ABSTRACT

Title of Dissertation: INTEGRATING AUTOMATED IMAGING AND A NOVEL IDENTIFICATION TECHNIQUE TO ESTIMATE MORTALITY AND IDENTIFY FACTORS THAT INFLUENCE THE VERTICAL DISTRIBUTION OF *CRASSOSTREA VIRGINICA* LARVAE

Jacob D. Goodwin, Doctor of Philosophy, 2015

Dissertation directed by: Associate Professor, Dr. Elizabeth North, Marine Estuarine Environmental Science, University of Maryland Center for Environmental Science.

Knowledge of the distribution, abundance, and transport of bivalve larvae has been limited due to their small size, similar morphologies between species, and lack of an automated approach for identification. Most of the literature and research to date has focused on juvenile and adult bivalves, much less is known about the larval stage. The objectives of this dissertation were to fill this knowledge gap by 1) creating a visual guide and key that would enhance the identification of *Crassostrea virginica* (eastern oyster) larvae in Choptank River using birefringent patterns that appear on the shells of bivalve larvae under crossed-polarized light, 2) testing and improving ShellBi, a novel supervised image classification method that uses pattern recognition software to identify images of bivalve larvae taken under cross-polarized light, 3) developing a benchtop automated image acquisition system to rapidly

capture images for use with ShellBi, and 4) applying these advances to identify factors that cue *C. virginica* vertical larval dispersal and to estimate their mortality rates in the field. Assessment tests of the ShellBi method indicated that error rates for identifying *C. virginica* larvae ranged from 1% to 22% when proportions of these larvae in a sample ranged from 2% to 90%. The automated image acquisition system increased image acquisition time from 2-13 hr to 46 min per sample and enabled *C. virginica* larvae to be rapidly imaged, measured, and identified with classification accuracies that ranged from 81-100% (mean 94% +/- 7 s.t.d.). Field collections of *C. virginica* larvae indicated that salinity appeared to be the dominant cue for vertical larval distributions, with > 90% of larvae < 200 μm found above a maximum salinity gradient of 1.2 m^{-1}. Estimated instantaneous daily mortality rates of 8-16 d-old larvae ranged 0.37 d^{-1} to 0.58 d^{-1}, with the most reliable rates being 0.37-0.38 d^{-1}. These findings advanced understanding of the larval ecology of *C. virginica.* The new techniques can be used to enhance image acquisition for other planktonic species and research results can be applied to validate larval transport models of *C. virginica* which have application for locating marine protected areas.

INTEGRATING AUTOMATED IMAGING AND A NOVEL IDENTIFICATION TECHNIQUE TO ESTIMATE MORTALITY AND FACTORS THAT DETERMINE THE VERTICAL DISTRIBUTION OF *CRASSOSTREA VIRGINICA* LARVAE

by

Jacob D. Goodwin

Dissertation submitted to the Faculty of the Graduate School of the
University of Maryland, College Park, in partial fulfillment
of the requirements for the degree of
Doctor of Philosophy
2015

Advisory Committee:
Professor Dr. Elizabeth North, Chair
Dr. William Boicourt
Dr. Kennedy Paynter
Dr. James Pierson
Dr. Michael Roman
Dr. Michael Wilberg
Deans representative: Dr. Paul Leisnham

Dedication

In memory of Ryan Saba who helped with some of this work. Ryan was a great friend and colleague and left us with good words to live by after he passed:

"This is the beginning of a new day. God has given me this day to use as I will. I can waste it or use it to do good. What I do today is very important because I am exchanging a day of my life for it. When tomorrow comes, this day will be gone forever leaving something in its place I have traded for it. I want it to be a gain, not a loss, good not evil, success not failure, In order that I shall not forget the price I paid for it. Success is a journey, not a destination, and the journey is The reward."

(*Source unknown*)

Acknowledgements

I would like to thank all of the people and agencies who supported this research and my graduate funding. The majority of funding that supported this research was provided by the National Science Foundation (OCE-0829512). Additional funding was provided by The Bailey Wildlife Foundation and Stolarz Foundation. Additional travel funds were provided by the Ryan Saba memorial fund and the Horn Point Laboratory Education Committee.

The key to my graduate success has been my advisor Elizabeth North who has guided me through this entire process and helped me develop into a better scientist and writer. She challenged and encouraged me during all stages of this research. There are no words to describe how much she has taught me but I am forever thankful. The lessons I have learned from her are invaluable and will stay with me throughout my career and life.

My committee, Bill Boicourt, Ken Paynter, Jamie Pierson, Mike Roman, Mike Wilberg have also been invaluable during my time as a graduate student. They provided much needed guidance, advice, feedback, and equipment. The door was always open to me whenever I needed and they always gave their careful guidance that helped this work tremendously.

Thanks to Ian Mitchell and Christine Thompson as this research would not have been possible without their programming skills. Both did much to help advance the automated image analysis system. Thanks to Vic Kennedy who helped spawn all the species (aside from oysters and marsh mussels) used in this study and offered guidance and support throughout my graduate career. Special thanks to Don Merritt

and Stephanie Alexander of the Horn Point Hatchery for providing *C. virginica* larvae over the years and to Lisa Guy for providing the algae to feed them. I thank the crew of the *R.V. Hugh Sharp* for their hard work and good spirits during the fixed station cruise. I thank Steve Suttles for processing the ADCP data and Erin Markin for processing the CTD data. Special thanks to Tom Wazniak who always provided support on all field ventures and helped process cruise reports. Thanks to Hanna McFadden and Ryan Saba for helping in the laboratory with imaging and tests for the automated system. I would like to thank Meg Maddox and the Horn Point laboratory analytical services group for processing TSS and Chlorophyll data. I would like to thank Rebecca Tay, Rachel Woodward, Adam Hardy, Adam Schlenger, Johanna Thalmann, Ford VanFossen, Aiden Fischer and Kaley Hanrahan for their help in the field and laboratory. I thank Jack Seabreese for custom pieces made for the automated imaging system and Ritchie Long for helping with the boat and field gear. I thank the entire maintenance and administrative staff at Horn Point Laboratory for their exceptional help whenever I needed it. The staff at Horn Point really make that laboratory an exceptional place to work.

Special thanks to Anne and Joe for helping me through these times. I thank my parents and Uncle JJ. I thank CJ Burnley, Tommy Bradley, Jeff Mitchell and Homero Macedo as well as friends from Cambridge for helping me get through rough times. Ashley Brandon Spear, Matt Bramble, Marc Bramble, Ann Barse, and Joe Byrne. I thank Ryan Saba, Blakey Clark and Will Vick and my sister Dana for helping me snowboard a lot of tension away. I thank Abby Kent for keeping me sane in the later stages of writing and supporting me.

Table of Contents

List of Tables

Slightly lower accuracies were reported when training sets included images of shells stored in formalin (95-96%) compared to those stored in ethanol (97-98%). Based on the high classification accuracies for shells stored in both types of fixatives, it is concluded that the fixative used does not interfere with the ability of ShellBi to classify larvae.

Table S2.2. Leave one-out (LOO) cross validation accuracy of training sets for classifying *C. virginica*. The first column lists the analysis in which the training set was applied. The second column gives the two letter code of each species used in the training set (CV: *Crassostrea virginica*, RC: *Rangia cuneata*, ML: *Mulinia lateralis*, TG: *Tagelus plebeius*, IR: *Ischadium recurvum*, and DF: *Mytilopsis leucophaeata*). The third column lists the number of images in each training set. The fourth column gives the LOO percent accuracy for classifying *C. virginica.* *Denotes that images of *C. virginica* larvae grown in different temperature and salinity treatments were added to the *C. virginica* training set category (Table S2.3).

Table S2.3. The number of images of *C. virginica* larvae that grown in different temperature and salinity treatments which were added to the *C. virginica* training set category denoted by CV* in Tables 2.2 and S2.2. Mean, standard deviation, and sample size for temperature and salinity measurements are reported.

Table S3.1. Information on the taxonomy and ages of the 8 species of bivalve larvae whose images were used to construct training sets for the validation experiments. The age groups represented were evenly distributed (a closely as possible) so that the total number of images for each species would contain an even representation of all ages. Each training set had three categories (Ostreoida (oysters), Mytiloida (mussels), and Veneroida (clams)which contained equal numbers of images. The two training sets (COM1000, COM7000) were bothed created using setting one (Table 3.3). However, color channel intensities for COM1000 were not measured and were different than those for COM7000.

Table 3S.2. Results from the two validation tests using three ShellBi training sets (COM1000, COM700, and COM1700) and two humans (Jake and Meghan) to manually classify images of C. virginica of various ages and quantities within 18 folders. Each folder had 100 images of different randomly picked bivalve larvae chosen from table S.3.1. Tables A and C show the actual number of C. virginica images “actual CV” in each of the 18 folders as well as how many were classified by ShellBi, Jake, and Meghan. Tables B and D show the classification accuracy (number correctly classified/actual). Blank values mean there were no *C. virginica* in those particular folders.

List of Figures

unknown larvae in different proportions. A 6-species training set (6-spec, solid lines) was composed of six categories, each for a separate species: *C. virginica, I. recurvum, M. lateralis, M. leucophaeata R. cuneata,* and *T. plebeius*). A second training set (order-based, dotted lines) contained images of these species grouped by order (clams: *M. lateralis, M. leucophaeata, R. cuneata, T. plebeius*; oyster: *C. virginica*, mussel: *I. recurvum*). These training sets were used to classify three different groups of images of "unknown" larvae: 1) *C. virginica*, *T. plebeius*, and *M. lateralis* (CV, TG, ML), 2) *C. virginica*, *T. plebieus,* and *I. recurvum* (CV, TG, IR), and 3) *C. virginica, R. cuneata*, and *M. lateralis* (CV, RC, ML). Each group contained "unknown" sets of images in which the percentage of *C. virginica* in the set ranged from 2 to 90%.

Fig. 2.6. Classification confidence intervals for the 6-species (no fill with solid gray line) and order-based (gray shading with dashed gray line) training sets. Confidence intervals were constructed around the correct percentage of *C. virginica* classified in a sample (solid line with triangles) using the highest number of false positives and false negatives from tests summarized in Fig. 5. False positives were added to the correct number of *C. virginica* images to construct the top lines and false negatives were subtracted from the correct number of *C. virginica* images to construct the bottom lines. The closer the gray lines are to the black line, the smaller the classification error, which ranged from 5-21% for the 6-species training set and from 1-22% for the 3-category order-based training set.

Fig. 3.1. Automated imaging acquisition system composed of 1) Infinity 2-3C digital microscope camera with metal braces on each side, 2) Semprex automated stage motor, 3) Semprex automated stage with Sedgwick Rafter slide in well plate holder, 4) stage motor controller hub, 5) Omax inverted polarizing microscope with metal braces on each side of base, 6) four metal braces (two on each side), and 7) aluminum baseplate clamped to benchtop.

Fig. 3.2. Percent classification accuracy of 9-d- old *C. virginica* larvae (upper panel) and concurrent color channel intensity measurements (bottom panel) taken over a span of 100 days. Each data point for classification accuracy was the result of classifying 50 images of 9-d-old C. virginica using a three species training set (*C. virginica, I. recurvum, and R. cuneata*). The color channel intensity values were calculated using five blanks captured from the automated stage and were compared to the acceptable range (hatched regions) (see procedures section). Arrows indicate the time when color channel intensity values dropped below the acceptable range due to a microscope light bulb malfunction, and when percent classification accuracies also dropped (from an average of 98 to 70%).

Chapter 1: Shedding light on bivalves of the Choptank River: how polarized light can enhance identification

Abstract

Understanding the population dynamics and complete life cycle of bivalves is important for effectively manage them. Most of the literature and research to date has focused on juvenile and adult bivalves, much less is known about larvae. The larval stage of the bivalve life cycle has been difficult to study due to the lack of a rapid automated approach for identifying species. However, a new technique, called ShellBi, has emerged that utilizes color patterns on the larval shell under polarized light to identify bivalve larvae. The objective of this chapter was to review the scientific basis for ShellBi and to apply it to bivalve larvae in Choptank River with the goal of distinguishing *C. virginica* from seven other species that spawn at the same time. A digital camera and polarized light microscope were used to capture images of the shells of bivalve larvae under standard and cross-polarized light. Images of *C. virginica* were distinguishable from other species based on these patterns, especially at later stages of development. These images could serve as a visual guide to identify *C. virginica* collected from the Choptank River and other tributaries with similar species in Chesapeake Bay.

Introduction

Bivalves have a complex life cycle with a pelagic larval stage (Kennedy 1996). Their population dynamics are based on birth, mortality, immigration, and emigration (Gotelli 2001). Larval ecology is crucial for understanding population dynamics because immigration, emigration, and mortality occur during the larval stage (Kennedy 1996). Many species of bivalves are ecologically and economically important yet little is known about their larval stage due to challenges in identification (Garland and Zimmer 2002). Using crossed polarized light is a new method that has potential for identifying bivalve larvae to species. It utilizes the color patterns from the shells of bivalve larvae emitted under polarized light (Tiwari and Gallager 2003). The goal of this chapter is to apply this new approach to eight species of bivalve larvae that spawn during summer in the Choptank River with the goal of distinguishing the larvae of *Crassostrea virginica*, the eastern oyster, from the other species whose larvae are in the plankton at the same time.

Development and shell formation in bivalve larvae

Although the larval stage is not the same for all bivalve species, it is usually occurs within several weeks (Gosling 2003). The bivalve larval stage is part of a complex life cycle. Bivalves' reproductive cycle involves growth, ripening of gametes, spawning and gonad redevelopment (Gosling 2003). They reproduce sexually and eggs and sperm combine and develop into larvae. It is during the larval stage when the shell begins to form (Kennedy 1996, Gosling 2003).

Bivalves progress through several stages of development including prodissoconch I, prodissoconch II, and dissoconch stages (Carriker 1996). All shell

development stages occur during the planktonic larval stages (prodissoconch I/II) except the dissoconch stage, which occurs after settlement (Carriker et al 1996). Bivalve larvae mineralize their shells. The biological definition of mineralization is the process through which an organic substance becomes impregnated by inorganic substances (IUPAC 2012). Larval shells are made mostly of aragonite rather than the less soluble calcite that makes up the shells of adult bivalves (Carriker 1996). It has been proposed that aragonite is harder than calcite and has greater strength as a structural material and is less prone to breakage by cleavage making it a better choice for life in the plankton (Carriker 1996). Shell mineralization occurs in an organic aragonite matrix formed in the shell field (Carriker 1996). The matrix that forms constitutes a brick-wall patterned biocomposite of bio-mineralized aragonite platelets surrounded by organic matter known as nacre (Checa et al. 2006). It is arranged in terraces that grow simultaneously (Schmidt 1924, Wada 1972). Within the terraces are three crystallographic axes of crystals (called a-,b-, and c-axis) with the c-axis perpendicular to the nacre surface and the other two axes parallel to the local growth direction of the shell margin (Wada 1972).

The mineralization of a bivalve larvae shell first takes place during the late stages of embryonic shell development. Mineralization of the larval shell occurs in the shell field (Carriker et al 1996). The shell field is an area of ectodermal cells in the dorsal region of a developing embryo that secretes the embroyonic shell (Carrkiker 1996). The first appearance of the shell field occurs in early embryogenesis (Moor 1983) when the shell field invaginates to form a “shell field invagination” (Eyster 1983). At this moment organic shell material is secreted by the

cells of the shell field externally and the epithelial cells in the shell field spread over the embryonic surface prior to mineralization (Carriker et al 1996). More recent studies conducted on adult *C. virginica* shells have shown that granulocytic hemocytes could be directly involved in shell crystal production in addition to the previously described process of extracellular shell field invagination (Mount et al. 2004). However, it is not known if this process begins at the larval stage. It is thought that there is only a single shell field invagination in bivalves, but the intricate process is still not fully understood (Carriker 1996, Mount et al. 2004). After the initial mineralization the larvae are often called trocophores and the new mineralized shell is homogenous and composed mostly of calcium carbonate (Eyster 1986).

Mineralization marks the end of the embryonic stage and the beginning of the prodissoconch I stage which for several species lasts between 24-30 hours at summer temperatures (Andrews 1979). Mineralization in two species, *Mercenaria mercenaria* and *Crassostrea gigas,* was found to begin with a precursor of aqueous calcium carbonate after three days, followed by a crystalline aragonitic phase (Weiss et al. 2002). Aragonite is a form of calcium carbonate with a different crystal structure (Chang 1996). Weiss et al. (2002) also postulated that other bivalve larvae would have the same developmental properties as the two species they studied. The prodissoconch I larvae in the crystalline aragonitic phase look like the letter "D" and are often called "D-stage larvae". Toward the end of the prodissoconch I stage, two equal-length aragonite valves form (Carriker and Palmer 1979) and can be noted by conspicuous punctate-stellate patterns on the surface of each valve when viewed under scanning electronic microscopy (Carriker 1996).

During prodissoconch II, the next shell development stage, the left valve grows considerably wider than the right valve (i.e., more convex) and an umbo begins to form (Carriker 1996). An umbo is the rounded elevated oldest part of each valve at the anterior end of the bivalve (Carriker 1996). As shell secretion continues, the valves become heavier (Carriker 1996). By the end of prodissoconch II, oyster larvae may be over 150 μm long and both abductor muscles are nearly equal in size (Carriker 1996). At this point some bivalve species exhibit growth striate that are visible in bands between aragonite layers (Millar 1968, Siddall 1980).

The Prodisoconch II stage ends with the formation of an actively crawling foot as the organism begins searching for a settling place (Nelson 1924, Carriker 1986, Carriker 1996). The settling behavior of several bivalves has been studied and some respond to chemical and biological cues that stimulate settlement (Carriker 1996, Kennedy 1996).The planktonic larval development ends after settlement and the homogenous aragonitic prodissoconch I and II shell secretion changes from aragonite to calcite to begin the adult dissoconch stage (Carriker and Palmer 1979).

Larval shells under polarized light

Polarized light as a tool for microscopy has been used in geology for 200 years (Carlton 2011). However, recent advances have made polarized light microscopy useful in biology to identify bivalve larvae because of the aragonite (crystalline) composition of bivalve larval shells (Gallager and Tiwari 2008, United States Patent #7415136). The shells of bivalve larvae contain anisotropic crystals with different orientations and are birefringent. Birefringent materials (e.g., calcite, mica, cellophane) have two different indices of refraction, i.e., light passes through in two

directions. When placed between crossed polarizers, birefringent materials produce interference colors (colors that differ from those under normal light) (Murphy et al. 2013). The crystalline shells of bivalve larvae are birefringent and form rainbow-like interference colors that are easily discernable in plankton samples (Fig. 1.1).

Visualizing patterns formed by the crystal structures under polarized light was first conducted in the early 1900s on a river mussel species in Germany (Schmidt 1924). The optical orientation of the crystals contained in the nacre of each species appears distinct (Tiwari and Gallager 2003). It is extremely difficult, at best, to visualize the crystal patterns or infer orientation under standard microscopy (Fig. 1.1A). However, as described by Tiwari and Gallager (2003), under cross-polarized light, the light that is not in the plane of the polarizer refracts off the shell in a fashion affected by its crystal orientation and a dark cross of light extinction becomes visible in the plane of the two polarization plates (Fig. 1.1B). With the addition of a full wave compensation plate (or λ plate), distinct colored interference patterns are produced as the polarized light refracts off the crystals (Fig. 1.1C). The patterns, investigated, are species-specific because the protein compliment of the shell matrix and the axial rotation of the crystals differ between species of bivalves (Tiwari and Gallager 2003). Thus the way that the crystals are laid down during shell formation differs, and the resulting patterns are distinct, between species. Some of these patterns can be discerned by eye or by using pattern recognition software to identify larvae to species (Thompson et al. 2012). This objective of this chapter was to capture birefringent images of different size classes of bivalve larvae that spawn the same time as *C. virginica* in the Choptank River, a sub-estuary of Chesapeake Bay.

Bivalves of the Choptank River

Although there are more than eight species of bivalves in the Choptank River, this research focuses on those that spawn the same time as *C. virginica*. One other species of clam *Gemma gemma* also reproduces at the same time as *C. virginica* but this species is not found in the plankton because it broods its young and they emerge as juveniles (Sellmer 1967). Therefore *Gemma gemma* is not included in this guide. The species that spawn and have larvae in the plankton the same time as *C. virginica* are: *Ischadium recurvum* (Chanley 1970), *Guekensia demissa* (Borrero 1987), *Macoma mitchelli* (Blundon and Kennedy 1982), *Mytilopsis leucophaeata* (Kennedy 2011a), *Mulinia lateralis* (Calabrese 1969), *Rangia cuneata* (Sunberg and Kennedy 1993), and *Tagelus plebeius* (Chanley and Castagna (1971). The following section reviews each species life history and larval ecology. Table 1.1 provides a summary of spawning conditions, larval salinity tolerances, and pelagic larval durations for these species.

C. virginica (Gmelin 1791), eastern oyster. The eastern oyster can reach up to 360 mm in shell length (Galtsoff 1964). The adult salinity tolerance varies from 5 to 40 although optimal ranges can vary by geographic location (Galtsoff 1964). They range from the Western Atlantic to the Gulf of St. Lawrence to Brazil and Argentina and have been introduced to the West Coast of the U. S. (Carriker and Gaffney 1996). When water temperatures reach 25 ^{o}C in the lower Chesapeake Bay, *C. virginica* spawn and the larvae produced may be present in the water column for up to 2-3 weeks (Shumway et al. 1996). Optimal temperatures and salinity for the larvae may vary by geographic location. Larvae from Long Island Sound grow well in

temperatures of 17.5 ^{o}C and salinities of 15–27 (Davis and Calabrese 1964). However, spat sets have been observed in salinities as low as 1.4 and tolerance of larvae may vary by geographic location (Shumway et al. 1996). Native *C. virginica* populations are economically important as a food source for humans (Rothschild et al. 1994, Mackenzie 2007) and ecologically (Wells 1961, Rodney and Paynter 2006, Fulford et al. 2010) important by providing habitat and food for other organisms (Rodney and Paynter 2006) and by filtering the algae from the water column (Newell 2004). Populations are declining in many parts of the world (Beck et al. 2011). In Chesapeake Bay the abundance of current *C. virginica* populations are less than one percent of historical levels (Wilberg et al. 2011).

I. recurvum (Rafinesque, 1820), hooked mussel. These mussels can reach 60 mm (Lipcius and Burke 2006). The range of *I. recurvum* stretches from Cape Cod through the Gulf of Mexico and the West Indies (Allen 1962). Their larvae have salinity and temperature requirements similar to *C. virginica* (salinities 6-20 and temperatures 25-30). This species is often found on oyster reefs in the Chesapeake Bay (Allen 1962, Shaw 1965, Chanley 1970). Settlement has been observed in Choptank River from April through December (Shaw 1965). Although little is known about their pelagic larval duration it took 14 days to rear our laboratory specimen. The hooked mussel is usually found on oyster bars and can affect the growth habits of oysters (Lipcius and Burke 2006). These mussels also provide food for surf scoters *Melanitta perspicillata* in Chesapeake Bay (Berlin 2008).

G. demissa (Dillwyn 1817), ribbed or marsh mussel. These mussels have a lifespan of around 15 years and reach 100 mm in length (Brousseau 1984). Their

geographical range is from the Gulf of Maine to Florida although the species was also introduced in San Francisco Bay (Franz 2001). There is usually one annual spawning event between June and September depending upon the region (Borrero 1987). The larvae are in the water, including in Chesapeake Bay, from early summer to the beginning of fall (Borrero 1987). Information on *G. demissa* larvae is scarce but planktonic larval duration can take 6–21 days and larvae can grow at 27 ^{o}C and salinities between 12-22 (obs. from Rutgers Hatchery unpublished data). Baker and Mann (2003) observed later-stage pediveliger larvae of the marsh mussel in surface waters during non-stratified conditions in one tributary of Chesapeake Bay. Populations of *G. demissa* are important because they affect the nutrient dynamics of marshes and estuaries (Jordan and Valiela 1982). Kuenzler (1961) found that the mussels can remove a third of the particulate phosphorus from suspension and deposit it on the mud surface. They can also alter the structure of microbiota (Kemp et al. 1990). Sometimes *G. demissa* can form dense aggregates altering the physical structure of the marsh and stimulating the growth of *Spartina alterniflora* (Bertness and Grosholz 1985). These mussels are also food sources for diamondback terrapins (Whitelaw and Zajac 2002) and are one of the few bivalves able to forage on small-sized bacterioplankton (Newell and Kambeck 1995).

M. mitchelli (Dall 1895) , Matagora macoma clam. This small clam reaches 16 mm in length (Blundon and Kennedy 1982). The exact geographic range of these clams is not known but there are occurrences of *M. mitchelli* in samples collected in the Atlantic and Gulf Coasts of the United States (e.g. Parker 1959, Tenor 1972, Redding 1975). They have a salinity range of 5-18 (Kennedy 1989). They are thought

to spawn between spring and fall but juveniles have been observed throughout the year (Blundon and Kennedy 1982). Their larval development time is 6-7 days and the larvae will grow at temperatures around 23 °C and salinity of 18 (Kennedy et al. 1989). The ecological role of this species is not well known although it was considered as a potential bio-indicator of pollution in the Neuse River Estuary (Waller 1996).

M. lateralis (Say 1822), coot clam or surf clam. This clam can be found in the upper 5 cm of the sediment of Chesapeake Bay and may reach up to 18 mm in length (Blundon and Kennedy 1982). It is found from Malpeque Bay Canada to northeastern Mexico and in the West Indies (Calabrese 1969). It can tolerate salinities ranging between 1.4 - 75.1 (Breuer 1957). The optimum salinity for both developing embryos and survival of larvae is 25-27.5 at 25 ^{o}C (Calabrese 1969). Temperature has the greatest influence on the duration of the larval stage and growth is "satisfactory" at temperatures from 22.5-27.5 ^{o}C and salinities from 20-35 (Calabrese 1969). Larval swimming is affected by salinity and larvae (of all stages) concentrated at the salinity discontinuity according to laboratory studies (Mann et al. 1991). Although this clam is not important commercially, its short generation time and high fecundity make it a perfect candidate for studies of pollution effects (Calabrese and Rhodes 1974). Waterfowl of the Chesapeake Bay also eat *M. lateralis* (Berlin 2008, Harmon 1962).

M. leucophaeata (Conrad 1831), dark false mussel. This mussel can reach 25.2 mm in length (Kennedy 2011a), although typical populations range between 15-20 mm (Sidall 1980). Although *M. leucophaeata* are native to the east coast of North America (Kennedy 2011a), they have been introduced in South America and Europe

(Kennedy 2011b). The species has a salinity range of 0.8-20.9 and temperature range of 15-27 °C (Verween et al. 2007). The adults spawn between summer and fall (Verween et al. 2005). The planktonic larval duration for *M. leucophaeata* is between 6-11 days depending on temperature and salinity (Verween et al. 2007). Larvae can survive in temperatures of 10-30 °C and salinities of 0-25 although their optimal growth conditions are 22 °C with salinity near 15 (Verween et al. 2007). Dark false mussels filter algae from the water column and provide food for fish species (e.g., pinfish (*Lagodon rhomboids*) and sheepshead (*Archosargus probatocephalus*)) and blue crabs (*Callinectes sapidus*) (Odum and Herald 1972). Perry et al. (2007) found these mussels in the gullet and gizzard of ducks shot on the Chester River in Maryland indicating their importance as a prey item for waterfowl.

R. cuneata (Sowerby, 1831) , Atlantic rangia. Atlantic rangia clams are suspension feeding bivalves that can reach over 70 mm in shell height (Chanley 1965). They are found from the upper Chesapeake Bay to areas in the Gulf of Mexico that have salinities less than 15 (Hopkins et al. 1973, Cain 1975). Gametogenesis begins in this species at water temperatures exceeding 15 ^{o}C and salinities less than 15 (Hopkins and Andrews 1970). Planktonic larval duration for *R. cuneata* is about one week before settlement and the larvae size range for pediveligers is between 160 and 300 µm (Sundberg and Kennedy 1992). Larval swimming is affected by salinity and larvae (of all stages) concentrated at the salinity discontinuity according to laboratory studies (Mann et al. 1991). The clam larvae can develop successfully at temperatures of 23-26 ^{o}C and salinities of 8-10 (Sundberg and Kennedy 1992). Although this species is not commercially harvested it is a non-

selective filter-feeder turning plant detritus and phytoplankton into clam biomass that animals can eat (Darnell 1958). In some areas of the country, mainly Texas, their shells are economically valuable (Hopkins and Andrews 1970).

T. plebeius (Lightfoot 1786), stout or razor clam. Razor clams can reach up to 75 mm (NMR 2013). These clams are an infaunal species ranging from Cape Cod to Argentina (Gosner 1979, Vazquez et al. 2006). They are common in salinities of 10–30 but can tolerate salinities below 10 (Chanley & Castagna 1971). Their gonads are mature from June through December but most spawning occurs in late August and September (Chanley and Castagna 1971). Larvae of *T. plebeius* have a length of 90 to 170 µm and complete their development at a smaller size than many other veliger bivalve larvae (Chanley and Castagna 1971). The pelagic larval duration is usually between 8-13 days (Chanley and Castagna 1971). Larvae of *T. plebeius* have been successfully reared at temperatures of 22-25 ^{o}C and salinities of 11-30 (Chanley and Castagna 1971, Table 1.1). This clam is becoming increasingly important commercially for use as bait in commercial crab and eel traps (Dungan et al. 2002). They are also food sources for diamondback terrapins (Whitelaw and Zajac 2002) and most likely other species in the Bay.

These eight species of larvae have diverse size ranges, pelagic larval durations, and ecological roles within the Choptank River. However, a rapid way to identify these larvae is needed. Furthermore, a full understanding of what cues swimming behavior or affects mortality is not known. Yet, this information is important for understanding larval transport and population connectivity, which in turn are important for advancing knowledge of the population dynamics of these

important commercial and ecological shellfish. Using image analysis with polarized light can help fill this knowledge gap by allowing for improved identification and enumeration of bivalve larvae. The objective of this chapter is to document the color patterns of eight species of bivalve larvae in the Choptank River under polarized light and to create a visual identification guide for distinguishing *C. virginica* using these patterns.

Methods

To create a visual guide and key for identifying bivalve larvae under polarized light, adult bivalves were spawned and their larvae reared. Images of the larvae at different stages of growth were captured under polarized light for all species. Finally, a visual guide and a key were created that could help distinguish *C. virginica* from the other species.

Spawning and rearing

Eight bivalve species that are found in Choptank River were spawned, their larvae were reared and images of their shells were taken (Table 1.1, Fig. 1.3-1.10). The adult bivalves that were collected from the Choptank River and reared in the laboratory consisted of: *I. recurvum* (hooked mussel), *M. lateralis* (dwarf surf clam), *M. leucophaeata* (dark false mussel), *M. mitchelli* (Matagora macoma clam), *R.cuneata* (Atlantic rangia clam), and *T. plebeius* (razor clam). Larvae of *C. virginica* (eastern oyster) were obtained from the Horn Point Hatchery and *G. demissa* (marsh mussel) were obtained from the Rutgers Cape Shore Laboratory. Spawning (using

temperature fluctuation) and rearing procedures were consistent with summer conditions in Choptank River and were explained in detail (see Goodwin et al. 2014 (Chapter 2)) for all species with the exception *G. demissa*. The *G. demissa* larvae were reared in conditions similar to Delaware Bay at a temperature of 24.9 ^{o}C at a salinity of 22.5 and fed *Isochrysis galbana*, *Pavlova lutheri*, and *Chaetoceros calcitrans*.

Imaging

Images used for this guide were captured under standard microscopy and with cross polarized light with a full wave (λ) compensation plate. Specimens of three age groups (2-3d) from each species were imaged to discern the differences in birefringence patterns over larval development (D-stage, early Prodissoconch II, and late Prodissoconch II) All bivalve larvae were imaged using an Omax M837PL trinocular inverted polarizing microscope. The microscope was equipped with an automatic stage and had a 5x ocular with an objective lens of 20x. The magnification was calculated to be 7x. An Infinity model 2-3C eight megapixel digital microscope camera was used to image both polarized light and standard light images. The software program used to capture images with the camera was Lumenera Infinity Analyze Software version 3.1. The camera software settings used to capture images used in this guide were: exposure (151.0), gain (10.6), gamma (0.82), light source setting (fluorescent), saturation (1.31), brightness (4), contrast (4), red (1.0), blue (1.0), green (1.0), averaging (1), and subsampling (1). Settings for Birefringent images and standard light images were both captured under these settings. First, larval shells were broken apart and tissue digested by immersing them in a 40% bleach and

buffered (Sodium Borate) DI water (see Chapter 3 for more details). Then, clean shells were pipetted in buffered (Sodium Borate) DI water onto a Sedgewick-Rafter slide. Birefringent images were captured using cross polarized light with a full wave (λ) compensation plate. Once an image of the shell of a bivalve larvae was captured, the polarizer was removed and the (λ) plate removed. A standard green glass filter was then placed over the light source and another image was captured under standard microscopy conditions.

A key was created from an image library that was taken with an automated image acquisition system (Chapter 3), using the same procedures mentioned above except for different software settings of the camera: exposure (151.0), gain (15.2), gamma (0.82), light source setting (fluorescent), saturation (1.31), brightness (4), contrast (4), red (1.0), blue (1.0), green (1.0), averaging (1), and subsampling (1). This online library represents 1000 images of Osteroida, Veneroida, and Mytiloida that spawn during summer in Choptank River (species listed above) for a total of 3000 images.

Results

Images that were captured under polarized light of larvae had similar color patterns at the taxonomic level of order: oysters (*C. virginica* (Fig. 1.3A-F)), mussels (*I. recurvum* (Fig. 1.4A-F) *and G. demissa* (Fig 1.5A-F)), and clams ((*M. mitchelli* (Fig 1.6A-F), *M. lateralis* (Fig. 1.7A-F), *M. leucophaeata* (Fig. 1.8A-F), *R. cuneata* (Fig. 1.9A-F), and *T. plebeius* (Fig. 1.10A-F)). A unique pattern of yellow coloration at the posterior and anterior edges of the D-stage shell (Fig. 1.3D) helped distinguish

C. virginica from clams and mussels at the D-stage. Patterns of mussels and clams at the D-stages vary but were harder to distinguish (panel D on Fig. 1.4, and 1.6-1.10) due to similar colors and patterns.

The taxonomic groups were more clearly distinguishable at the prodissoconch II level. The *C. virginica* (Fig. 1.3E,F) and mussel species (panels E,F on Fig. 1.4-5) had a more yellow in their shell patterns than clams. Prodissoconch II mussels had the brightest patterns of yellow on their shells (Fig. 1.4E,F). The dark banding patterns of the oyster *C. virignica* and the mussel *I. recurvum* were similar (Fig. 1.3F, 1.4F) but the species were distinguishable because the mussel had a more circular shell with a less pronounced umbo. The birefringent images of clam species had a majority of red and blue coloration (panels E,F on Fig. 1.6-1.9) with little yellow making it difficult to distinguish between clam species, but useful for distinguishing them from mussels and *C. virginica*. One exception is later stage larvae of *T. plebeius* (Fig. 1.10E,F) which had some yellow coloration but still less than 20% of the shell. The more circular shape of *T. plebeius* helped distinguish these images from *C. virginica* and mussels (Fig. 1.10).

An identification key was created to help distinguish *C. virginica* larvae apart from other species that spawn the same time as *C. virginica* (Fig. 11.1). The key identifies larvae based on stage (e.g. D-stage, umbo). Larger *C. virginica* larvae were easier to distinguish because of their color (yellow and orange) and shape (pronounced umbo). Smaller *C. virginica* D-stage larvae were distinguishable because they were generally dull in color compared to other D-stage larvae. This key was made to use with a set of images called COM1000 that is available online

(http://northweb.hpl.umces.edu/TRANSPORT/home.htm) and was used as a training set for computer-assisted classification of bivalve larvae (see Chapter 3).

Discussion

These images of birefringent larval shells at different stages in their development could be used as a visual identification guide for bivalve larvae in the Choptank River. Previous work has been conducted that utilizes pattern recognition software (ShellBi) to identify bivalve larvae using birefringent patterns under polarized light (Gallager 2008, Thompson et al. 2012, Goodwin et al. 2014). An automated image acquisition system coupled with ShellBi could rapidly and accurately measure and classify larvae (see Chapter 3) and cost ~$17,000 plus an additional $16,000 for the ShellBi software. However, this visual guide (coupled with a digital library of multiple images for each species/stage) could be used for identification with a polarized microscope and digital camera for substantially less ($3,600).

The patterns in interference colors on the shells of bivalve larvae under polarized light were sensitive to camera settings and some settings may be better than others at distinguishing different species (see Chapter 3). The settings used in these images were optimized to distinguish *C. virginica* larvae. However, if another target species was being identified, different settings may perform better. For example, under these settings, it was difficult to distinguish clam species from each other (*M. mitchelli*, *M. lateralis*, *M. leucophaeata*, and *R. cuneata*), but altering the software

settings of the camera could bring out species-specific differences among them. A key (Fig. 1.11) was created to help identify oyster larvae. However, this key was created to target *C. virginica* and was best used with an established reference image library under the same camera settings as described in this study.

The objective of this chapter was to create a guide that could be used to visually identify *C. virginica*. It is important to identify *C. virginica* larvae so that more information can be gathered on this important life stage that governs transport and connectivity of populations (Kennedy 1996, Cowen and Sponagle 2009). The ultimate goal of this dissertation was to enhance our understanding of processes that affect the vertical and horizontal distribution and the mortality of *C. virginica* larvae. First, tests of the ShellBi software were conducted to determine its performance when distinguishing *C. virginica* larvae from the other seven species of bivalve larvae that spawn in the Choptank River at the same time as *C. virginica* (Chapter Two). Second, an automated image acquisition system was developed for use with ShellBi and tested to determine classification accuracies for identifying *C. virginica* from the other seven species (Chapter Three). Finally, ShellBi and the automated image acquisition system were applied to field samples from the Choptank River to characterize the distribution of *C. virginica* larvae in relation to physical and biological parameters, to infer their swimming behavior, and to calculate larval mortality rates (Chapter 4). By testing the ShellBi technology (Chapter 2), automating image capture (Chapter 3), and applying these advancements to field samples (Chapter 4), this research will help provide fundamental knowledge on the ecology of *C. virginica* which will support management of this species.

Literature cited

Allen, J.F. 1962. Gonad development and spawning of *brachidontes recurvus* in Chesapke. Bay. Naut. 75(4):149-156.

Andrews, J.D. 1979. Pelecypoda: Ostreidae. *In:* A.C. Giese and J.S. Pearse (eds). Reproduction of marine invertebrates, vol. 5. Academic Press, New York. Pages 293-341.

Baker, S. and R. Mann. 2003. Late stage bivalve larvae in a well-mixed estuary are not inert particles. Estuaries. 26(4A):837-845.

Beck, M.W., R.D., Brumbaugh, L. Airoldi, A. Carranza, L.D. Coen, C. Crawford, O. Defeo, G.J. Edgar, B. Hancock, M.C. Kay, H.S. Lenihan, M.W. Luckenbach, C.L. Toropova, G. Zhang, and X. Guo. 2011. Oyster reefs at risk and recommendations for conservation, restoration, and management. BioScience, 61:107-116.

Berlin, A. 2008. Foraging values of *Mulinea lateralis* and *Ischadium recurvum*: energetics of surf scoters wintering in the Chesapeake Bay. MEES Dissertation University of Maryland. 2008.

Bertness, M.D. and E. Grosholz. 1985. Population dynamics of the ribbed mussel, *Geukensia demissa*: The costs and benefits of an aggregated distribution. Oecologia 67:192-204.

Blundon, J.A. and V.S. Kennedy. 1982. Refuges for infaunal bivalves from blue crab, *Callinectes sapidus* (Rathbun), and predation on Chesapeake Bay bivalves. J. Exp. Mar. Biol. Ecol. 65:67-81.

Borrero, F.J. 1987. Tidal height and gametogenesis: reproductive variation among populations of *Geukensia demissa*. Biological Bulletin 173:160-168.

Breuer, J.P. 1957. An ecological survey of Baffin and Aluzan Bay Tx. Publ. Inst. Marine. Sci. 4:134-155.

Brousseau, D.J. 1984. Age and growth rate determinations for the Atlantic ribbed mussel, *Geukensia demissa* Dillwyn (Bivalvia: Mytilidae). Estuaries and Coasts 7:233-241.

Cain, T.D. 1975. Reproduction and recruitment of the brackish water clam *Rangia cuneata* in the James River, Virginia. Fish. Bull. 73:412-430.

Calabrese, A. 1969. The early life history and larval ecology of the coot clam, *Mulinia lateralis* (Say) (Mactridae: Pelecypoda). Dissertation, Univ. of Connecticut, 1969. 101 pp.

Calabrese, A., and E.W. Rhodes 1974. Culture of *Mulinia lateralis* and *Crepidula fornicate* embryos and larvae for studies of pollution effects. Thal. Jugoslavica 10:89-102.

Carriker, M.R., and Gaffney P.M. 1996. A catalogue of selected species of living oysters (Ostreacea) of the world. *In*: V.S. Kennedy, I.E. Newell, and E.F. Eble (eds). The eastern oyster *Crassostrea virginica* Chapter 1. Maryland Sea Grant pp 1-18.

Carriker, M.R. 1996. Chapter 3. The shell and ligament. *In*: Kennedy, V.S., R.I. E. Newell, and A.F. Eble (eds). The eastern oyster *Crassostrea virginica*. Maryland Sea Grant, College Park, Maryland.

Carriker, M.R. 1986. Influence of suspended particles on biology of oyster larvae in estuaries. Amer. Malcol. Bull., spec. ed. 3:41-49.
Carriker M.R. and R.E. Palmer. 1979. A new mineralized layer in the hinge of the oyster. Science 206:691-693.
Chang, L.L.Y., R.A. Howie, and J. Zussman 1996. Rock-forming minerals, (2nd edition), v. 5B, non-silicates, 108–135.
Chanley, P. 1965. Larval development of the brackish water mactrid clam, *Rangia cuneata*. Chesapeake Sci. 6(4):209-213.
Chanley, P. 1970. Larval development of the hooked mussel, *Brachiodontes recurves* Rafineque (Bivalvia: Mytilidae) including a literature review of larval characteristics of the Mytilidae. Proc. Natl. Shell. Assoc. 60:86-94.
Chanley, P., and M. Castagna. 1971. Larval Development of the Stout Razor Clam, *Tagelus plebeius* Chesapeake Sci. 12(3):167-172.
Checa, A.G., T. Okamoto, and J. Ramirez. 2006. Organization pattern of nacre in Pteriidae (Bivalvia:Mollusca) explained by crystal competition. Proc. Biol. Sci. 273(1592):1329-1337.
Darnell, R.M. 1958. Food habits of fishes and large invertebrate of Lake Pontchartrain, Louisiana, an estuarine community. Publ. Inst. Mar. Sci. Univ. Tex. 5:353-416.
Davis, H.C., and A. Calabrese. 1964. Combined effects of temperature and salinity on development of eggs and growth of larvae of *M. mercenaria* and *C. virginica*. U.S. Fish Wildl. Serv., Fish. Bull. 63:643-655.
Dungan, C.F., R.M. Hamilton, K.L. Hudson, C.B. McCollough, and K.S. Reece. 2002. Two epizootic diseases in Chesapeake Bay commercial clams, *Mya arenaria* and *Tagelus plebeius*. Dis. Aquat. Org. 50:67-78.
Eyster, L.S. 1983. Ultrastructure of early embryonic shell formation in the opisthobranch gastropod *Aeolidia papillosa*. Biol. Bull. 165:394-408.
Eyster, L.S. 1986. Shell inorganic composition and onset of shell mineralization during bivalve and gastropod embryogenesis. Biol. Bull. 170:211-231.
Fogarty, M.J., and L.W. Botsford. 2007. Population Connectivity and Spatial Management of Marine Fish. Oceanogr. 20:112-123.
Franz, D. 2001. Recruitment, survivorship, and age structure of a New York ribbed mussel population (*Geukensia demissa*) in relation to shore level-A nine year study. Estuaries, 24(3):319-327.
Fulford, R.S., D.L Breitburg, M. Luckenbach, and R.E. Newell. 2010. Evaluating ecosystem response to oyster restoration and nutrient load reduction with a multispecies bioenergetics model. Ecol. Applications, 20, 915-934.
Gallager, S., and S. Tiwari. 2008. Optical method and system for rapid identification of multiple refractive index materials using multiscale texture and color invariants. *United States Patent 7,415,136*. Washington, DC: U.S.
Galtsoff, P.S. 1964. The American oyster, *Crassostrea virginica* (Gmelin) Fishery Bull. Fish Wildl. Serv. U.S. 64:1-480.
Garland, E.D., and C.A. Zimmer. 2002. Techniques for the identification of bivalve larvae. Mar. Ecol. Prog. Ser. 225:299-310.

Gosner, K.L. 1979. A field guide to the Atlantic seashore: invertebrates and seaweeds of the Atlantic Coat from the Bay of Fundy to Cape Hatteras: Houghton Mifflin Press, Boston, MA.

Gotelli, N.J. (2001) A primer of ecology. Sunderland, MA: Sinauer Associates, Inc., 265pp.

Harmon, B.G. 1962. Molluscs as food of lesser scaup along the Louisiana coast. Trans. N. Am. Wildlife. Nat. Resour. 27:132-137.

Hopkins, S.H., and J.D. Andrews. 1970. *Rangia cuneata* on the east coast: Thousand mile range extension, or resurgence? Science. 167:868-869.

Hopkins, S.H., J.W. Anderson, and K. Horvath. 1973. The brackish water clam *Rangia cuneata* as an indicator of ecological effects of salinity changes in coastal waters. Report to U.S. Army Corps of Engineers, Waterways Experimental Station, Vicksburg, Mississippi. Contract Rep. H-73-1. 250 pp.

IUPAC, International Union of Pure and Applied Chemistry. Terminology for biorelated polymers and applications (IUPAC Recommendations 2012). Pure and applied Chemistry 84(2):377-410.

Jordan, T.E., and I. Valiela. 1982. A nitrogen budget of the ribbed mussel, *Geukensia demissa*, and its significance in nitrogen flow in a New England salt marsh. Limnol. and Oceanogr. 27: 75-90.

Kemp, P.F., S.Y Newall, and C. Krambeck, 1990. Effects of filter-feeding by the ribbed mussel *Geukensia demissa* on the water-column microbiota of *Spartina alterniflora* saltmarsh. Mar. Ecol. Prog. Ser. 50:119-125.

Kennedy, V. S. 1989. Larval and Early Postlarval Development of *Macoma mitchelli* Dall (Bivalvia: Tellinidae), The Veliger 32(1):29-38.

Kennedy, V. S. 1996. Biology of larvae and spat. p. 371-421. *In* V. S. Kennedy, R. E.Newell, and A.F. Eble (eds.). The Eastern Oyster *Crassostrea virginica*. Maryland Sea Grant

Kennedy, V. S. 2011a. The invasive dark false mussel *Mytilopsis leucophaeata* (Bivalvia: Dreissenidae): A literature review. Aqua. Ecol. 45:163-183.

Kennedy, V. S. 2011b. Biology of the uncommon dreissenid bivalve *Mytilopsis leucophaeata* (Conrad 1831) in central Chesapeake Bay. J. Mull. Stud. 77:154-164.

Kuenzler, E.J. 1961. Phosphorus budget of a mussel population. Limnology and Oceanography 6: 400-415.

Lipcius, R.N., and R.P. Burke. 2006. Abundance, biomass and size structure of eastern oyster and hooked mussel on a modular artificial reef in the Rappahannock River, Chesapeake Bay. Appl. Mar. Sci. Oc. Engineering. 390:1-19.

Mackenzie, C.L. 2007. Causes underlying the historical decline in eastern oyster (*Crassostrea virginica* Gmelin, (1791) landings. J. of Shell. Res., 26, 927-938.

Millar, R.H. 1968. Growth lines in the larvae and adults of bivalve mollusks. Nature 217:683.

Moor, B. 1983. Organogenesis. *In*: N.H. Verdonk, J.M. Van den Biggelaar, and A.S. Tompa (eds.). The Mollusca, Vol. 3, Development. Academic Press, New York. Pages 123-177

Mount, A.S., A.P. Wheeler, R.P. Paradkar, and D. Snider. 2004. Hemocyte-mediated shell mineralization in the eastern oyster. Science 304:297-300.
Murphy, D.B, R.S. Kenneth, T.J. Fellers, and M.W. Davidson. 2013. Introduction to Optical Birefringence. Nikon Microscopy U. https://www.microscopyu.com/articles/polarized/birefringenceintro.html
Natural History Museum Rotterdam (NMR). 2013. *Tagelus plebeius*, Brazil Rio de Janeiro NMR 17208. http://www.nmr-pics.nl/Solecurtidae/album/slides/Tagelus%20plebeius.html Last updated January 9, 2013.
Nelson, T.C. 1924. The attachment of oyster larvae. Biol. Bull. 46:143-151.
Newell, R.E. 2004. Ecosystem influences of natural and cultivated populations of suspension of feeding bivalve molluscs: A review. J. of Shell. Res. 23(1):51-61.
Newell SY and C Krambeck. 1995. Responses of bacterioplankton to tidal inundations of a saltmarsh in a flume and adjacent mussel enclosures. J. of Exper. Mar. Biol. and Ecol. 190:79-95.
North, E.W., Z. Schlag, R.R. Hood, M. Li, L. Zhong, T.F. Gross, and V.S. Kennedy. 2008. Vertical swimming behavior influences the dispersal of simulated oyster larvae in a coupled particle-tracking and hydrodynamic model of Chesapeake Bay. Mar. Ecol. Progr. Ser. 359: 99-115.
Odum, W. E. and E. J. Heald. 1972. Trophic analyses of an estuarine mangrove community. Bull. Mar. Sci. 22:671–738.
Parker, R. H. 1959. Macro-invertebrate assemblages of central Texas coastal bays and Laguna Madre. Bull. Amer. Assoc. Pet. Geol. 43:2100-2166.
Perry, M. C., A. M. Wells-Berlin, D. M. Kidwell, and P. C. Osenton. 2007. Temporal changes of populations and trophic relationships of wintering diving ducks in Chesapeake Bay. Waterbirds 30:4–16.
Redding, J.M. and R.L. Cory. 1975. Macroscopic benthic fauna of three tidal creeks adjoining the Rhode River, Maryland. U.S. Geological Survey, Water-Resources investigations 39-75. 23 pp.
Rodney, W.S. and Paynter, K.T. 2006. Comparisons of macrofaunal assemblages on restored and non-restored oyster reefs in mesohaline regions of Chesapeake Bay in Maryland. J. of Exp.Mar. Biol. and Ecol., 335, 39-51.
Rothschild, B.J., Ault, J.S., Goulletquer, P. and Heral, M. 1994. Decline of the Chesapeake Bay oyster population: a century of habitat destruction and overfishing. Mar. Ecol. Prog. Ser., 111, 29-39.
Schmidt, W.J. 1924. Die Bausteine des Tierkorpers in Polarisiertem Lichte. Bonn: Freidrich Cohen.
Sellmer, G.P. 1967. Functional morphology and ecological life history of the gem clam, *Gemma gemma* (Eulamellibranchia: Veneridae). Maclacol. 5:137-233.
Shaw, W.N. 1965. Seasonal setting patterns of five species of bivalves in the Tred Avon River, Maryland. Chesapeake Science 6(1):337-347.
Shumway, S.E. 1996. Natural environmental factors. *In*:The eastern oyster *Crassostrea virginica* V.S. Kennedy, I.E. Newell, and E.F. Eble (eds). Chapter 1. Maryland Sea Grant pp. 467-513.
Sidall, S.E. 1980. Early development of *Mytilopsis leucophaeata* (Bivalvia: Dreissenacea). Veliger 22:378–379.

Spires, J.E. 2015. The exchange of easter oyster (*Crassostrea virginica*) larvae between subpopulations in the Choptank and Little Choptank rivers: Model simulations, the influence of salinity, and implications for restoration. M.S. Thesis. University of Maryland Center for Environmental Science.

Sundberg, K., and V.S. Kennedy. 1992. Growth and development in larval and post-metamorphic *Rangia cuneata* (Sowerby, 1831). J. Shell. Res. 11:9-12.

Sundberg K., and V.S. Kennedy, V.S. 1993. Larval Settlement of Atlantic Rangia, Rangia cuneata Bivalvia: Mactridae). Estuaries 16(2): 223-228.

Tenore, K.R. 1972. Macrobenthos of the Pamlico River estuary, North Carolina. Ecol. Monogr. 42:51-69.

Tiwari, S., and S. Gallager. 2003. Machine learning and multiscale methods in the identification of bivalve larvae. Proceedings of the Ninth IEEE International Conference on Computer Vision, Nice, France, October 14-17, 2003.

Thompson, C.M., M.P. Hare and S.M. Gallager. 2012. Semi-automated image analysis for the identification of bivalve larvae from a Cape Cod estuary. Limnol. Oceanogr. Methods 10:538-554.

Vazquez NN, Ituarte C, Navone GT, Cremonte F. 2006. Parasites of the stout razor clam *Tagelus plebeius* (Psemmobiidae) from the southwestern Atlantic Ocean. J. Shell. Res. 25:877-886.

Verween, A., M., V. J. Mees, and S. Degraer. 2005. Seasonal variability of *Mytilopsis leucophaeata* larvae in the harbour of Antwerp: implications for ecologically and economically sound biofouling control. Belg. J. Zool 135(1):91-93.

Verween, A., M. Vincx, and S. Degraer. 2007. The effect of temperature and salinity of *Mytilopsis leucophaeata* larvae (Mollusca, Bivalvia): The search for environmental limits. 38:11-120.

Waller, L.M. 1996. In: The population dynamics of the Clam *Macoma mitchelli* and its potential as a bioindicator in the Neuse River Estuary, North Carolina. North Carolina State University. 1996.140 pp.

Wada, K. 1972. Nucleation and growth of aragonite crystals in the nacre of some bivalve molluscs. Biomineralisation 4:141-159.

Weiss, I.M., N. Tuross, L. Addadi, and S. Weiner. 2002. Mollusc larval shell formation: amorphous calcium carbonate is a precursor phase for aragonite. Exper. Zool. 293:478-491.

Wells, H.W. 1961. Fauna of oyster beds, with special reference to salinity factor. Ecol. Monographs, 31, 239-266.

Whitelaw, D. M., and R. N. Zajac. 2002. Assessment of prey availability for diamond back terrapins in a Connecticut salt marsh. Northeast. Naturalist 9(4):407-418.

Wilberg, M.J., M.E. Livings, J.S. Barkman, J.M. Robinson, and B.T. Morris. 2011. Overfishing, disease, habitat loss, and potential extirpation of oysters in upper Chesapeake Bay. Mar. Ecol. Prog. Ser. 436: 131-144.

Tables and figures

Table 1.1. Spawning conditions for seven species of bivalves that are found in the mesohaline region of the Choptank River. All species except for *C. virginica* and *G. demissa* were successfully spawned and reared in laboratory conditions of ~23 ^{o}C and salinities between 11-13. The larval development times for all bivalves was observed in the laboratory for all species except *C. virginica* (HPL hatchery) and *G. demissa* (Rutgers hatchery).

Scientific name	**Spawning temperature** ^{o}C	**Larval salinity tolerance**	**Larval development time in lab (days)**	**Spawning time**
Crassostrea virginica	28-30 (Shumway et al. 1996)	5-27 (Shumway et al. 1996)	16	Summer to fall (Kennedy 1996)
Macoma mitchelli	26-30 (Kennedy et al. 1989)	5–18 (Kennedy et al. 1989)	7	Year round (Blundon and Kennedy 1982)
Mytilopsis leucophaeata	30 (Kennedy 2011b)	0.5-18 (Kennedy 2011b)	13	Summer to fall (Kennedy 2011a)
Mulinia lateralis	28-30 (Calabrese and Rhodes 1974)	7.5-37.5 (Calabrese and Rhodes 1974)	13	May-Oct (Calabrese 1969)
Rangia cuneata	30 (Sundberg and Kennedy 1992)	<15 (Sundberg and Kennedy 1992)	8	Late spring to early fall (Sundberg and Kennedy 1993)
Tagelus plebeius	30-32 (Chanley and Castagna 1971)	10-30 (Chanley and Castagna 1971)	13	June-Nov (Chanley and Castagna 1971)
Guekensia demissa	27 (Rutgers hatchery unpub)	12 -22.5 (Rutgers hatchery unpub)	7-21	Early summer to fall (Borrero 1987)
Ischadium recurvum	25-30 (Chanley 1970)	20 (Chanley 1970)	14	June-Nov (Chanley 1970)

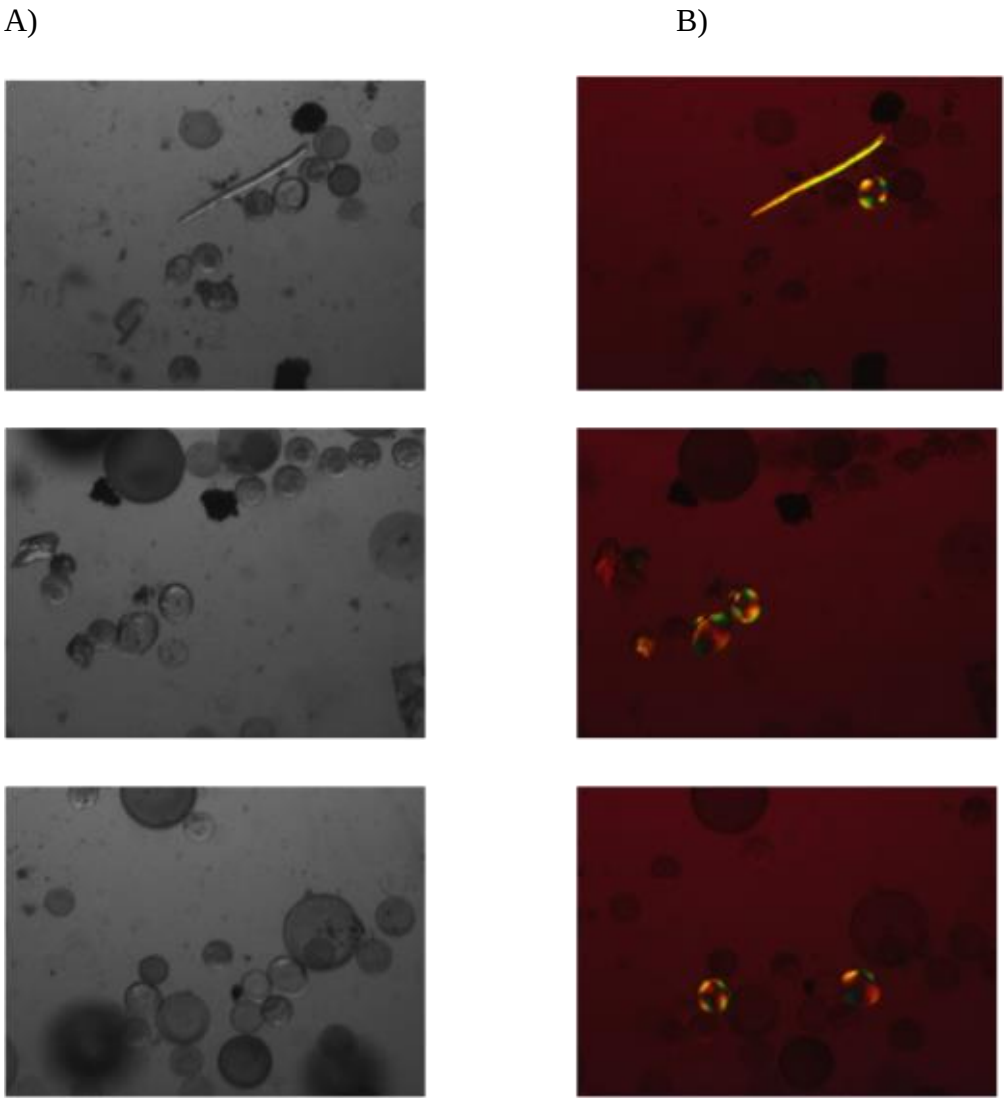

Fig. 1.1. Three images of field samples under A) regular light and B) cross polarized light with a full wave compensation (λ) plate. Bivalve larvae from panel B can be distinguished to the species level using pattern recognition software

A) B) C)

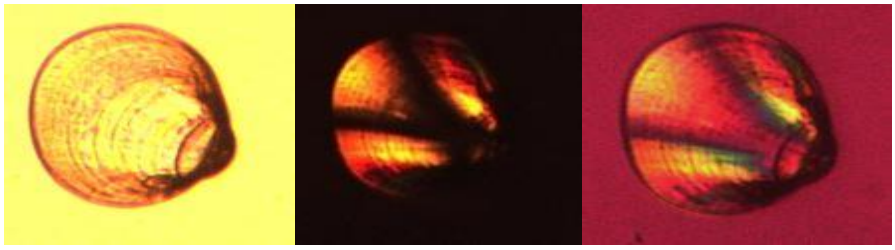

Fig. 1.2. Two 11 day old *C. virginica* captured at 20x magnification under a) standard light, b) polarized light, and c) polarized light with a full wave (λ) compensation plate.

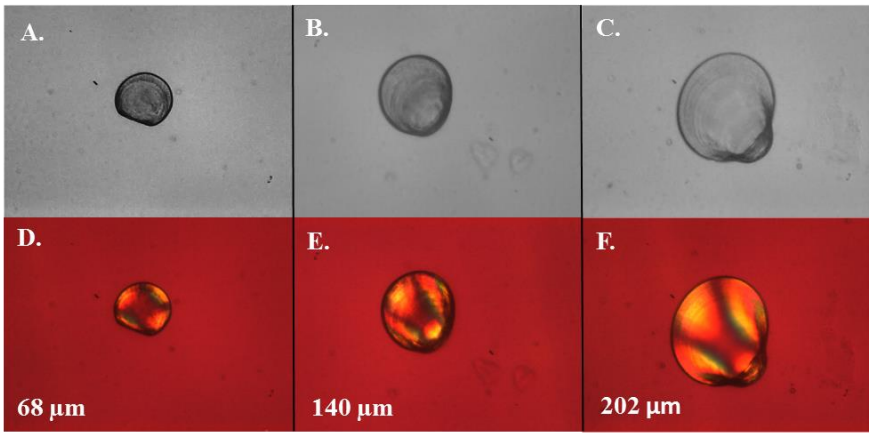

Fig. 1.3. Images of *C. virginica* larvae captured under A-C) standard and D-F) polarized light at a magnification of 7x. Larvae are A,D) 2-d, B,E) 6-d, and C,F)12-d old. Shell heights are listed in panels D-F.

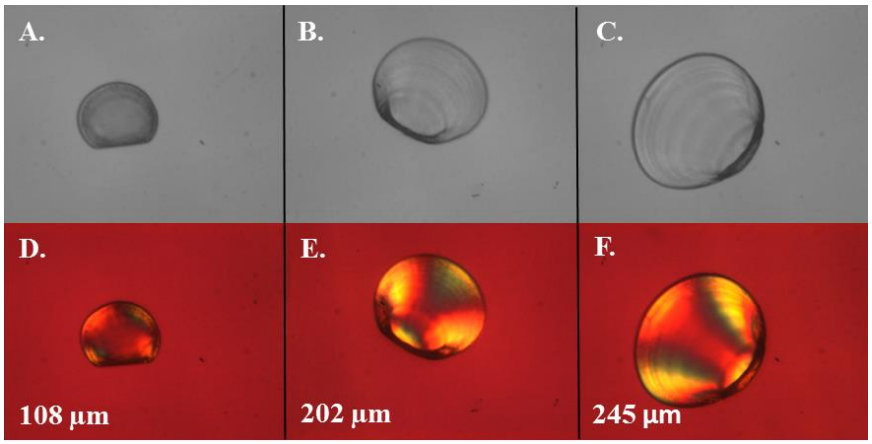

Fig. 1.4. Images of *I. recurvum* larvae captured under A-C) standard and D-F) polarized light at a magnification of 7x. Larvae are A,D) 3-d, B,E) 7-d, and C,F)13-d old. Shell heights are listed in panels D-F.

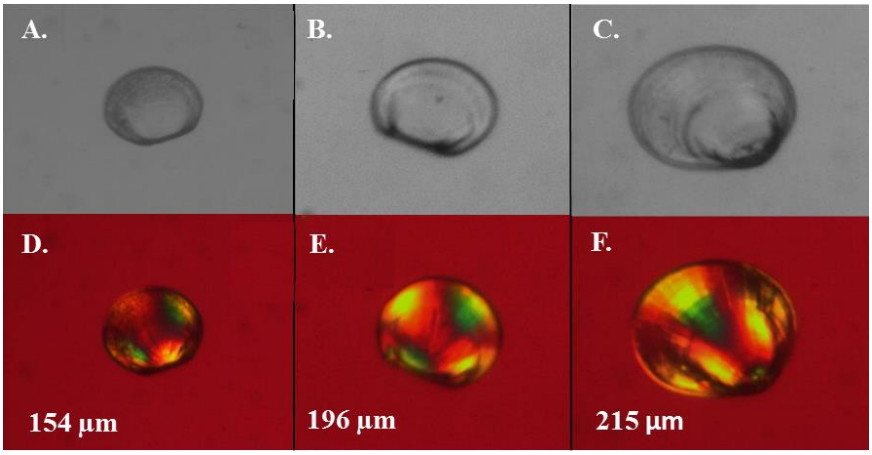

Fig. 1.5. Images of *G. demissa* larvae captured under A-C) standard and D-F) polarized light at a magnification of 7x. Larvae are A,D) 3-d, B,E) 6-d, and C,F)13-d old. Shell heights are listed in panels D-F.

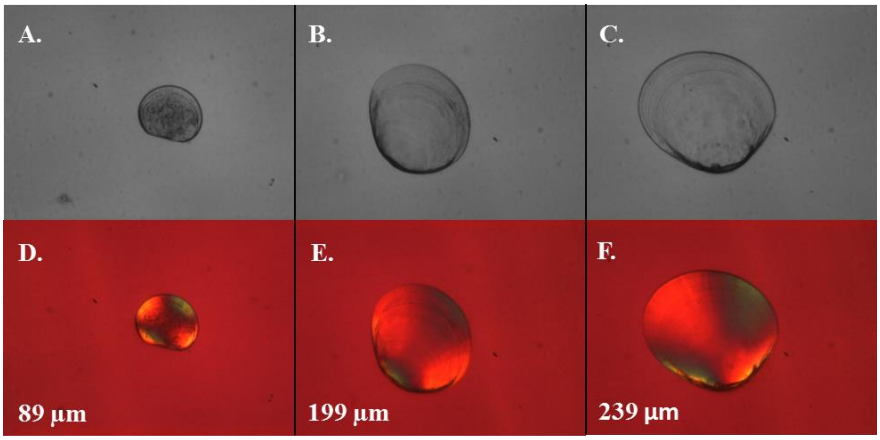

Fig. 1.6. Images of *M. mitchelli* larvae captured under A-C) standard and D-F) polarized light at a magnification of 7x. Larvae are A,D) 2-d, B,E) 8-d, and C,F)10-d old. Shell heights are listed in panels D-F.

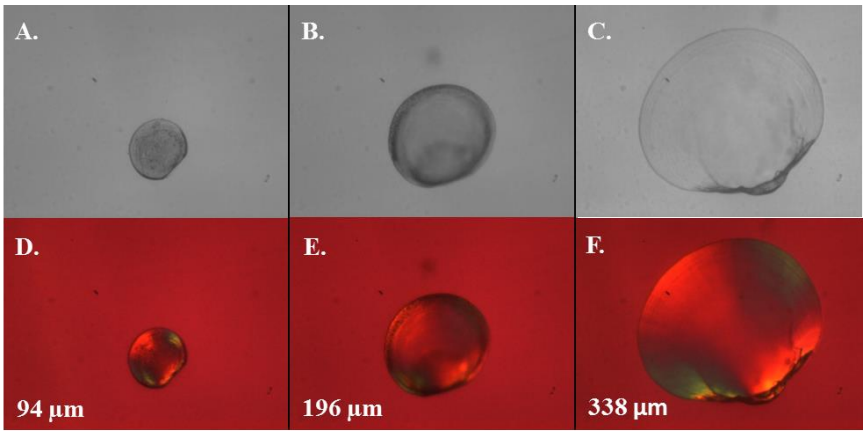

Fig. 1.7. Images of *M. lateralis* larvae captured under A-C) standard and D-F) polarized light at a magnification of 7x. Larvae are A,D) 4-d, B,E) 10-d, and C,F)13-d old. Shell heights are listed in panels D-F.

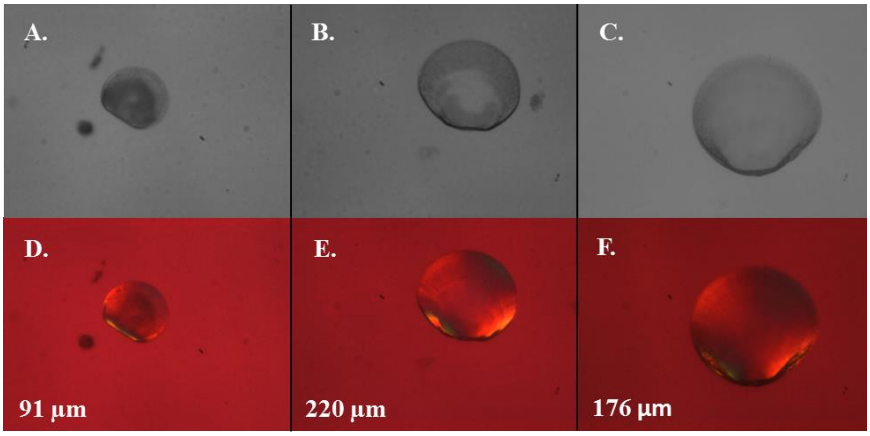

Fig. 1.8. Images of *M. leucophaeata* larvae captured under A-C) standard and D-F) polarized light at a magnification of 7x. Larvae are A,D) 2-d, B,E) 6-d, and C,F)8-d old. Shell heights are listed in panels D-F.

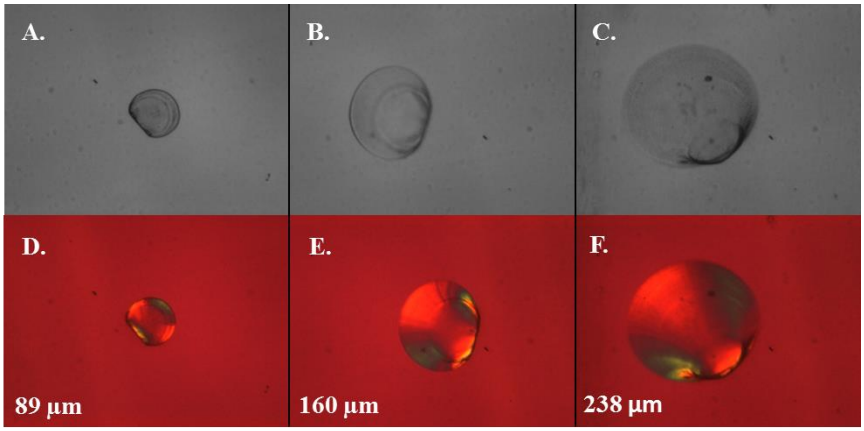

Fig. 1.9. Images of *R. cuneata* larvae captured under A-C) standard and D-F) polarized light at a magnification of 7x. Larvae are A,D) 2-d, B,E) 4-d, and C,F)8-d old. Shell heights are listed in panels D-F.

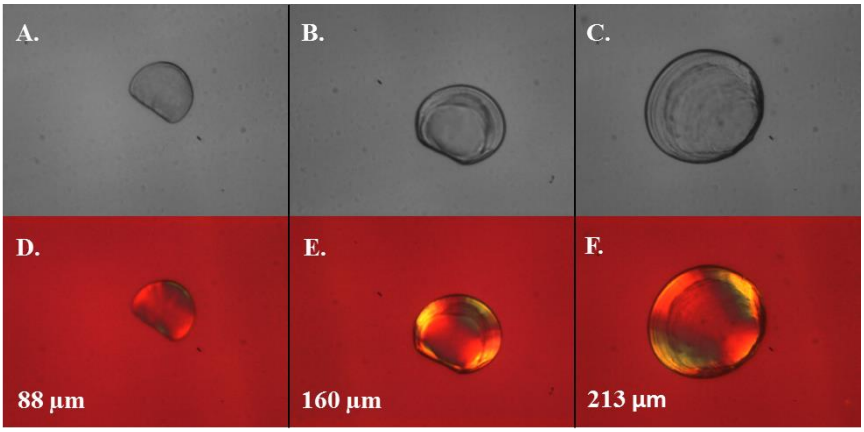

Fig. 1.10. Images of *T. pleibeius* larvae captured under A-C) standard and D-F) polarized light at a magnification of 7x. Larvae are A,D) 2-d, B,E) 4-d, and C,F) 8-d old. Shell heights are listed in panels D-F.

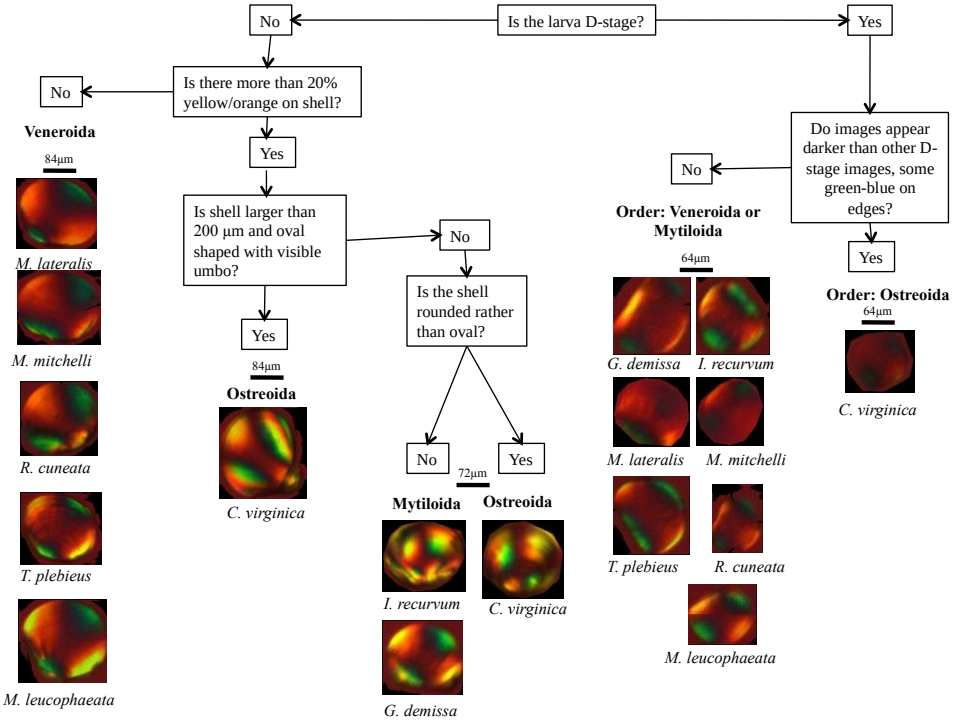

Fig. 1.11 Larval identification key based on shell birefringence, size, and morphology. Size bars correspond with images underneath them.

Chapter 2: Evaluating and improving a semi-automated image analysis technique for identifying bivalve larvae[1]

Abstract

Knowledge of the distribution, abundance, and transport of bivalve larvae is limited due to their small size, similar morphologies between species, and lack of an automated approach for identification. The objective of this research is to evaluate and improve the accuracy of ShellBi, a novel supervised image classification method that uses birefringence patterns on the shells of bivalve larvae under polarized light to identify species. The performance of the ShellBi method was tested by rearing *Crassostrea virginica* (eastern oyster) larvae at different temperatures (21.3 and 27.5 ^{o}C) and salinities (10.3, 14.1, 14.4, and 20.5). Differences in rearing temperatures resulted in differences in classification accuracy, as did large variations in salinity (≥10 units). Classification accuracies increased from 67-88% to 97-99% when training sets included images of larvae reared in conditions similar to those of the larvae being classified. Additional tests indicate that misclassification rates ranged from 0 to 13% for false positives and from 0 to 22% for false negatives, depending on the proportion of oyster larvae in the sample. Results suggest that this technique could be applied to field samples with high accuracy as long as the images that are used to make classifications include larvae that were reared in conditions that are similar to those *in situ*. In addition, these findings demonstrate that the ShellBi method can be

[1] Published: Goodwin, J.D., E.W. North, and C.M. Thompson. 2014. Evaluating and improving a semi-automated image analysis technique for identifying bivalve larvae. Limnology and Oceanography Methods 12:548-562.

used to measure and identify bivalve larvae in a different system than the one for which it was developed, suggesting that the method has broad applicability in marine and estuarine systems.

Introduction

Understanding dispersal pathways and connectivity is important for effective fisheries management strategies (Fogarty and Botsford 2007). The larval stage of bivalves is the least understood aspect of their life history, but it is important to understand because it is the stage during which dispersal takes place, which in turn influences population connectivity and gene flow (Kennedy et al. 1996, Pineda et al. 2007, Dame 2012, Munroe et al. 2012). Species identification is important for understanding dispersal and its effect on the population connectivity of bivalves because larvae of different species can exhibit variations in behavior that may result in large divergences in transport (Shanks and Brink 2005, North et al. 2008). However, studies of bivalve larvae are difficult to conduct because of identification challenges, small sizes of individuals, high mortality rates, and spatial patchiness (Boicourt 1988, Garland and Zimmer 2002).

Many identification techniques of bivalve larvae are too time consuming or expensive to apply when conducting sampling on a large scale. Accordingly, specific pros and cons of identification techniques of bivalve larvae are reviewed in Garland and Zimmer (2002), Hendriks et al. (2005), and Thompson et al. (2012a). Identification can involve time-consuming methods that rely on morphological differences (Loosanoff et al. 1966, Chanley and Andrews 1971, Lutz et al. 1982).

More rapid molecular techniques include multiplex PCR (Hare et al. 2000), quantitative PCR (Wight et al. 2009) and fluorescent *in situ* hybridization with DNA probes (Henzler et al. 2010). Although quantitative PCR can provide some insight into the quantity of bivalve larvae, it does not provide information on the sizes of those larvae. Furthermore, these methods can have high costs and limitations on sample volume.

An alternative method for rapid identification is ShellBi. ShellBi can be an accurate, cost effective, and rapid approach for identifying and measuring bivalve larval shells once the initial effort to prepare this technique for use in a new system is complete. ShellBi is a semi-automated image-processing approach that uses birefringence patterns on the shells of larvae that appear when subjected to polarized light (Twari and Gallager 2003a, 2003b, Gallager and Tiwari 2008, United States Patent #7415136, Thompson et al. 2012a). Under polarized light, color and texture-based features are extracted from digital images of the larval shells by pattern recognition software. The algorithm used in this work, a Support Vector Machine (SVM), generates decision boundaries that maximize differences between labeled categories (training images) and then applies the decision boundaries to classify new observations into those categories. For the ShellBi method, the categories are defined as groups of images of larval shells from known bivalve species (called 'training sets') and the observations are images of shells that need to be identified (called 'unknown sets'). In short, the classifier (the SVM) uses color and texture-based features from the training set images to identify images of larval shells in the unknown set (Twari and Gallager 2003a, 2003b,Thompson et al. 2012a).

Thompson et al. (2012a) validated the ShellBi method with DNA and visual classification methods and improved it showing 98% identification accuracy for four hatchery-reared species *Argopecten irradians* (bay scallop), *Crassostrea virginica* (eastern oyster), *Mercenaria mercenaria* (quahog), and *Mya arenaria* (soft-shell clam). However, the species featured in their hatchery-reared training sets represented a simplified sample relative to field-caught larvae and larvae *in-situ* may have had different growth rates due to environmental heterogeneities (Thompson et al. 2012a). Therefore, although obtained accuracies are high for identifying larvae reared in the hatchery, the effect of different growth conditions on shell formation between larvae reared in the hatchery and in the field may cause drops in accuracy. Therefore, improvements to the ShellBi method are needed when applied to field samples.

The overall objective of this research was to evaluate the use of the ShellBi method for identifying *C. virginica* bivalve larvae in the Choptank River, a tributary of Chesapeake Bay in Maryland. Initially ShellBi was tested using bivalve species native to Cape Cod, Massachusetts and found in Waquoit Bay (Tiwari and Gallager 2003b, Thompson et al. 2012a). The bivalve species and physical characteristics of the mesohaline Choptank River differ from Waquoit Bay. Salinities near the surface of the Choptank River during the spawning season of oysters (May-October) are 0 to 14 and temperatures range from 17 to 27 ^{o}C (MDNR 2012). In contrast, Waquoit Bay water temperatures during May-October are 13 to 26 ^{o}C and salinities range from 28 to 32 (Thompson et al. 2012b). In addition to the overall objective of testing the ShellBi technique in a different system, the three specific objectives that guided this research were to: 1) determine the influence of growth conditions on classification

accuracy, 2) evaluate the influence of training set composition on classification accuracy, and 3) estimate misclassification rates of this method when applied to distinguish *C. virginica* larvae from other bivalve species found in the Choptank River.

Materials and procedures

Six bivalve species that are found in the Choptank River were spawned, their larvae were reared, and images of their shells were used to create training sets (Fig. 2.1). In addition, *C. virginica* larvae were reared in different growth conditions and imaged. A series of classification tests were conducted with the training sets and *C. virginica* images. Methods for spawning, rearing, imaging, and classifying larvae are described in this section.

Spawning and rearing bivalve larvae from the Choptank River

Six species of bivalve larvae were reared to obtain images for training sets: *C. virginica* (the target organism) and five other species that are abundant in the plankton along the mesohaline portion of Chesapeake Bay (Table 2.1). Adult specimens of the five species, *Ischadium recurvum* (hooked mussel), *Mulinia lateralis* (dwarf surf clam), *Mytilopsis leucophaeata* (dark false mussel), *Rangia cuneata* (Atlantic rangia) and *Tagelus plebeius* (razor clam) were collected from Choptank River field sites and brought to lab for spawning in 2009, 2010, 2011, and 2012. Some specimens of *M. lateralis* also were collected from the Corsica River (a tributary of Chesapeake Bay that is north of the Choptank River). Temperature

fluctuation and strip spawning techniques were used to induce spawning (Chanley 1970, Kennedy et al. 1989). Larvae were raised at room temperature 23.0 +/- 0.5 ^{o}C (n=30) (here and henceforth numbers after '+/-' are the standard deviation) and fed fresh *Isochrysis galbana* and *Thalassiosira pseodonana* (for D-stage and veliger larvae) and *Tetraselmis chui* (for pediveliger larvae). A subset of larvae was preserved in 80% ethanol buffered with sodium borate every two days from prodissoconch 1 through pediveliger stages so that different age/size classes for each species could be incorporated into training sets. The fixative was buffered to a target pH of 8.0 in order to inhibit dissolution of larval shells (Thompson, pers. obs.).

In 2009, 2010, and 2011, multiple ages of *C. virginica* larvae (2-, 4-, 6-, 8-, 10-, 12-, 14- and 16-days old) were obtained from the Horn Point Oyster Hatchery where they had been reared at an average temperature of 25.9 +/- 1.5 ^{o}C (n=30) and average salinity of 10.3 +/- 0.9 (n=30). These hatchery-reared *C. virginica* larvae were fed *Isochrysis galbana* and *Thalassiosira pseodonana* as D-stage larvae. For veliger stages, *Chaetoceros mulleri* was added. Pediveligers were fed *Tetraselmis chui* plus *Chaetoceros mulleri*. Algal concentrations averaged 5.7 x 10^{4} cells ml^{-1} over the duration of the larval stages for hatchery-reared larvae. Larvae of *C. virginica* from 2009 were preserved in 80% ethanol buffered with sodium borate (Thompson et al. 2012a), larvae from 2010 and 2011 were preserved in 4% formalin buffered with sodium borate because larval shells stored in buffered ethanol began to crack after 2 years (Thompson and Goodwin, pers. obs.). The preservative used to store larvae (formalin vs. ethanol) did not interfere with the ability of ShellBi to classify bivalve larvae (Table S2.1).

In 2011, 1-day old D-stage *C. virginica* larvae were obtained from the hatchery and were reared at a mean temperature of 22.3 +/- 0.4 ^{o}C (n=30) and mean salinity of 11.5 +/- 0.3 (n=30). Larvae were fed live cultures of *Isochrysis galbana* and *Thalassiosira pseodonana* (fed to D-stage and veliger larvae) and *Tetraselmis chui* (fed to pediveliger larvae) at an average concentration of 5.7 x 10^4 cells ml^{-1}. Subsets of larvae were preserved in 4% formalin buffered with sodium borate every two days up to day 20.

Rearing *C. virginica* larvae in different growth conditions

Larvae of *C. virginica* were reared at different temperatures, salinities, and food concentrations (parameters known to affect growth (Kennedy et al. 1996)) to investigate how different growth conditions affect the classification accuracy of the ShellBi method.

Newly spawned *C. virginica* were obtained from Horn Point Oyster Hatchery and placed in 3-L glass rearing chambers within two temperature-controlled rooms. Water was collected from three sites within the Choptank River system (Tred Avon River, Harris Creek, and Choptank River at the Horn Point dock), and an external site (Chincoteague Bay) on the eastern shore of Maryland. Water was filtered to 1 µm in the field using a battery-operated pump (JABSCO model 50840-0012) and polypropylene cartridge system. Prior to rearing the larvae, salinity was adjusted to provide a range of salinities that reflect conditions *in-situ* in Chesapeake Bay. Salinity of the water collected at the Horn Point dock was raised to 10.3 and waters from the Tred Avon and Harris Creek were raised to 14.1 and 14.4, respectively, using Crystal Sea Marinemix (Marine Enterprises, Inc.). The salinity of the Chincoteague Bay

water was lowered to 20.5 using deionized (DI) water. Before starting this experiment, the water was filtered to 1 µm a second time.

The average water temperatures in the temperature-controlled rooms were 21.3 +/- 1.0 ^{o}C (n=48) and 27.5 +/- 0.6 ^{o}C (n=67). Each room contained 8 rearing chambers that held four salinity treatments (10.3 +/- 0.7 (n=58), 14.1 +/- 0.7 (n=63), 14.4 +/- 0.6 (n=53), and 20.5 +/-1.0 (n=44)) using two chambers and two levels of food concentrations (high and low) within each salinity treatment. The concentration of algae fed to the larvae was based on the concentration of larvae in the containers (Helm et al. 2004), with low food treatments fed half the concentrations of the high food treatments. The ratio of larvae to algae in the high food treatments was on average 1:1.6x10^{4}, with the objective that the larvae would be fed to satiation. The average concentration of algae in the high and low food treatments were 9.2x10^{4} cells ml^{-1} and 7.9x10^{3} cells ml^{-1}, respectively. Algae were obtained from the Horn Point Oyster Hatchery and were composed of live cultures of *Isochrysis galbana* and *Thalassiosira pseodonana* (fed to D-stage and veliger larvae) and *Tetraselmis chui* (fed to pediveliger larvae). Subsets of larvae were preserved in 4% formalin buffered with sodium borate every 2, 4, 6, 8, 12 and 14 days in the warm chambers. In the cool conditions larvae took longer to develop to the pediveliger stage and were preserved every two days up to day 20.

Image acquisition for training and unknown sets

Images of all larval shells were taken by an Infinity 2.3C digital 8 megapixel camera mounted on a custom-built compound microscope fitted with a polarization filter and full wave compensation plate (λ). Larvae were first soaked in 40% bleach

and 60% DI water buffered with sodium borate (hereafter referred to as buffered DI water) for a period of 15 minutes to remove tissue and break apart the valves of the shells. The larval shells were then sieved and rinsed with buffered DI water onto a Sedgewick Rafter slide. Digital images of individual shells were taken under 50x magnification at a resolution of 96 dpi. The microscope stage was moved manually or with a joystick attached to an automated stage to image one shell after another. Images were captured with shells at random orientations. A 12V 100W incandescent microscope bulb was used as a light source. Lumenera Analyze software (version 5.0.3 Lumenera Corporation) was used in conjunction with the digital camera to capture JPEG images. Settings on the software were adjusted so that they matched background color and cross polarization pattern as suggested in Thompson et al. (2012a) and kept constant between images. Major background color differences occurred throughout the day when a metal bracket was used for the full wave compensation plate which was near the light source of the microscope. Because these differences affected classification accuracies (results not shown), a plastic housing was used for the wave compensation plate to prevent background color drift.

To create a species category within a training set, 250 images of individual shells were selected for each species so that the images spanned the range of stages and sizes of the larvae (prodissoconch-1 through pediveliger). Thompson et al. (2012a) found that at least 200 images should be used in a training set. Training sets were composed of different numbers of species. For example, a 6-species training set included 250 images of *C. virginica, I. recurvum, M. lateralis, M. leucophaeata, R. cuneata* and *T. plebeius* for a total of 1,500 images. All training sets were balanced:

each species category had an equal quantity of images (250) with similar age representations of bivalve larvae.

Images of *C. virginica* shells from the experiment were used as unknown sets. The same imaging procedures that were used for the training sets were also used for *C. virginica* larvae reared in the growth experiment. There were 3,288 images of larvae captured from the experiment. Those images were used to represent warm and cool conditions as well as four different salinity treatments.

Images were pre-processed prior to classification so that each larval shell, a region of interest (ROI), was defined and distinguished from its background (Thompson et al. 2012a) using MATLAB (version R2009a, Mathworks Inc.) and its image Processing Toolbox (version 6.3, Mathworks Inc.). The pre-processing (i.e., cropping) was performed using an automated ROI masking routine in MATLAB (Thompson et al. 2012a).

Image classification and analysis

Image classification was accomplished by extracting features from training sets, cross validating the training sets, extracting features from unknown images, and using the training features to classify unknown images (Thompson et al. 2012a). All images were processed using the Bivalve Larval Identification (BivLID) software implemented in MATLAB by C. Thompson based on algorithms used in Tiwari and Gallager (2003b) and Thompson et al. (2012a). Training set feature extraction and cross-validation were conducted before the classification of unknown images. The feature extraction process calculated 1,104 Gabor texture features and 9 color-angle features for each image. A Principle Component Analysis (PCA) was then conducted

using the Gabor texture features and color angles to isolate the 25 Gabor features that encompassed the most variability in the training set and to remove redundancy and noise (Zhao et al. 2010, Thompson et al. 2012a). After extracting and transforming features from the training set and unknown images, a Support Vector Machine (SVM) in BivLID was used for cross-validation and classification (Cawley 2000, http://theoval.cmp.uea.ac.uk/svm/toolbox/).

A leave-one-out cross validation procedure (LOO, Fukunaga and Hummels 1989) was run to assess performance of the training sets. This procedure left out one image from the training set, used features from the remaining images to classify the left-out image, and repeated this for all images to calculate cross validation accuracy for each category. Classification tests were also conducted. To classify an image, the SVM mapped the same features from the unknown image to the decision boundaries created with the training set using a one-to-one approach for each category (Lou et al. 2003). An "other" category was created so unknown images would not be classified as false positives, i.e. forced into a training set category to which they were not closely related (Davis et al. 2004). The output of the program indicates how many unknown images were classified into each training set category and the "other" category.

Larval shells were measured and statistical tests were performed to compare shell heights. To accomplish this, a script was created in MATLAB (version R2009b, Mathworks Inc.) to measure the maximum axis of a masked ROI of a larval shell as a measure of shell height. Non parametric statistical tests were conducted because shell heights in all treatments were not normally distributed (Shapiro-Wilk, $\alpha = 0.05$, p

<0.01). Shell heights of *C. virginica* in the high and low food treatments were paired by salinity and temperature treatments for an even comparison (Sokal and Rohlf 1987). Median shell heights were not significantly different between larvae reared in high (95.9 μm, n=177) and low (91.0 μm, n=177) food treatments (Wilcoxon rank sum = 32750, Z = 1.39, p<0.17, n=354). Therefore images from high and low food treatments were pooled within each salinity and temperature treatment in further analyses. To determine if there was a difference in median shell heights between warm and cool treatments, a Wilcoxon rank sum test was employed with data pooled across salinity treatments. A Kruskal-Wallis one-way analysis of variance by ranks was used to test for differences in median shell heights between salinity treatments. After conducting the Kruskal-Wallis test, intergroup comparisons between salinity treatments were made using Mann-Whitley U tests. A Bonferroni adjustment was used to reduce type I error so that the p-value for significance was set to 0.008 (Bland and Altman 1995). The number of larvae reared in warm and cool conditions was similarly represented across salinity treatments and therefore did not bias larval growth across salinity treatments for these tests. All statistical tests were performed using MATLAB (version R2012a, Mathworks Inc.).

Assessment

Tests were conducted to evaluate the influence of growth conditions on the classification accuracy of the ShellBi method, to determine the influence of training set composition on classification accuracy, and to estimate misclassification rates. A leave-one-out (Fukunaga and Hummels 1989) cross validation resulted in high cross

validation classification accuracies (>90.8%) for all training sets except for a 6-species training set (74.7%) (Table S2.2).

The influence of growth conditions on classification accuracy

The effect of temperature on classification accuracy of a hatchery composed training set was tested using two training sets that contained *C. virginica* reared in warm conditions (a 3-species training set composed of 250 images each of *C. virginica*, *M. lateralis*, and *R. cuneata* and a 4-species training set that also included 250 images of *T. plebeius*). For both training sets, *C. virginica* larvae were reared in the hatchery at an average temperature of 25.9 +/- 1.5 ^{o}C (n=30). The other species were reared in our laboratory at room temperature 23.0 +/- 0.5 ^{o}C (n=30). The training sets contained images of larvae at similar age ranges (2-14 days old).

The 3- and 4-species training sets were used to conduct four classification tests in which the training sets remained the same and the "unknown" images of *C. virginica* shells from the experiment were varied. The two test sets were comprised of images of larvae reared in 1) the warm (27.5 +/-1.0 ^{o}C, n=67) treatment, 2) and the cool (21.3 +/- 1.0 ^{o}C, n=48) treatment. Each of these unknown sets included images of larval shells grown at all salinity levels and age ranges between 2-20 days old. The temperatures at which larvae were reared significantly influenced growth of the two treatments: larvae reared in cooler treatments had shorter median shell heights (77.0 μm, n=365) than those reared in warm conditions (88.8 μm, n=365) (Wilcoxon rank sum: 97903, Z=-12.7, $p<0.01$, n=730). The median shell height of larvae from the warm treatment was shorter, but not significantly, than the median shell height of the hatchery-reared *C. virginica* larvae in the training sets (114 μm, n=916) (Wilcoxon

rank sum: 107222, Z=-0.88, p=0.39). On average, the accuracy of ShellBi for identifying *C. virginica* reared in the warm treatment was ~20% higher than the accuracy for identifying *C. virginica* reared in the cool treatment using 3-species and 4-species training sets (Fig. 2.2). In other words, the classification accuracy for *C. virginica* was highest when the temperature at which larvae in the unknown set were reared was similar to that of the training sets.

An additional analysis was conducted to test the effect of rearing temperature on classification accuracy using another training set composed of larvae reared in cool conditions. In this case, the training set was composed 250 images of each species reared in similar cool temperature conditions, *C. virginica* (22.3 +/- 1.2 ^{o}C, n=58), and *Rangia cuneata* and *Mulinea lateralis* (23.0 +/- 0.5 ^{o}C, n=30). This training set was used to classify *C. virginica* larvae from two treatments 1) warm (27.5 ^{o}C, n = 1,624) and 2) cool (21.3 ^{o}C, n=1,664). The accuracy for identifying larvae from the cool treatment was 25% higher (91.0%) than the classification accuracy for larvae from warm treatment (66.0%) (Fig. 2.2). Because shell heights differed between larvae grown in warm and cool conditions and because of the strong influence of temperature on classification accuracies, it is concluded that differences in temperature-dependent growth conditions between training sets and unknown sets influence the classification accuracy of the ShellBi method.

In addition to temperature, the effect of salinity on classification accuracy was tested using 3-species training sets composed of *C. virginica*, *R. cuneata* and *I. recurvum*. The *C. virginica* used in the training sets and for the unknown sets were reared in the experiment at four salinities (10.3, 14.1, 14.4 and 20.5) and were pooled

across temperatures. The images of *C. virginica* reared at the four salinities were used to create four different 3-species training sets. In addition to 250 images of *C. virginica*, each training set also had 250 images of *R. cuneata* and *I. recurvum* (reared in a salinity of 11.3). Each of the four training sets were then used to classify four unknown sets of 250 different *C. virginica* images from each of the three other salinity treatments. For example, the training set with *C. virginica* larvae raised in salinity of 10.3 was used to classify larvae from the three other treatments (14.1, 14.4, and 20.5). A total of 12 tests were conducted. High classification accuracies (>95%) occurred when training sets with larvae from low salinity treatments (10.3, 14.1, and 14.4) were used to identify "unknown" *C. virginica* larvae reared in the same low salinity treatments (Fig. 2.3). Accuracy dropped by 10% when these training sets were used to classify larvae raised in the higher salinity treatment (20.5) (Fig. 2.3). Training sets with larvae raised in the high salinity treatment (20.5) classified "unknown" larvae from the three lower salinity treatments with >95% accuracy.

Shell height increased with increasing salinity. Median shell heights in treatments (n=250 for each treatment) with salinities of 10.3, 14.1, 14.4 and 20.5 were 76.1 μm, 80.0 μm, 83.9 μm, and 98.3 μm, respectively. Shell heights were significantly different between the four treatments (Kruskal-Wallis test, df=999, $p<0.01$). Post-hoc pairwise comparisons were made using Mann-Whitney U tests. Salinity treatments were significantly different ($p<0.008$, df=499), except for salinity treatments 14.1 and 14.4 ($p=0.13$, df = 499). Based on this and the results of the classification tests above, it is concluded that large (10 unit) differences in salinity-

dependent growth conditions between training sets and unknown sets influence the classification accuracy of ShellBi.

The influence of training set composition on classification accuracy

Three tests were conducted to determine if the composition of images in a training set influenced classification accuracy. (1) The first examined how changing the larval stage (D-stage versus veliger) within the *C. virginica* portion of the training set altered classification accuracy. (2) The second test was designed to identify how the number of categories in a training set influenced classification accuracy. (3) A third test was conducted to determine if increasing variation of growth conditions of larvae in the *C. virginica* portion of the training set affected classification accuracy.

(1) Larval images were broken down into two groups 1) D-stage larvae (comprised of larvae between 2-3 days old), and 2) veliger larvae (comprised of larvae between 6-20 days old). Two training sets composed of *C. virginica*, *M. lateralis and T. plebeius* were created. All training sets contained the same images of *M. lateralis* and *T. plebeius*. Images in the *C. virginica* category were varied to form the two training sets that were comprised of 1) images of D-stage larvae raised in the hatchery, and 2) images of veliger larvae raised in the hatchery. These training sets were used to classify unknown sets that were comprised of *C. virginica* images of 1) D-stage larvae from the hatchery, 2) D-stage larvae from the experiment, 3) veliger larvae from the hatchery, and 4) veliger larvae from the experiment. Results indicate that training sets containing images of D-stage *C. virginica* larvae classified "unknown" D-stage and "unknown" *C. virginica* veliger images with high accuracies (>98%). Training sets comprised of images of *C. virginica* veliger larvae and used to

classify “unknown” D-stage *C. virginica* images had low accuracies (<29%). Based on these results, it is concluded that a training set should contain images of both D-stage and veliger larvae.

(2) Classification tests were conducted using training sets with various numbers of categories and the same set of unknown larvae. Images of *C. virginica, I. recurvum, T. plebeius, R. cuneata, M. lateralis* and *M. leucophaeata* larvae were used to create nine 3-species training sets, seven 4-species training sets, five 5-species training sets and one 6-species training set. These training sets were used to classify one unknown set comprised of *C. virginica* larvae from the warm and cool treatments of the experiment (n=998). Results comparing the number of categories in a training set indicated that mean accuracies were 82% for 3-species categories (n=9), 75% for 4-species categories (n=7), 70% for 5-species categories (n=5), and 67% for 6-species categories (n=1) (Table 2.2). When the number of training set categories increased from 3 to 6, the accuracy of ShellBi dropped on average by 17% (Fig. 2.4). Within the 3-, 4-, and 5-species category training sets, classification accuracies varied by as much as 30% depending on which species combinations were used for each training set (Table 2.2). When the 6 species training set was grouped into a 3-category training set based on taxonomic order [1: Ostreoida, oysters (*C. virginica*), 2: Veneroida, clams (*M. lateralis, M. leucophaeata, R. cuneata, T. plebeius*), 3: Mytiloida, mussels (*I. recurvum*)], classification accuracy improved compared to the 6-species training set, from 66.8% to 87.8%. Therefore the number of categories in a training set and the species composition within them are important factors that affect the classification accuracy of *C. virginica* using the ShellBi approach.

(3) Four training sets composed of *C. virginica*, *M. lateralis* and *T. plebeius* (250 images for each species) were created. All training sets contained the same (250) images of *M. lateralis* and *T. plebeius.* Images in the *C. virginica* category were varied to form the four different training sets, which were comprised of images of larvae raised: 1) in the hatchery in 2009, 2) in the hatchery in 2009 and 2010, 3) in the hatchery in 2009, 2010, and 2011, and 4) in the hatchery in 2009, 2010, and 2011 and images of *C. virginica* larvae from the warm and cool treatments of the experiment (Tables S2.2 and S2.3). The mean temperature and salinity at which the larvae were raised in each training set were 1) 25.4 ^{o}C +/- 1.6 and 10.6 +/- 0.4 (n=30), 2) 26.6 ^{o}C +/- 2.3 and 11.2 +/- 0.4 (n=60), 3) 25.9 ^{o}C +/- 1.1 and 9.1 +/- 0.2 (n=90), and 4) 25.3 ^{o}C +/- 2.3 and 13.2 +/- 0.4 (n=153), respectively. These training sets were used to classify the same unknown set which was composed of images of *C. virginica* from the warm and cool treatments of the experiment (n=424). Results indicate that as the variation in growth conditions increased within the *C. virginica* portion of the training set, classification accuracies increased from 76.7% to 98.5% (Table 2.3). In a second test, a 6-species training set and the 3-category training set based on taxonomic order (Ostreoida, Veneroida, Mytiloida) were used, with some (n=100) of the *C. virginica* images replaced with those from the warm and cool treatments. These training sets were employed to classify the same unknown set used in the test in the previous experiment, which was composed of other images of *C. virginica* from the warm and cool treatment of the experiment (n=424). When larvae from the experiment were added to the *C. virginica* portion of the training set, classification accuracy with the 6-category training set improved from 66.8% to 97.1%.

Classification accuracies with the 3-category training set were slightly higher than those with the 6-category training set, improving from 87.8% to 98.3% when images of larvae from the experiment were included in the training set. Based on these findings, it is recommended that the images of larvae used to create training sets be representative of the growth conditions of larvae in need of identification, especially in terms of temperature and salinity.

Estimating misclassification rates

Classification tests were performed to determine how well the ShellBi method could identify the target species *C. virginica* given various proportions in a sample. Two training sets were used: a 6-species training set composed of 250 images each of *C. virginica, M. lateralis, T. plebeius, R. cuneata, M. leucophaeata*, and *I. recurvum* larvae, and a 3-category order-based training set, using the same 6 species categorized by taxonomic order [1: Ostreoida, oysters (*C. virginica*), 2: Veneroida, clams (*M. lateralis, M. leucophaeata, R. cuneata, T. plebeius*), 3: Mytiloida, mussels (*I. recurvum*)]. Both training sets contained images of larvae from warm and cool treatments of the experiment to ensure wide variation in growth conditions within the training sets (Tables S2.2, S2.3). Three different groups of unknown sets were classified: 1) *C. virginica*, *T. plebeius*, and *M. lateralis*, 2) *C. virginica*, *T. plebeius*, and *I. recurvum*, and 3) *C. virginica*, *R. cuneata*, and *M. lateralis*. Each group contained 7 sets of 100 images of "unknown" larvae in which the percentage of images of *C. virginica* varied (2, 10, 25, 33, 50, 75, and 90%), with the remaining percentages comprised of equal number of images of two other species. Indices of classifier performance were calculated based on the actual number of *C. virginica*

images and on true positives, false positives, and false negatives for *C. virginica*. A true positive occurs when an image of *C. virginica* is classified as *C. virginica*. A false positive occurs when an image of a species other than *C. virginica* is classified as *C. virginica*. A false negative occurs when an image of *C. virginica* is misclassified as any other species. Probability of detection (i.e. the probability that the classifier will identify images correctly, P_D = true positive counts / (true positive counts + false negative counts) (Hu and Davis 2006)), specificity (i.e. the probability that the classifier's prediction is correct for each category, SP = true positive counts / (true positive counts + false positive counts) (Baldi and Brunak 2001)), and the ratios of false positives and false negatives to the actual number of *C. virginica* images (e.g. if a sample had 2 images of *C. virginica* and 4 images of mussels were classified as *C. virginica,* then the false positive ratio would be 4:2 or 2.0) were calculated. All indices of classifier performance (P_D, SP, false positive and false negative ratios) were calculated for the 3-category and 6-species training sets which were applied to each of the unknown groups.

Use of the order-based training set resulted in a similar number of misclassifications as the 6-species training set, except when the proportion of images of *C. virginica* in a sample was very low (Fig. 2.5). The probability of detection (P_D) was generally equal or higher for classifications by the order-based training set than for the 6-species training set except when the proportion of images of *C. virginica* comprised 2% of the sample (Fig. 5A). Specificity increased for both training sets as the proportion of images of *C. virginica* in a sample increased, with the 6-species training set performing slightly better when the number of *C. virginica* was high (Fig.

2.5B). False negative ratios did not exceed 0.33 except for the order-based training set when it was used to classify low percentages of *C. virginica* (2%) (Fig. 2.5C). The ratio of false positives to actual numbers was higher with the order-based training set when there were relatively few images of *C. virginica* in a sample (Fig. 2.5D), but this corresponded to a low number of misclassified images (3-8). These metrics show that higher proportions of *C. virginica* in a sample will result in greater classification accuracy, particularly with the order-based training set.

The highest number of false positive and false negative misclassifications from each training set was used to construct confidence intervals that depict the misclassifications that can be expected for different proportions of *C. virginica* in a sample (Fig. 2.6). The actual *C. virginica* images present plus the highest number of false positives was used to construct the upper line of the interval and the actual *C. virginica* minus the highest number of false negatives was used to construct the lower line of the interval. The confidence interval for the 6-species training set varied from <5% error at low percentages (2% *C. virginica* larvae) to <21% error at higher percentages (90% *C. virginica* larvae). The higher misclassifications at higher percentages are a result of more *C. virginica* being classified as other bivalves (i.e., false negatives) (Fig. 2.6). The confidence interval for the 3-category order-based training set varied from <1% error at low percentages (2% *C. virginica* larvae) to <22% error at medium percentages (33% *C. virginica* larvae) to <11% at the highest percentages (90% *C. virginica* larvae). The highest error for the 3-category order-based training set is a combined effect of increased false positives and false negatives in the middle ranges (33% *C. virginica*). Based on these results, it is expected that

misclassification rates will be within 5 to 21% for the 6-species training set and within 1 to 22% for the 3-category order-based training set depending on the proportion of *C. virginica* in a given sample.

Discussion

Our evaluation shows that the ShellBi technique can be applied with success to distinguish *C. virginica* larvae from the larvae of other bivalve species that are found in the Choptank River, indicating that this approach has application to different species and systems than the one in which it was developed (Waquoit Bay). Results indicate that 1) classification accuracies can increase by as much as 30% when training sets include images of larvae grown in conditions similar to those that are being classified, 2) accuracies can increase by 69% when larvae of different stages (both D-stage and veligers) are included in training sets, and 3) average accuracies are 15% higher when the number of categories within a training set is three compared to six. Although the first two points are novel and specific to this method, the third point has been shown in other image processing methods that are used to identify plankton (Davis et al. 2004, Grosjean et al. 2004). Finally, misclassification rates were estimated for our target species *C. virginica*, which suggest that this technique can be applied with error rates from 1-22% when proportions of the target organisms in the sample range from 2 to 90% (Fig. 2.6). Results indicate that further methods development aimed at reducing false positive and negative classification rates is a priority.

Differences in growth conditions based on salinity and temperature influenced median shell heights as well as the accuracy of classifying *C. virginica.* Higher temperatures and salinities correspond to faster growth in *C. virginica* (Kennedy et al. 1996) and influence growth in other bivalve larvae (Chanley 1970, Sundberg and Kennedy 1992). Shell heights of *C. virginica* in warm treatments were larger than those in cool treatments, but were shorter than those of hatchery-reared larvae grown at similar warm temperatures. This could be due to the lower assortment of algae fed to the experimental treatments compared to the diet of hatchery *C. virginica* (Langdon and Newell 1996). Regardless of the cause of variation, our results indicate that using images in training sets of larvae that were grown in similar conditions as the unknown sets resulted in higher classification accuracies. This suggests that differences in growth conditions may influence the formation of the shells of bivalve larvae, and hence alter birefringence patterns and classification accuracies. However, potential changes in shell structure and birefringence patterns under different growth conditions warrants further investigation.

The number of categories in a training set and the composition of species in a training set altered the classification accuracy of *C. virginica*. As the number of training set categories increased from 3 to 6, the average accuracy dropped by ~15%, which is consistent with previous studies (Davis et al. 2004, Grosjean et al. 2004, Thompson et al. 2012a). A training set in which 6 species were grouped into 3 categories based on taxonomic order increased classification accuracy of *C. virginica* from 66.8 to 87.8%. These findings suggest that ShellBi would perform well in systems with low numbers of bivalve species in the plankton at any given time (e.g., a

system in which 3 species spawn during spring) or in systems where non-target species can be aggregated into a few (≤ 3) categories.

The composition of the training set was also important. When used to identify the same unknown set, a training set composed of *C. virginica, R. cuneata*, and *T. plebeius* had 69.5% accuracy, while one of *C. virginica, M. leucophaeata*, and *I. recurvum* had 99.8% accuracy (Table 2.2). This may be explained, to some degree, because smaller *C. virginica* appear to have similar colors as later stage *T. plebeius* (Fig. 2.1). This suggests that some species of bivalves at different stages may have birefringence patterns that are similar, resulting in lower classification accuracies, while others have patterns that are more distinct, resulting in higher classification accuracies. Although further investigation is needed to determine how shell patterns compare between species throughout development and influence classification accuracies, grouping similar species into a small number of categories can help improve classification accuracies and could be optimized through a machine learning technique (Fernandes et al. 2009).

The confidence range for misclassifications that can be expected for different proportions of *C. virginica* in a sample may be a conservative estimate. The training sets used in this study were balanced (contain equal numbers of images in each species category) and the SVM classifier assumes that the unknown set contains equal representations of each category (Provost 2000, Lin et al. 2002), but the proportion of *C. virginica* in our unknown sets was varied. Adjusting the cost function (C parameter) of an SVM can help avoid false positives (Sun et al. 2007) and could result in narrower confidence intervals. Future directions to improve ShellBi include

adjusting the cost function given different percentages of target species (*C. virginica*) in a sample.

Although the initial set up of ShellBi requires time and effort, ShellBi is the fastest way to both identify and measure different species of bivalve larvae to date once training sets are established. Microscope techniques require a significant time investment while many molecular techniques require time and expense to set up primer or antibody designs or to sequence adult DNA (Garland and Zimmer 2002, Hendriks et al. 2005). When compared with multiplex PCR, ShellBi is less expensive and time consuming for bivalve larvae because individual larvae do not have to be isolated (Thompson et al. 2012a). Although quantitative PCR can provide some insight into the quantity of bivalve larvae, it does not provide information on the sizes of those larvae, which ShellBi does. Another promising technique is fluorescence *in situ* hybridization with DNA probes (Henzler et al. 2010), but the costs are currently prohibitive for large sampling efforts.

Results of this study suggest that ShellBi has broad applicability for the study of size-specific changes in the distribution and abundance of bivalve larvae in estuarine and marine systems. ShellBi has been used successfully to identify larvae in Waquoit Bay (Thompson et al. 2012b) and is being used to help enhance current understanding of *C.virginica* larval dispersal and connectivity in the Choptank River (Goodwin, unpublished data). This technique could be applied to other ecologically and economically important bivalves, both in the laboratory with samples collected from sediment-laden estuaries or in flow-through systems for underway identification of early stage bivalves in marine waters (the tissues of early-stage larvae do not

impede resolving birefringent patterns allowing flow-through imaging under field conditions) (S. Gallager, pers. comm.). Furthermore, ShellBi may provide insight into the dynamics of other calcareous organisms with shells that show birefringent patterns under polarized light (e.g., pteropods, Goodwin, pers. observation). Finally, because this image-based approach has the potential to be fully automated, it has promise to radically expand our knowledge of the dynamics of bivalve larvae via *in situ* monitoring platforms and gliders.

Comments and recommendations

Based on the experiments carried out in this study, several improvements are recommended for future applications and research. The first is to establish training sets with several ages of bivalve larvae reared in a range of environmental conditions similar to the system of study. In addition, we recommend the use of the fewest number of categories in a training set as possible. We found that a 3-category training set based on taxonomic order was slightly more accurate at classifying oyster larvae than a 6-category training set in which each category represented a separate species. It is possible that the species grouped by order (e.g., clam larvae) could be distinguished with a second classification test using categories that correspond to species (e.g., *R. cuneata, T. plebeius, M. lateralis, M. leucophaeata*).

Another recommendation is to ensure that the microscope and camera image capture settings are configured so that the background color in all images is uniform for both training and unknown sets. Thompson et al. (2012a) found that training sets created with different microscope settings were not compatible. We found that major

background color differences could negatively affect classification accuracies (results not shown), but that minor background color differences (see Fig. 2.1) for tests conducted in this manuscript did not result in in poor classification accuracies. To avoid major background color variations, we recommend against using metal brackets for polarizers or full wave compensation plates when they are near the light source of the microscope. Changes in temperature due to heating by the light source can lead to large differences in the background color of images when using metal housings. A non-metal or plastic housing for a polarizer or wave compensation plate near the light source offers more stable conditions that provide similar background colors between images.

The next step for improving the ShellBi method is to increase the speed of image acquisition, ROI extraction, and classification. For the tests presented here, the microscope stage was moved manually or with a joystick attached to an automated stage before an image was taken. A person can image about 100 larval shells per hour with this approach. Currently, efforts toward automation have been made using an automated camera and stage system that will automatically image an entire slide in 46 minutes (regardless of the number of shells per slide). With this system, 50% of the larvae in a field sample are being imaged in 46 minutes (half of two slides) which is faster and more likely to detect rare species than manual identification which most often relies on subsamples much smaller than half of the sample. In addition, efforts are underway to automate post processing of the bivalve images with automatic ROI detection, ROI cropping, and classification steps, with care taken to assess and minimize errors that can be introduced by subsampling and automation of image

analysis (Bachiller et al. 2012). As these enhancements improve how we apply the ShellBi method, so will our ability to rapidly process samples and to conduct field studies with greater spatial and temporal resolution, thereby increasing our understanding of the occurrence and patterns in the presence of bivalve larvae in the field.

Literature cited

Bachiller, E., J. A. Fernandes, and X. Irigoien. 2012. Improving semiautomated zooplankton classification using an internal control and different imaging devices. Limnol. Oceanogr. Methods. 10:1-9.

Baldi, P., and S. Brunak. 2001. Bioinformatics-the machine learning approach, MIT Press, Cambridge, MA.

Boicourt, W. C. 1988. Recruitment dependence on planktonic transport in coastal waters, p. 183-202. *In* B.J. Rothschild (ed.), Toward a theory on biological-physical interactions in the world ocean. Kluwer Academic Publishers.

Bland, J. M., and D. G. Altman. 1995. Multiple significance tests: the Bonferroni method. BMJ 310:170.

Calabrese, A. 1969. *Mulinia lateralis*: Molluscan fruit fly? Proceedings of the National Shellfisheries Association 59:65-66.

Calabrese, A., and E. W. Rhodes. 1974. Culture of *Mulinia lateralis* and *Crepidula fornicate* embryos and larvae for studies of pollution effects. Thalassia Jugosl. 10:89-102.

Cawley, G. C. 2000. (MATLAB) Support vector machine toolbox (v0.55\beta). University of East Anglia, School of information systems, Norwich, Norfolk, U.K. NR4 7TJ. http://theoval.cmp.uea.ac.uk/svm/toolbox/

Chanley, P. 1970. Larval development of the hooked mussel, *Brachiodontes recurves* Rafinesque (Bivalvia: Mytilidae) including a literature review of larval characteristics of the Mytilidae. Proceedings of the National Shellfisheries Association 60:86-94.

Chanley, P., and J. D. Andrews. 1971. Aids for identification of bivalve larvae of Virginia. Malacol. 11:45-119.

Chanley, P., and M. Castagna. 1971. Larval development of the stout razor clam, *Tagelus plebeius* solander (solecurtidae: Bivalvia). Ches. Sci. 12:167-172.

Dame, R. F. 2012. Population processes p. 75-103. *In*: (eds) P. Petrailia, and H. Linna. Ecology of marine bivalves an ecosystem approach 2nd edition. CRC Press Taylor Frances Group. Boca Raton, FL.

Davis, C. S., Q. Hu, S. M. Gallager, X. Tang, and C. J. Ashjian. 2004. Real-time observation of taxa-specific plankton distributions: an optical sampling method. Mar. Ecol. Prog. Ser. 284:77-96.

Fernandes, F. A., X. Irigoien, G. Boyra, J. A. Lozano, and I. Inza 2009. Optimizing the number of classes in automated zooplankton classification. J. Plankton Res. 31(1):19-29.

Fogarty, M. J., and L.W. Botsford. 2007. Population connectivity and spatial management of Mar. Fish. *Oceanogr.* 20(3):112–123,http://dx.doi.org/10.5670/oceanog.2007.34.

Fukunaga, K., and D. M. Hummels. 1989. Leave-one-out procedures for nonparametric error estimates. IEEE Trans. Pattern Anal. Mach. Intellig. 11:421-423.

Garland, E. D., and C. A. Zimmer. 2002. Techniques for the identification of bivalve larvae. Mar. Ecol. Prog. Ser. 225: 299-310.

Grosjean, P., M. Picheral, C. Warembourg, and G. Gorsky. 2004. Enumeration, measurement, and identification of new zooplankton samples using the ZOOSCAN digital imaging system. J. Mar. Sci. 61:518-525.

Hare, M. P., S. R. Palumbi, and C. A. Butman. 2000. Single-step species identification of bivalve larvae using multiplex polymerase chain reaction. Mar. Biol. 137:953-961.

Helm, M., N. Bourne, and A. Lovatelli. 2004. Hatchery culture of bivalves: A Practical manual, FAO Fisheries Technical Paper 471, Rome.

Hendriks, I. E., L. A. van Duren, and P. M. J. Herman. 2005. Image analysis techniques: a tool for the identification of bivalve larvae? J. Sea Res. 54:151-162.

Henzler, C. M., E. A. Hoaglund, and S. D. Gaines. 2010. FISH-CS - a rapid method for counting and sorting species of marine zooplankton. Mar. Ecol. Prog. Ser. 410:1-11.

Hu, Q., and C. Davis. 2006. Accurate automatic quantification of taxa-specific plankton abundance using dual classification with correction. Mar. Ecol. Prog. Ser. 306:51-61.

Kennedy, V.S., R. A. Lutz, and C. A. Fuller. 1989. Larval and early postlarval development of *Macoma mitchelli* Dall (Bivalvia: Tellinidae). The Veliger 32:29-38.

Kennedy, V. S. 1996. Biology of larvae and spat. p. 371-421. *In* (eds.) V. S. Kennedy, R. E. Newell, and A. F. Eble. The Eastern Oyster *Crassostrea virginica.* Maryland Sea Grant.

Kennedy, V. S. 2011a. The invasive dark false mussel *Mytilopsis leucophaeata* (Bivalvia: Dreissenidae): A literature review. Aqua. Ecol. 45:163-183.

Kennedy, V. S. 2011b. Biology of the uncommon dreissenid bivalve *Mytilopsis leucophaeata* (Conrad 1831) in central Chesapeake Bay. J. Mull. Stud. 77:154-164.

Langdon, C. J. and I. E. Newell. 1996. Digestion and Nutrition in Larvae and Adults. p. 231-269. *In* (eds.) V. S. Kennedy, R. E. Newell, and A. F. Eble. The Eastern Oyster *Crassostrea virginica.* Maryland Sea Grant.

Lin, Y., Y. Lee and G. Wahba. 2002. Support Vector Machines for classification in nonstandard situations. Mach. Learn. 46(1-3):191-202.

Loosanoff, V. L., H. C. Davis, and P. E. Chanley. 1966. Dimensions and shapes of larvae of some marine bivalve mollusks. Malacol. 4:351-435.

Lou, T., K. Kramer, D. Goldgof, L.O. Hall, S. Samson, A. Remsen, and T. Hopkins. 2003. Learning to recognize plankton, p. 888-893. In Proceedings of the IEEE International Conference on Systems, Man and Cybernetics. Washington C.C. October 2003.

Lutz, R. J., and others. 1982. Preliminary observations on the usefulness of hinge structures for identification of bivalve larvae. J. Shell. Res. 2(1): 65-70.

(MDNR) Maryland Department of Natural Resources 2012. Fixed station monthly monitoring buoy EE1.1 http://mddnr.chesapeakebay.net/bay_cond/bay_cond.cfm?param=wt&station=EE11

Munroe, D. M., J. M. Klinck, E. E. Hofmann, and E. N. Powell. 2012. The role of larval dispersal in metapopulation gene flow: local population dynamics matter. J. of Mar. Res. 70:441-467.

North, E., Z. Schlag, R. Hood, M. Li, L. Zhong, T. Gross, and V. S. Kennedy. 2008. Vertical swimming behavior influences the dispersal of simulated oyster larvae in a coupled particle tracking and hydrodynamic model of Chesapeake Bay. Mar. Ecol. Prog. Ser. 359: 99-115.

Pineda, J., J. A. Hare, and S. Sponaugle. 2007. Larval transport and dispersal in the coastal ocean and consequences for population connectivity. Oceanogr. 20(3):22-39.

Provost, F. 2000. Machine learning from imbalanced data sets 101, p. 1-3. *In* Proceedings of the AAAI,00 workshop on learning from imbalanced data sets, Austin, TX. AAAI.

Shanks, A. L., and L. Brink. 2005. Upwelling, downwelling, and cross-shelf transport of bivalve larvae: test of a hypothesis. Mar. Ecol. Prog. Ser. 302:1-12.

Sokal, R., and J. Rohlf. 1987. p. 225-227. *In* Sokal, R. and J. Rohlf (eds). Non parametric methods *in lieu* of ANOVA Introduction to biostatistics. W.H. Freeman and Company.

Sun, Y., M. M. Karnel, A. K. C. Wong, and Y. Wang. 2007. Cost-sensitive boosting for classification imbalanced data. Patt. Recogn. 40:3358-3378.

Sundberg, K., and V. S. Kennedy. 1992. Growth and development in larval and post-metamorphic *Rangia cuneata* (Sowerby, 1831). J. Shell. Res. 11:9-12.

Sundberg, K., and V. S. Kennedy. 1993. Larval settlement of Atlantic Rangia, *Rangia cuneata* Bivalvia: Mactridae). Estuaries 16(2):223-228.

Thompson, C. M., M. P. Hare, and S. M. Gallager. 2012a. Semi-automated image analysis for the identification of bivalve larvae from a Cape Cod estuary. Limnol. Oceanogr. Methods: 10:538-554.

Thompson, C. M., R. H. York, and S.M. Gallager. 2012b. Species-specific abundance of bivalve larvae in relation to biological and physical conditions in a Cape Cod estuary: Waquoit Bay, Massachusetts (USA). Mar. Ecol. Prog. Ser. 469:53-69.

Tiwari, S., and S. M. Gallager. 2003a. Optimizing multiscale invariants for the identification of bivalve larvae. Proceedings of the 2003 IEEE International Conference on Image Processing, Barcelona, Spain, September 14-17, 2003.

Tiwari, S., and S. Gallager. 2003b. Machine learning and multiscale methods in the identification of bivalve larvae. Proceedings of the Ninth IEEE International Conference on Computer Vision, Nice, France, October 14-17, 2003.

Wight, N. A., J. Suzuki, B. Vadopalas, and C.S. Friedman. 2009. Development and optimization of quantitative PCR assays to aid *Ostrea lurida* Carpenter 1984 restoration efforts. J. Shell. Res. 28(1): 33-41.

Zhao, F., F. Lin, and H. S. Sea. 2010. Binary SIPPER plankton image classification using random subspace. Neurocomp. 73:1853-1860.

Tables and Figures

Table 2.1. Spawning conditions for six species of bivalves that are found in the mesohaline region of the Choptank River.

Scientific name	**Temperature**	**Salinity**	**Season**
Ischadium recurvum	25-30 ^{o}C (Chanley 1970)	20 (Chanley 1970)	June-Nov (Chanley 1970)
Rangia cuneata	30 ^{o}C (Sundberg and Kennedy 1992)	<15 (Sundberg and Kennedy 1992)	late spring to early fall (Sundberg and Kennedy 1993)
Mytilopsis leucophaeata	30 ^{o}C (Kennedy 2011b)	0.5-18 (Kennedy 2011b)	Summer to fall (Kennedy 2011a)
Tagelus plebeius	30-32 ^{o}C (Chanley and Castagna 1971)	10-30 (Chanley and Castagna 1971)	June-Nov (Chanley and Castagna 1971)
Mulinia lateralis	28-30 ^{o}C (Calabrese and Rhodes 1974)	20-30 (Calabrese and Rhodes 1974)	May-Oct (Calabrese 1969)
Crassostrea virginica	28-30 ^{o}C (Kennedy et al. 1996)	12-27 (Kennedy et al. 1996)	Summer to fall (Kennedy 1996)

Table 2.2. Percent classification accuracy of unknown *C. virginica* larvae from experiments (n = 3,288) using training sets with different numbers and compositions of species. Training sets of 3-, 4-, 5-, and 6-species categories were comprised of *C. virginica* (CV), *R. cuneata* (RC), *T. plebeius* (TG), *I. recurvum* (IR), *M. lateralis* (ML), and/or *M. leucophaeata* (DF). 250 images were used for each category. *Denotes that images of *C. virginica* larvae grown in different temperature and salinity treatments were added to the *C. virginica* training set category (Table S3).

Training set	Percent classification accuracy	Number of images in training set
CV, RC, TG	69.5	750
CV, RC, IR	72.1	750
CV, ML, IR	82.1	750
CV, DF, RC	72.1	750
CV, DF, IR	99.8	750
CV, DF, TG	96.9	750
CV, IR, TG	97.1	750
CV, TG, ML	79.5	750
CV, ML, RC	71.8	750
CV, RC, TG, ML	66.7	1000
CV, RC, IR, ML	69.1	1000
CV, RC, IR, DF	72.2	1000
CV, DF, TG, IR	96.9	1000
CV, RC, DF, ML	69.2	1000
CV, DF, TG, ML	79.7	1000
CV, RC, TG, IR	69.5	1000
CV, RC, IR, TG, ML	66.6	1250
CV, RC, IR, TG, DF	69.6	1250
CV, RC, IR, ML, DF	69.3	1250
CV, RC, TG, ML, DF	66.8	1250
CV, IR, TG, ML, DF	79.6	1250
CV, RC, IR, TG, ML, DF	66.8	1500
CV*,RC, IR, TG, ML, DF	97.1	1500
order-based: (CV), (IR), (RC, TG, ML, DF)	87.8	750
order-based: (CV*), (IR), (RC, TG, ML, DF)	98.3	750

Table 2.3. Percent classification accuracy using four training sets to identify "unknown" *C. virginica* larvae that were raised in the experiment. The training sets were composed images of *M. lateralis*, *T. plebeius* and *C. virginica*, the latter of which were varied to incorporate larvae grown in different conditions: 1) in the hatchery in 2009 (CV-2009), 2) in the hatchery in 2009 and 2010 (CV-2009-2010), 3) in the hatchery in 2009, 2010, and 2011 (CV-2009-2010-2011) and 4) in the hatchery in 2009, 2010, and 2011, and in the temperature-controlled experiment (CV-2009-2010-2011-exp).

Training Set	Percent accuracy
CV-2009	76.7
CV-2009-2010	76.8
CV-2009-2010-2011	84.7
CV-2009-2010-2011-exp	98.5

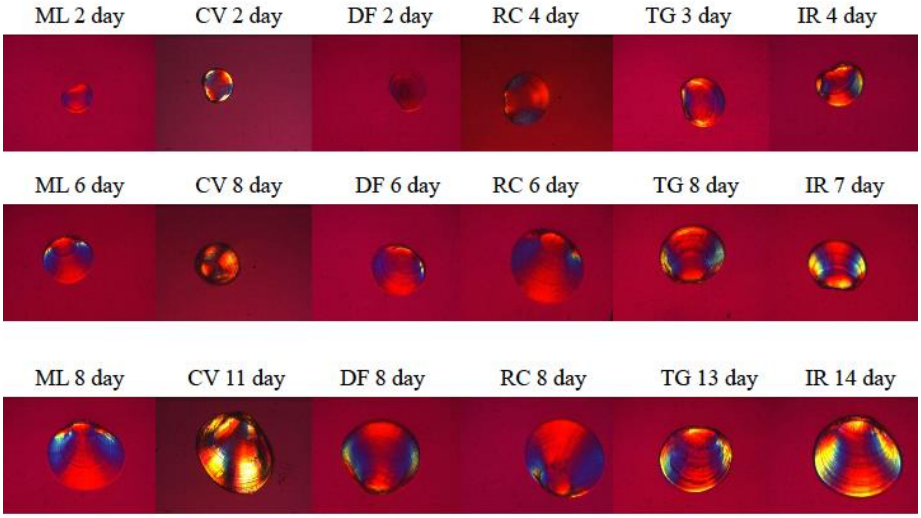

Fig. 2.2. Images under polarized light of the shells of six species of bivalve larvae used in the analysis ranging from early-stage veliger (top row, 2-4 days old) to late stage veliger (bottom row, 8-14 days old). Species pictured are *Mulinia lateralis* (ML), *Crassostrea virginica* (CV), *Mytilopsis leucophaeata* (DF), *Rangia cuneata* (RC), *Tagelus plebeius* (TG), and *Ischadium recurvum* (IR).Sizes of larvae range from 72-88 µm (top row), 95-155 µm (middle row), and 157-246 µm (bottom row).

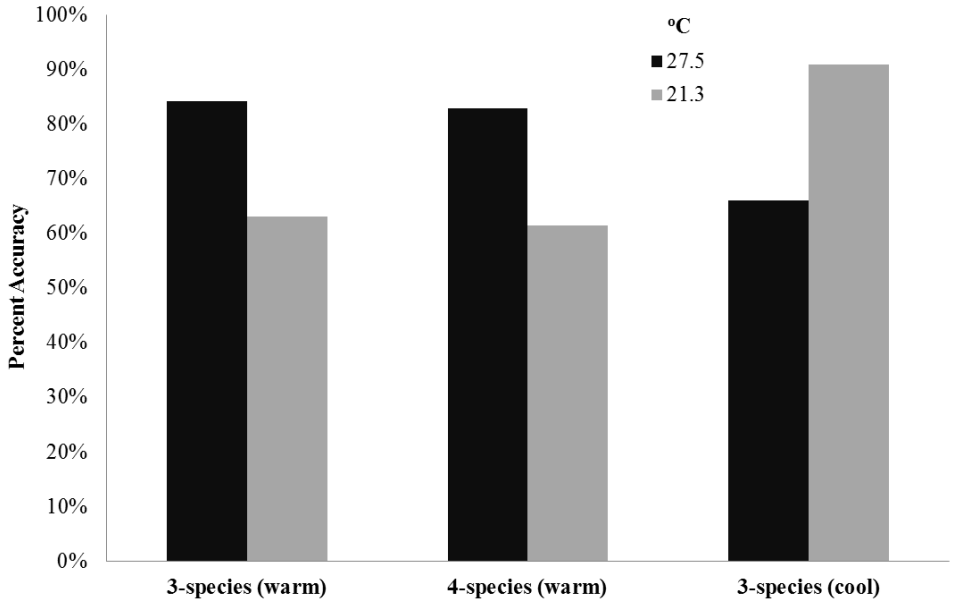

Fig. 2.2. Classification accuracy for *C. virginica* using two 3-species training sets (*C. virginica*, *M. lateralis*, and *R. cuneata)* and one 4-species training set (*C. virginica, M. lateralis*, *R. cuneata,* and *T. plebeius*). Images of shells of *C. virginica* were reared at 25.9 ^{o}C for 'warm' training sets and at 23.3 ^{o}C for the 'cool' training set. All three training sets were used to classify shells of *C. virginica* from warm (darker bars) and cool (lighter bars) treatments.

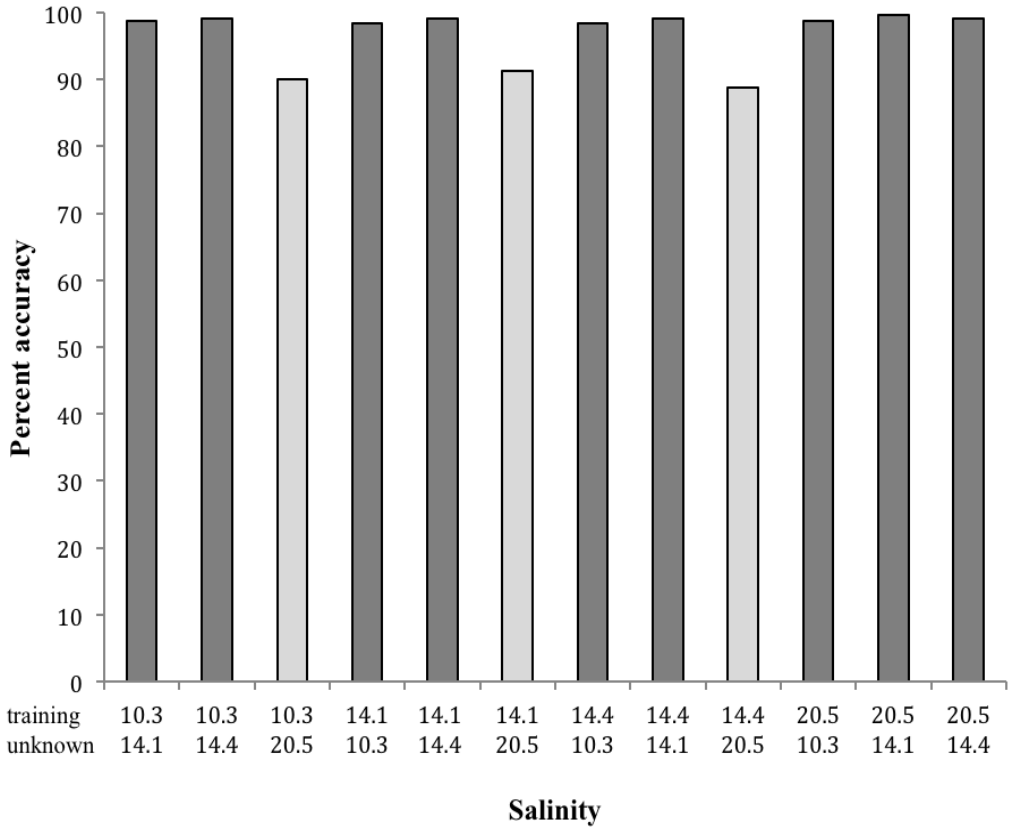

Fig. 2.3. Classification accuracies for shells of "unknown" *C. virginica* larvae raised in four different salinities (10.3, 14.1, 14.4, and 20.5) when classified with training sets composed of *R. cuneata*, *I. recurvum* and *C. virginica* larvae, the latter of which were raised in the same four salinities. Numbers under each bar represent the salinity at which *C. virginica* were reared in the training set (upper number) and in the unknown set (lower number). Lighter bars indicate training sets reared at the first three lower salinities used to classify the high salinity treatment (20.5).

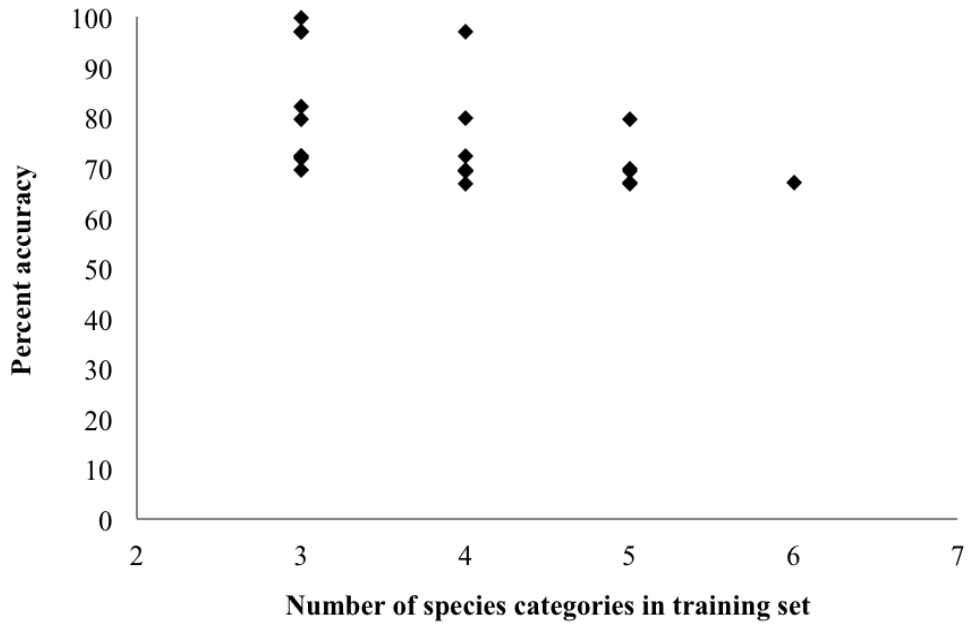

Fig. 2.4. Percent classification accuracy of ShellBi when classifying images of *C. virginica* shells using training sets with different numbers of species categories (see Table 2.2 for details). Training sets of 3-, 4-, 5-, and 6-species categories were comprised of hatchery-reared *C. virginica,* and the following species reared in the laboratory: *I. recurvum*, *M. lateralis*, *M. leucophaeata*, *T. plebeius*, and *R. cuneata.* . Diamonds represent training sets, each with a different set of species comprising the categories in the training set.

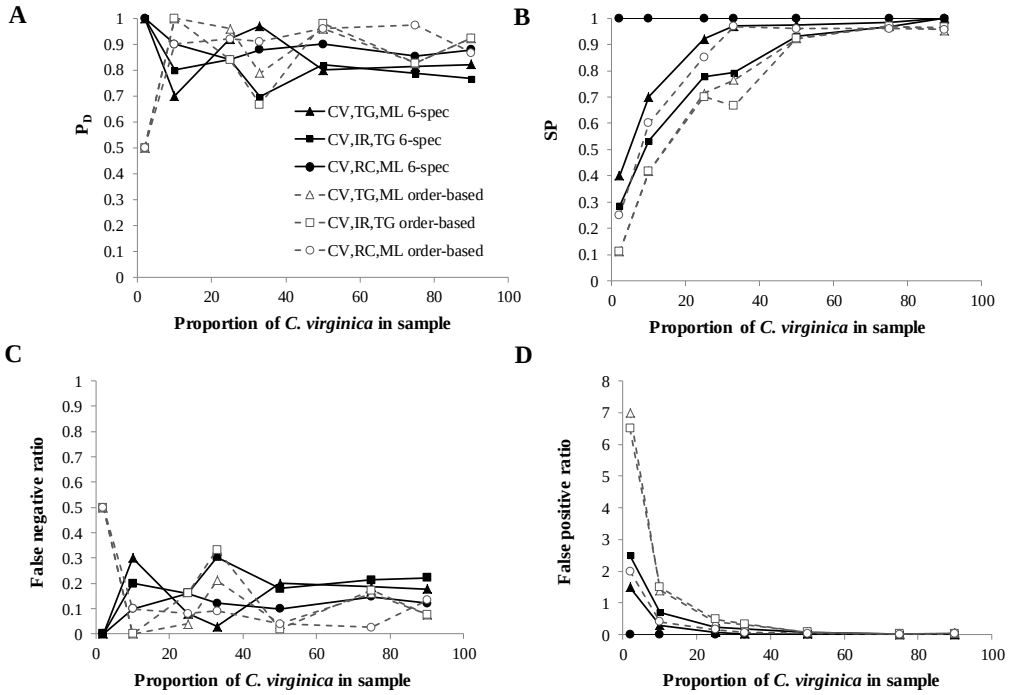

Fig. 2.5. Misclassification metrics versus the proportion of *C. virginia* (CV) images in a sample: A) probability of detection (P_D), B) specificity (SP), C) the ratio of false positives to actual *C. virginica* images, and D) the ratio of false negatives to actual *C. virginica* images. For all panels, two training sets were used to classify three groups of unknown larvae in different proportions. A 6-species training set (6-spec, solid lines) was composed of six categories, each for a separate species: *C. virginica*, *I. recurvum*, *M. lateralis*, *M. leucophaeata R. cuneata*, and *T. plebeius*). A second training set (order-based, dotted lines) contained images of these species grouped by order (clams: *M. lateralis*, *M. leucophaeata*, *R. cuneata*, *T. plebeius*; oyster: *C. virginica*, mussel: *I. recurvum*). These training sets were used to classify three different groups of images of "unknown" larvae: 1) *C. virginica*, *T. plebeius*, and *M. lateralis* (CV, TG, ML), 2) *C. virginica*, *T. plebieus*, and *I. recurvum* (CV, TG, IR), and 3) *C. virginica*, *R. cuneata*, and *M. lateralis* (CV, RC, ML). Each group contained "unknown" sets of images in which the percentage of *C. virginica* in the set ranged from 2 to 90%.

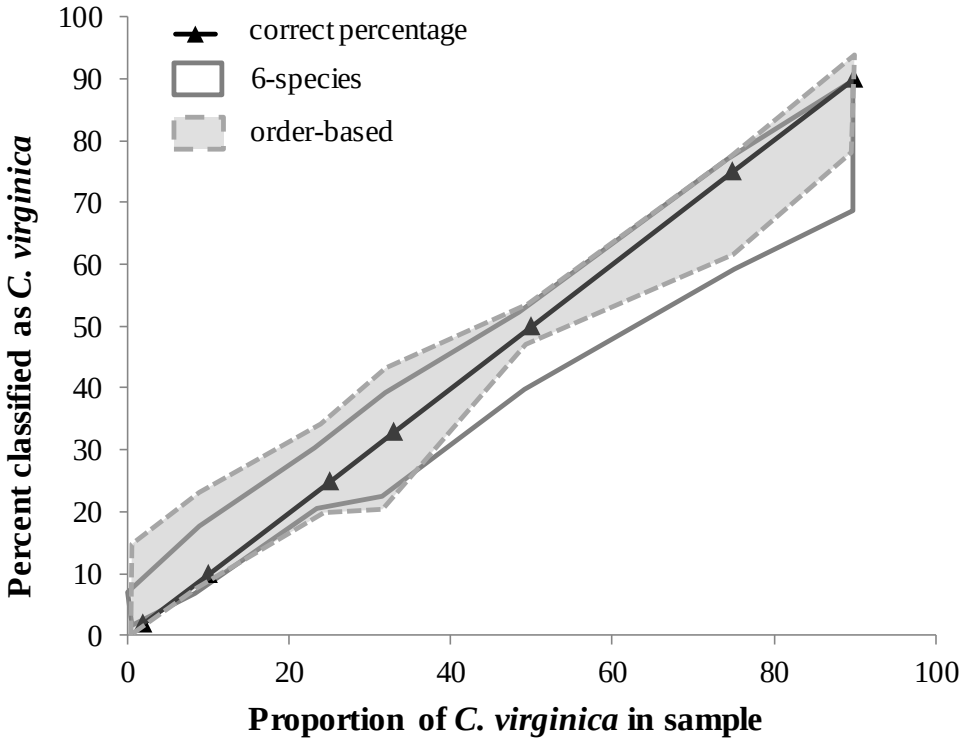

Fig. 2.6. Classification confidence intervals for the 6-species (no fill with solid gray line) and order-based (gray shading with dashed gray line) training sets. Confidence intervals were constructed around the correct percentage of *C. virginica* classified in a sample (solid line with triangles) using the highest number of false positives and false negatives from tests summarized in Fig. 5. False positives were added to the correct number of *C. virginica* images to construct the top lines and false negatives were subtracted from the correct number of *C. virginica* images to construct the bottom lines. The closer the gray lines are to the black line, the smaller the classification error, which ranged from 5-21% for the 6-species training set and from 1-22% for the 3-category order-based training set.

Supplementary tables

Table S2.1. Results of classification tests designed to determine if fixative type (ethanol vs. formalin) influenced the classification accuracy of the ShellBi method. All fixatives for training sets and 'unknowns' were buffered with sodium borate. Training sets were composed of 250 images of the following species: *Crassostrea virginica*, *Ischadium recurvum*, *Mytilopsis leucophaeata* and *Rangia cuneata.* Images of larvae in the training sets that were stored in either ethanol or formalin were used to classify images of *M. leucophaeata* that had been stored in either ethanol or formalin. Treatments denoted "ethanol & formalin" are composed of 100 images of *M. leucophaeata* that were stored in ethanol and 100 images of *M. leucophaeata* that were stored in formalin. The *M. leucophaeata* larvae were taken from the same cohort and stored in formalin or ethanol for an equal amount of time (11 months). All training sets had classification accuracies >95%. Slightly lower accuracies were reported when training sets included images of shells stored in formalin (95-96%) compared to those stored in ethanol (97-98%). Based on the high classification accuracies for shells stored in both types of fixatives, it is concluded that the fixative used does not interfere with the ability of ShellBi to classify larvae.

Test Number	**Fixative of training set**	**Fixative of unknown set**	**Percent classification accuracy**
1	ethanol	ethanol	98.1
2	ethanol	formalin	95.2
3	ethanol	ethanol & formalin	97.3
4	formalin	ethanol	98.3
5	formalin	formalin	95.8
6	formalin	ethanol & formalin	96.1
7	ethanol & formalin	ethanol	97.1
8	ethanol & formalin	formalin	94.9
9	ethanol & formalin	ethanol & formalin	96.7

Table S2.2. Leave one-out (LOO) cross validation accuracy of training sets for classifying *C. virginica*. The first column lists the analysis in which the training set was applied. The second column gives the two letter code of each species used in the training set (CV: *Crassostrea virginica*, RC: *Rangia cuneata*, ML: *Mulinia lateralis*, TG: *Tagelus plebeius*, IR: *Ischadium recurvum*, and DF: *Mytilopsis leucophaeata*). The third column lists the number of images in each training set. The fourth column gives the LOO percent accuracy for classifying *C. virginica.* *Denotes that images of *C. virginica* larvae grown in different temperature and salinity treatments were added to the *C. virginica* training set category (Table S2.3).

Analysis	Training set	Number of images	Percent cross validation accuracy
Temperature			
26.4 (hatchery 3-species)	CV, RC, ML	750	98.1
26.4 (hatchery 4-species)	CV, RC, ML, TG	1000	98.9
22.3 (cool Exp)	CV, RC, ML	750	97.1
Salinity			
10.3	CV, IR, RC	750	98.8
14.1	CV, IR, RC	750	99.6
14.3	CV, IR, RC	750	99.6
20.5	CV, IR, RC	750	99.2
Variation in growth conditions			
RC, ML, CV-2009	CV, RC, ML	750	99.6
RC, ML, CV-2009-2010	CV, RC, ML	750	98.5
RC, ML, CV-2009-2010-2011	CV, RC, ML	750	98.1
RC,ML,CV-2009-2010-2011-exp	CV, RC, ML	750	96.7
Larval stage			
Veliger	CV, ML, TG	750	99.0
D-stage	CV, ML, TG	750	96.4
Training set composition			
3-species	CV, RC, TG	750	95.6
3-species	CV, IR, RC	750	95.7
3-species	CV, ML, IR	750	92.4
3-species	CV, DF, RC	750	98.8
3-species	CV, DF, IR	750	95.6

3-species	CV, DF, TG	750	97.2
3-species	CV, IR, TG	750	94.8
3-species	CV, TG, ML	750	95.2
3-species	CV, ML, RC	750	98.1
4-species	CV, RC, TG, ML	1000	92.4
4-species	CV, RC, IR, ML	1000	92.4
4-species	CV, RC, IR, DF	1000	94.0
4-species	CV, DF, TG, IR	1000	94.0
4-species	CV, RC, DF, ML	1000	97.2
4-species	CV, DF, TG, ML	1000	94.0
4-species	CV, RC, TG, IR	1000	94.0
5-species	CV, RC, IR, TG, ML	1250	90.8
5-species	CV, RC, IR, TG, DF	1250	92.8
5-species	CV, RC, IR, ML, DF	1250	91.6
5-species	CV, RC, TG, ML, DF	1250	95.6
5-species	CV, IR, TG, ML, DF	1250	90.8
6-species	CV, RC, IR, TG, ML, DF	1500	74.7
6-species	CV*, RC, IR, TG, ML, DF	1500	92.1
3-category order-based (clams, oysters, mussels)	(CV), (IR), (RC, ML, DF,TG)	750	90.7
3-category order-based (clams, oysters, mussels)	(CV*), (IR), (RC, ML, DF,TG)	750	98.9

Table S2.3. The number of images of *C. virginica* larvae that grown in different temperature and salinity treatments which were added to the *C. virginica* training set category denoted by CV* in Tables 2.2 and S2.2. Mean, standard deviation, and sample size for temperature and salinity measurements are reported.

Source	Temperature	Salinity	Number of images
Experimental chamber	27.9 +/- 0.7 (n=12)	10.3 +/- 0.7 (n=25)	8
Experimental chamber	27.7 +/- 0.6 (n=17)	14.1 +/- 0.6 (n=32)	27
Experimental chamber	27.5 +/- 0.6 (n=15)	14.4 +/- 0.7 (n=30)	12
Experimental chamber	27.6 +/- 0.6 (n=20)	20.5 +/- 1.0 (n=50)	20
Experimental chamber	21.1 +/- 1.0 (n=13)	10.3 +/- 0.7 (n=25)	19
Experimental chamber	20.9 +/- 1.0 (n=15)	14.1 +/- 0.6 (n=32)	34
Experimental chamber	21.4 +/- 1.0 (n=15)	14.4 +/- 0.7 (n=30)	6
Experimental chamber	22.7 +/- 1.0 (n=16)	20.5 +/- 1.0 (n=50)	19
Hatchery	25.9 +/- 1.0 (n=30)	10.3 +/- 0.9 (n=30)	105
TOTAL			250

Chapter 3: Improving a semi-automated classification technique for bivalve larvae: automated image acquisition and measures of quality control

Abstract

Bivalve larvae are small (50-400 μm) and difficult to identify using standard microscopy, thus limiting inferences from samples collected in the field. With the advent of ShellBi, an image analysis technique, accurate identification of bivalve larvae is now possible but rapid image acquisition and processing remains a challenge. The objectives of this research were to 1) develop a benchtop automated image acquisition system for use with ShellBi, 2) evaluate the system, and 3) create a protocol that would maintain high classification accuracies for bivalve larvae. These improvements decreased image acquisition time from 2-13 hr to 46 min per slide. This system was used to capture images of three species of bivalve larvae at three magnifications (7x, 21x, and 41x). Classification accuracies were highest, and image acquisition time was shortest (46 min), at the lowest (7x) magnification. Quality control tests indicated that classification accuracies were sensitive to camera and light source settings and that measuring changes in light source and color channel intensities over time was an important part of quality control during routine operations. Validation experiments indicated that under proper settings, automated image acquisition coupled with ShellBi could rapidly classify *C. virginica* larvae with high accuracies (80-93%). Results suggest that this automated image acquisition system coupled with ShellBi can be used to rapidly image plankton samples and classify bivalve larvae allowing for expanded capability to understand bivalve larval

ecology in the field. Additionally, the automated system has application for rapidly imaging other planktonic organisms at high magnification.

Introduction

Populations of ecologically and commercially important shellfish have a transient planktonic larval stage and sessile juvenile and adult phases (Kennedy 1996). However, little is known about the planktonic stage of larvae although it influences the recruitment patterns of a population (Gaines and Roughgarden 1985, Kennedy 1996). Discerning patterns in abundance and changes in distributions of planktonic bivalve larvae requires a large number of samples over space and time (Steele 1989, Wiens 1989). Recently, semi-automated plankton imaging techniques have been developed to expand the spatial and temporal scales of sampling (Grosjean et al. 2004, Benfield et al. 2007, Macleod et al. 2010, Thompson et al. 2012), with both *in situ* (e.g., Video Plankton Recorder (Davis et al. 1996), ISIIS (Cowen and Guigand 2008)) and benchtop (e.g., Zooscan (Gorsky et al. 2010) approaches. However, these techniques do not identify bivalve larvae to the species level. One semi-automated imaging technique called ShellBi uses machine learning to identify images of bivalve larvae taken under polarized light (Twari & Gallager 2003, Thompson et al. 2012, Goodwin et al. 2014). However, the acquisition of those images is still completed manually and can take up to 12 hours per sample (Thompson et al. 2012, Goodwin et al. 2014). Therefore, a more rapid benchtop approach for image acquisition of bivalve larvae is needed to decrease processing time for samples collected from turbid waters like estuaries where flow-through *in*

situ technologies are not effective. The objective of this research was to develop and test such an approach.

Traditional methods of identifying bivalve larvae focus on hinge structures or other morphological cues (Chanley and Andrews 1971, Lutz et al. 1982). These methods often require experts, intensive labor, and are subject to a degree of individual subjectivity (Garland and Zimmer 2002). More recent genetic-based methods include polymerase chain reaction (PCR) (Hare et al. 2000, Garland and Zimmer 2002, Larsen et al. 2005). However, these methods are still susceptible to misclassification and are often time consuming or expensive (Laresn et al. 2005, Thompson et al. 2012). Furthermore, many genetic-based methods must meet the challenge of designing primers to discriminate between sequences at the species level while retaining insensitivity to polymorphism (which creates false negative results) within the target species (Hare et al. 2000). Another recent genetic-based method utilizes fluorescence *in situ* hybridization (FISH), but this method is still susceptible to problems encountered when using DNA probes (Henzler et al. 2010). More pros and cons of bivalve identification methods are reviewed in Garland and Zimmer (2002) and Hendricks et al. (2005).

A more recently developed method for identifying bivalve larvae is ShellBi. ShellBi utilizes the color and texture-based features extracted from digital images of bivalve larvae taken under polarized light (Gallager and Tiwari 2008). This method uses an image library, or training set, to classify 'unknown' images (for more detail see Thompson et al. 2012). The images of the bivalve larvae are classified using pattern recognition software (Gallager and Tiwari 2008). ShellBi was validated by

applying DNA and visual classification methods to bivalve species in Cape Cod, yielding high (98%) classification accuracies for hatchery reared larvae but lower accuracies (68-88%) for field samples (Thompson et al. 2012). Further testing of ShellBi showed that identification accuracies increased from 67-88% to 97-99% when training sets included larvae reared under similar environmental conditions as the larvae being classified (Goodwin et al. 2014). Goodwin et al. (2014) also demonstrated that ShellBi was effective for distinguishing different species of bivalves than those that Thompson et al. (2012) tested, suggesting that this method has broad applicability in estuarine and marine systems.

Although ShellBi offers a quantitative way to identify and measure bivalve larvae, image acquisition speed has been limited to ~100 images h^{-1} (Goodwin et al. 2014) while capturing images of larvae under a microscope by manually moving the stage or by using a joy-stick-assisted motorized stage. Both techniques necessitate substantial time investment of a trained technician especially if target organisms are rare and subsampling is not possible. Automating image acquisition would greatly enhance sample processing speed and enable greater spatial and temporal coverage during field surveys for bivalve larvae. In addition, increased speed of acquisition of high resolution images at high magnification has applications for enhancing surveys of other types of plankton such as copepods and fish eggs.

Another challenge with automated image acquisition is identifying and cropping (selecting) regions of interest (ROI). For ShellBI, the ROI is the shell of bivalve larvae. Currently, cropping for ShellBi is done manually by clicking with a mouse around the ROI because automated ROI detection software is not effective.

The main objective of this research was to create an automated image acquisition system which would enable faster image acquisition and improved cropping while maintaining a standard of quality control which enabled consistent and high-accuracy classification of bivalve larvae. Custom software was created that enabled a digital camera and automated stage to image the contents of a Sedgwick-Rafter slide automatically, and ROI detection software was improved. The system was tested to determine how magnification, software settings, and other factors affected the classification accuracy of bivalve larvae. Quality control measures were developed to ensure that the image acquisition system captured images with consistent alignment, brightness, and color. Methods for sample preparation and storage were also developed.

Materials and procedures

This section describes the automated image acquisition system which was combined with ShellBi software to create a rapid system for identifying bivalve larvae. It also includes procedures which were developed to maintain image quality and classification accuracies and to prepare field samples for use with the automated imaging system.

Hardware

An automated image acquisition system was developed that integrated hardware and software components to improve image capture, image processing, and overall sample processing speeds for imaging bivalve larvae. The hardware consisted

of an automated stage, stage motor controller, digital camera, microscope, metal braces and a desktop computer (Fig. 3.1, Table 3.1). The automated stage, a Semprex KPL53 Servo motor-controlled stage, was configured with a micro-plate holder that fit Sedgewick-Rafter slides and an aluminum baseplate that was clamped to the benchtop to reduce vibration. This system was run without the use of a manual joystick that is available and can also control the stage. An Omax M837PL trinocular inverted polarizing microscope with factory stage removed was bolted to the aluminum baseplate. The microscope was fitted with a polarizer (slides into place over the light source), a condenser (which rotates), and a full wave compensation (λ) plate (slides into place). The microscope was fitted with an ocular of 5x and objective lenses of 4, 10, and 20x. The factory stage was removed and therefore the exact magnification could not be calculated by multiplying the ocular by the objective. Hence, magnification was calculated by imaging an American Optical 2-mm reticle and measuring a 100 µm increment on it. The image of the100 µm increment was converted to pixels using ImageJ software and then the camera conversion factor of 3.45µm/pixel (specific to the camera used) was applied to calculate actual magnifications of 7, 21, and 41x for objective lenses 4, 10, and 20x, respectively.

An Infinity model 2-3C eight-megapixel digital microscope camera was fitted onto the microscope using a digital camera extension piece (Fig. 3.1). The camera was further secured by two metal braces that screwed into the side of the camera and rested tightly at the head of the microscope. The braces were secured in place to help maintain camera alignment. Other metal braces were installed at each side of the base of the microscope so that the microscope could be secured to the aluminum baseplate

of the automated stage. The digital camera and automated stage motor controller were connected to a windows PC desktop computer.

The Semprex KPL53 Servo motor-controlled stage was equipped with x, y, and z directions. The z direction is the vertical height the stage can move toward or away from the objective lenses. The height of the stage was adjusted manually so that 9-day old *C. virginica* larvae were in focus, which resulted in younger (2-4 day) and older (> 14 day old) larvae not being in sharp focus. Some Sedgewick Rafter slides did not provide as level a surface as others when placed in the well plate holder of the automated stage. In order to select the best Sedgwick rafter slides, we measured the vertical height at which D-stage larvae were in focus at the four corners and center of several Sedgewick Rafter slides, and chose to use the slides with the least change in height across the slide for processing samples (<0.1 mm difference). We did not use the automatic focus in the z direction (which is available with the automated stage) because setting the autofocus could result in additional processing time (up to 30 s) per bivalve and sometimes there were > 1,000 bivalves in samples from the field.

Software

Custom software was developed to enable the computer to control both the camera and the automated stage so that images could be captured rapidly. The custom software called on libraries from both the automated stage software (Semprex) and the camera software (Software Development Kit (SDK) from Lumen*era*). The custom software was written in Microsoft Visual Basic .NET (VB.NET). Permission from Semprex (Lou Volk, LouV@Semprex.com) and the purchase of the Lumen*era* SDK (available from lumenera.com) was required to use the custom software. The custom

software made calls to both the stage controller and camera. First the custom software signaled the controller to move the stage to a "home" position. After the home position was reached, the stage was then signaled to move in a series of steps down the length of the Sedgwick Rafter slide and the camera was programmed to capture images at designated points. Between each step the program executed a pause (referred to as settling time) to wait for any vibrations to dampen and then the program called the camera to capture an image. This process was repeated until an entire column of the Sedgwick Rafter cell was imaged. The stage then was programmed to move to the next column and capture images in a similar stepwise fashion. This pattern was repeated until the entire area of the slide was imaged. A binning factor was implemented to speed up image acquisition so that a 4x4 pixel square on the camera sensor was summed to become 1 pixel in the final image. This resulted in smaller, brighter images allowing for shorter exposures and less time between successive image captures. The camera captured images in a raw file format created by the 2-3C Infinity camera and this was the format in which images were transferred to the computer. After imaging the Sedgewick-Rafter slide was complete, the raw image files on the computer were converted into BMP images using another custom program. This post-acquisition image processing was implemented to reduce the time needed to capture images and thereby speed up the image acquisition process. After post-processing, the images were ready to be cropped, measured, and classified with the ShellBi software package.

Procedures

Based on tests described in the Assessment section below, recommended steps and procedures were created to optimize the automated image acquisition system and ensure quality control. These steps were 1) maintain alignment, 2) standardize microscope and camera settings, 3) create training set, 4) check color channel intensity, and 5) classify a standard. In addition, recommendations for how to prepare and store field samples for image acquisition were developed.

Maintain alignment. In order to ensure that a Sedgewick Rafter slide was entirely imaged (and therefor all organisms on the slide would be imaged), an alignment protocol was established. A Sedgewick Rafter slide with grid lines was used. After an entire gridded Sedgwick Rafter slide was imaged (n = 1,920 images), the images were stitched together in a mosaic MATLAB (R2012b) software. The mosaic was examined by zooming in on the grid line sections of each slide and checked to 1) ensure that the entire area of the Sedgewick Rafter slide was captured and 2) the grid lines on the slide lined up across the image. If the entire slide was not imaged, the 'home' position was reprogrammed. If the grid lines did not line up, the camera was rotated slightly until proper grid alignment was achieved. This alignment procedure was repeated until the system was aligned. We found that conducting the alignment protocol at least weekly was necessary while samples were being processed.

*Standardize microscope and camera settings***.** Optimal microscope and camera settings were determined and then remained fixed so that consistent images were taken for training sets and unknown specimens. For the microscope, the objective

lens, the light source, and the rotation of the condenser were set. The rotation of the condenser was set by sliding the polarizer into place, focusing on a bivalve shell under full light extinction, and then rotating the condenser until a black cross formed on the shell (see Tiwari and Gallager 2003). Once full extinction was reached, a lambda (λ) plate was then inserted and a magenta background became apparent (see Fig. 2.1). The objective lens used was 4x (see Assessment section for explanation). The light intensity level was controlled using a dial near the base of the microscope. A white line was marked on the base of the scope just above the dial position to ensure the dial did not move from this position. The camera settings were originally chosen in the Infinity Analyze software program which allowed each setting to be named and saved within the program. The settings were then programmed into the custom software where they were saved.

*Create training sets***.** Once optimal settings were chosen and saved, training sets of images of specimens of different species of bivalve larvae were created so that they could be used for classifying unknown specimens and for use in quality control of the automated image acquisition system. The training sets were created from laboratory reared specimen (see Assessment section for information on the specimen library used to create training sets). At least 200 images were used in each category of all training sets based on Thompson et al. (2012).

Check color channel intensity. ShellBi depends on consistent software settings to maintain stable accuracies for bivalve larvae identification (Thompson et al. 2012) although some minor fluctuation is tolerable (see Goodwin et al. 2014). Changes in light intensity, specifically color channel intensity, can alter the color of light detected

on larval shells as well as the background color of the images. We found that color channel intensity fluctuated over the course of a day and over the lifespan of the light bulb in the Omax microscope. Therefore a protocol was developed to measure light intensity of individual RGB color channels (red, green, blue) from a bitmap image using code developed in MATLAB (R2012b). First an acceptable range in variation of color channel intensity was determined, and then a protocol was established to maintain color channel intensities within that range. Color channel intensities were reported as binned values out of a range of 0-255 with 0 being no light and 255 being maximum possible intensity. This range was unit-less and was determined by the 8-bit bit depth of each color channel value that made up the output file (in this case a bitmap image).

An 'acceptable' light intensity range was determined by measuring the daily variation in light intensity, then assessing whether that range affected ShellBi classification accuracies for our target organism, *C. virginica*. First, 'blanks' were taken by imaging the light from the light source without a Sedgewick Rafter or any other slide in the stage. Five of the blank images were then analyzed in MATLAB to calculate the color channel intensity of red, blue, green, and overall average values. This process was repeated hourly over the course of 6 days to determine the variability in color channel intensity, which ranged from 97.0-115.5, 14.0-15.83, 19.9-23.3, and 43.7-51.6 for red, green, blue, and average color channel intensities, respectively. A 'quality control' training set was created by capturing and cropping images of *Crassostrea virginica*, *Ischadium recurvum*, and *Rangia cuneata* (n = 200 for each species) when color channel intensity was set to the mean of the average

color channel intensities (49.9). This training set was used to classify three sets of 50 images of 9-day old C. *virginca* larvae which had been captured at the mean, maximum, and minimum of the daily range in color channel intensities and then cropped. Classification accuracies of *C. virginica* ranged from 92-100%, indicating that the maximum and minimum in daily color channel intensity fluctuations resulted in high classification accuracies and provided an acceptable range.

Once the acceptable range in color channel intensities was determined, five blanks were captured and analyzed three times per day to ensure color channel intensity values remained within the acceptable range. If the color channel intensities were not within the acceptable ranges, the intensity of the light source was adjusted until they were within the acceptable range or the bulb was replaced on the microscope.

Repeated classification of a standard. A performance-based test was conducted to ensure quality control for the automated image acquisition system. Specifically, 50 images of 9-d-old *C. virginica* larvae were imaged once per week, cropped, and then classified using the ShellBi software with the 'quality control' training set (described above). This helped ensure that high classification accuracies were maintained over the months that field samples were being imaged.

Preparing field samples for image acquisition. New protocols were developed for preparing field samples for imaging bivalve larvae by reducing the number of other organisms and small sediment particles present in the sample and by removing tissue of the larvae which inhibits detection of birefringent patterns in veliger and pediveliger larvae. Samples collected from the Choptank River were stored in 200 ml

jars with 4% formalin seawater solution buffered with sodium borate. Under a fume hood, a sample was poured through a 350 µm sieve into a 300 ml beaker to remove larger particles. The sample in the beaker was poured through a 44 µm sieve. The 44 µm sieve was rinsed using 40% bleach and 60% Deionized (DI) water buffered with sodium borate into a centrifuge tube. The sample was left for 20 minutes to digest tissue and break apart valve hinges and then poured through another 44 µm sieve. The sample was then rinsed from the sieve into a 15 ml centrifuge tube using buffered DI water (buffered with sodium borate) and left for five minutes to settle (the time it took for the smallest shells to sink to the bottom). The supernatant was carefully pipetted off until a 2 ml sample volume was left in the tube. The supernatant was discarded after observing that no bivalve larvae were present (n = 270). The remaining sample was mixed and resuspended within the 2 ml of solution by pipetting the sample up and down 3-4 times within the centrifuge tube (in an up and down fashion avoiding circular motion). Then a 1-ml aliquot was pipetted from the centrifuge tube and placed (from left to right) onto the center of a Sedgewick Rafter slide (non-gridded). A coverslip was carefully placed on top of the Sedgwick Rafter slide and the slide was then placed in a well plate holder on the automated stage. The remaining 1-ml aliquot was pipetted onto another Sedgewick Rafter slide in the same manner.

Subsamples of the two aliquots were conducted by imaging half of the Sedgwick Rafter slide (lengthwise). Tests performed indicated that the first 1-ml aliquot pipetted onto the Sedgewick Rafter slide had unequal numbers of larvae compared with the second aliquot, but that there was no statistically significant difference in the number of bivalve shells on the left compared to the right half of

each slide (Students t-test, $p = 0.37$, $n = 60$). Therefore, half of each slide with the first and second 1-ml aliquots was imaged. By imaging half of each slide in 23 min (including start up time), 50% of the sample was imaged. Note that the count of larvae in a plankton sample would be calculated as two times the number of ROIs (to take into account the 50% subsampling) divided by two (to take into account the fact that each larva had two shells).

Images of known specimens that were reared to create training sets underwent the same procedure, except that sieving was not necessary and full slides (rather than 50%) were imaged.

Sample storage. Sample storage considerations are important for this method. Although Goodwin et al. (2014) found no difference in classification accuracy using ShellBi when samples were preserved in buffered 95% ethanol or buffered 4% formaldehyde, buffered 4% formaldehyde solution should be used for long term storage > 2 yrs because shells of bivalve larvae stored in buffered 95% ethanol cracked after two years (Goodwin, Thompson pers. obs.). To prepare samples for long term storage, the samples should be preserved with 4% formaldehyde buffered to a pH of 8.0-8.1with sodium borate (pH 10.1). The pH of the samples should be monitored over time. O'Meara et al. (2013) found that birefringence is lost on veliger mussel (*Dreissena bugensis*) larvae if they are not stored in basic (pH 7.0-9.0) conditions. However, larval shells can dissolve when sample pH drops below 8.0 (Goodwin, pers. obs). Therefore, pH should be tested one or two days after sample collection, after the first week, after the first month and then quarterly thereafter. If

pH drops near or below 8.0, buffer should be added to bring pH back up to the 8.0-8.1 ranges, then retested a few days to a week later to ensure that the pH remains stable.

Assessment

Tests were conducted to evaluate the automated image acquisition system and improvements to the ShellBi software in order to attain optimum classification accuracies. Specifically, magnification and image resolution, color channel intensity, ROI detection, and camera software settings were assessed. Finally, two blind validation experiments were conducted to test classification accuracies of the automated image acquisition system.

An image library of the shells of bivalve larvae was used in these tests. Eight bivalve species that are found in Choptank River were spawned, their larvae were reared and images of their shells were used for all tests. The adult bivalves that were collected from the Choptank River and reared in the laboratory consisted of: *Ischadium recurvum* (hooked mussel), *Mulinia lateralis* (dwarf surf clam), *Mytilopsis leucophaeata* (dark false mussel), *Macoma mitchelli* (matagora macoma clam), *Rangia cuneata* (Atlantic rangia clam), and *Tagelus plebeius* (razor clam). Larvae of *Crassostrea virginica* (eastern oyster) were obtained from the Horn Point Hatchery and *Guekensia demissa* (marsh mussel) were obtained from the Rutgers Cape Shore Laboratory. Spawning and rearing procedures were consistent with summer conditions in Choptank River and were explained in detail (see Goodwin et al. 2014) for all species with the exception *G. demissa*. The *G. demissa* larvae were reared in

conditions similar to Delaware Bay at a temperature of 24.9 ^{o}C at a salinity of 22.5 and fed *Isochrysis galbana*, *Pavlova lutheri*, and *Chaetoceros calcitrans*.

Magnification and image resolution tests

The objectives of the magnification and image resolution tests were 1) to choose the lowest magnification that resulted in high classification accuracies and the fastest image acquisition time, and 2) to determine how changes in image resolution within the ShellBi software influenced classification accuracies. Previous research with the ShellBi technique was conducted at a magnification of 50x (Thompson et al. 2012, Goodwin et al. 2014). To test a range of magnifications, the automated stage and software was used to image bivalve larvae on a Sedgewick Rafter slide at three different magnifications: 7, 21, and 41x. It took 46, 120, and 160 minutes to image a slide at magnifications of 7, 21, and 41x, respectively. Images of bivalve larvae were captured at each magnification using consistent hardware and software components, except that objective lenses (4, 10, and 20x) were changed to create the different magnifications.

Training sets composed of 200 images of four species of bivalve larvae (*C. virginica*, *I. recurvum*, *R. cuneata*, and *M. leucophaeata*) (n = 800 total images) were created and used to classify 'unknown' images of each species (n = 25 for each species). These training sets were created for each magnification and images of the 'unknown' specimens were also captured at each magnification.

In addition to testing the effect of magnification on classification accuracy, the influence of image resolution within the ShellBi software was also determined. In the research performed by Goodwin et al. (2014), the software did not reduce the

resolution of images. The resolution of images taken at different magnifications was reduced by 40, 20 and 0% and classification tests were performed to determine the influence of image resolution on classification accuracies.

Classification accuracies of images captured at different magnifications and with different image resolutions ranged from 88-100%. Classification accuracy for images taken under magnification settings of 7x were highest for all four species (98-100%) regardless of the reduction setting used (Table 3.2). There were no differences in classification accuracy when image resolution was reduced at a magnification of 7x and little difference in accuracies (< 1%) when image resolution was reduced at magnifications of 21x or 41x. Based on the results of these classification tests, it was concluded that the low magnification setting of 7x yielded highest accuracies and fastest sample imaging time (46 min) and that reducing image resolution in the software had a little effect on classification accuracy.

Color channel intensity

Over a period of 100 days, color channel intensities were measured and monitored and a standard set of 50 images of 9-day old *C. virginica* larvae were classified (Fig. 3.2) as part of the protocol for maintaining high classification accuracies (described in the Materials and Procedures section). Classification accuracies were consistent (98-100%) until the color channel intensity for red, green, and blue dropped. The intensity drop was due to a faulty light bulb which led to lower classification accuracy (70%) of the standard unknown set. The light bulb was replaced and color channel intensity was restored to acceptable levels, as indicated by classification tests (98-100%) (Fig. 3.2). Based on these observations, color channel

intensity influences the classification accuracy of ShellBi and should therefore be monitored daily to be maintained within an acceptable range.

ROI detection

Tests were conducted to assess the ability of the updated ROI detection software to automate the post processing of images. Samples (n = 23) that included oysters (*C. virginica*), mussels (*G. demissa*, *I. recurvum*), and clams (*M. mitchelli*, *M. lateralis*, *M. leucophaeata*, *R. cuneata*, *T. plebeius*) were imaged with the automated image acquisition system. The larvae that were imaged ranged in ages (2-16 days) and lengths (44-330 µm). Images with birefringence were sorted into folders using the automated sorting software. Trained technicians counted the bivalve shells in the folders, after which the automated ROI detection software was used to enumerate the number of ROIs in the images. The same procedure was repeated with 30 samples (200 l^{-1}) that had been collected from the Choptank River in July of 2012. These samples included clam, mussel and oyster larvae of various sizes.

When applied to clean samples with specimens that had been reared in the laboratory or hatchery, the counts of bivalve larvae generated by the automated ROI detection software compared favorably with those of trained technicians, except at very high numbers of bivalve larvae (> 800) but did not compare favorably for field samples (Fig. 3.3). The automated ROI detection software performed better on laboratory reared specimen than it did on the field-collected samples (Fig. 3.3). For field samples, the automated ROI detection software systematically underestimated the number of bivalve larvae compared to trained technicians (Fig. 3.3). Based on these results, we conclude that this software has use in laboratory and hatchery

applications but field samples should be manually cropped until further improvements in the software are made.

Camera software setting performance

Tests were conducted with the automated image acquisition system to determine the influence of camera software settings on the performance of ShellBi. Five different camera settings (labeled 1-5) were created by altering specific attributes in the Infinity Analyze software program (Table 3.3). Varying the attributes created different backgrounds in the images (Fig. 3.4). All settings and attributes were identical except for the exposure, gain, light source setting, saturation, brightness, contrast, and hue. Five three-species training sets composed of 200 images each of *C. virginica*, *I. recurvum*, and *R. cuneata* were created with images taken under the five settings using the automated image acquisition system. A larger training set (labeled "All (1-5)") was constructed as a compilation of the five different training sets (n=3,000 images).

The six training sets were used to classify 150 images of "unknown" *C. virginica*, *I. recurvum*, and *R. cuneata* (50 images of each species) which were taken under each of the five settings, for a total of 30 tests of ShellBi classification accuracy (Table 3.4). Classification accuracies for unknown *C. virginica, I. recurvum, and R. cuneata* ranged from 4 to 100% and differed between species and between camera settings (Table 3.4 A-D). In general, the highest accuracies (82-100%) occurred when the settings of the training sets and those of the 'unknown' sets were the same (Fig. 3.4, especially overall accuracies reported in panel D). The training set composed of images taken under all settings (All(1-5)) had classification accuracies from 85-95%.

These tests indicate that using the same settings for training sets and the unknown images yielded high overall classification accuracies and that different settings may be optimal for different species.

Validation experiments

Two validation experiments were conducted to assess the accuracy of both the ShellBi software and trained technicians to classify images of shells of bivalve larvae which had been captured using the automated image acquisition system.

Three training sets were constructed with the automated imaging acquisition system and used to classify shells of bivalve larvae with ShellBi in both validation experiments. These training sets were composed of images of eight species of bivalve larvae found in the Choptank River grouped into three categories (oysters: *C. virginica;* mussels: *I. recurvum, G. demissa;* clams: *M. leucophaeata, M. lateralis, M. mitchelli, R. cuneata,* and *T. plebeius*). Each category included images of larvae of different ages. One training set, called COM1000, had 1,000 images per category (Table S3.1) and was taken with camera settings 2 (Table 3.3). A second training set (COM700) was composed of images using setting 1 (Table 3.3). Furthermore, COM700 contained fewer total images of bivalves (700 images per category), fewer images of *M. lateralis* and *T. plebeius* and no images of *G. demissa*. However, different ages and species were all represented as equally as possible (Table S3.1). The third training set (COM1700) was simply a combination of COM700 and COM1000, so that each category had 1,700 images.

Each validation experiment consisted of 18 separate tests of the ability of trained technicians and ShellBi to identify images of *C. virginica* from those of other

bivalves. The 18 tests were each composed of 100 ‘unknown’ images (n = 1,800 total unknown images). Unknown images for validation One were taken under the same settings as the training set COM1000. Unknown images for validation Two were taken under the same settings as COM700. For each experiment, a lab member (who did not undertake classifications) created 18 folders which contained 100 images of different ages of *C. virginica, I. recurvum, G. demissa, M. leucophaeata, M. lateralis, M. mitchelli, R. cuneata, and T. plebeius*. Care was taken to vary the number of images of species and ages (sizes) to simulate differences that might be found in field samples (e.g., the number of *C. virginica* in folders ranged from zero to 44). For validation test Two, there were no *G. demissa* images and fewer *M. lateralis* and *T. plebeius* because specimens were not available (Table S3.1). The original folders that contained the species name and age were stored on a password protected secure server. For the validation experiments, a copy of the 18 folders was created and all images were renamed so that the identity and ages of the bivalves would not be known by the trained technicians who undertook the classifications.

Two trained technicians used the training sets COM1000 (for experiment one) and COM700 (for experiment two) as visual keys to assist with identifying the images of bivalve larvae within the 18 folders for each experiment. They sorted images of oysters into separate folders. Misclassification was assessed by matching each of these images to those in the original folders stored on the server to determine if each image was *C. virginica* and noting if any *C. virginica* images were not correctly identified (i.e., only true positives were counted).

In addition, images in each of the 18 folders were classified using ShellBi and each of the three training sets. Misclassifications for ShellBi were calculated using a script written in MATLAB that calculated true positives (in this case *C. virginica* larvae that were properly classified).

Trained technicians were able to classify images of *C. virginica* larvae with high accuracies (> 92% on average for both validation experiments) (Table 3.5). In contrast, classification of images of *C. virginica* with ShellBi ranged from averages of 60 to 94% for both experiments. ShellBi had highest accuracies (80 to 93% on average) when training sets contained images of larvae that were taken under the same settings as those of the "unknown" images. Accuracies dropped (60-74% on average) when training sets were used to classify "unknown images" that had been taken under different settings (Table 3.5). Based on these tests, we conclude that the automated image acquisition system can capture images which can be classified with high accuracy by a trained technician. In addition, this system can be used with ShellBi to successfully classify images with high speed and accuracies > 85% on average for *C. virginica* larvae from the Choptank River of Chesapeake Bay, as long as camera settings used to create training sets and unknown images correspond. We recommend that trained technicians check and correct ShellBi classifications, thereby ensuring high accuracies while taking advantage of the rapid image classification by the ShellBi software.

Discussion

Our goal was to create an automated image acquisition system and improve ShellBi software (Thompson et al. 2012, Goodwin et al. 2014) to rapidly and accurately identify and measure larvae of a target bivalve species (*C. virginica*). Results indicate that automated image acquisition system at 7x magnification was able to image an entire Sedgewick Rafter slide in 46 min. In addition, the ShellBi software distinguished *C. virginica* larvae that were imaged with the system with high accuracies (>85% on average) which could be improved to >92% on average if a trained technician were to check and correct the computer-based classifications. The increase in sample processing time was faster than previous efforts where manual image acquisition was needed to pre-process images for ShellBi (Goodwin et al. 2014).

Our research showed that higher accuracies and faster processing times could be achieved with lower (7x) magnifications. Previous research with the ShellBi technique was conducted at magnifications of 50x (Thompson et al. 2012, Goodwin et al. 2014). The higher accuracy when using lower magnification could be because the Support Vector Machine that the ShellBi software uses to distinguish between species works better with less information because details in texture features and color angles are smoothed out at lower resolutions. Further testing may reveal that magnifications lower than 7x could be equally accurate, although there may be a point at which lower magnifications would have too little information to distinguish larvae, especially for small D-stage larvae.

The automated ROI detection performed well for laboratory-reared samples but poorly for field samples (Fig. 3.3). This was mostly due to other birefringent material in the samples from the eutrophic Choptank River (Fig. 3.5). This material confounded the edge detection and ROI extraction process. Performance may be better in oligotrophic waters if there are less birefringent particles there. Further improvements in the software may enable more accurate ROI detection and automated cropping. Newer ROI detection methods are constantly being developed for many applications in the medical field (Chun-Chu and Shyr-Shen 2015, Molder et al. 2015, Vishrutha and Ravishankar 2015). Improvements could help ROI extraction for ShellBi and should be evaluated in future studies. However, without any further advances, our automated ROI detection software could be used "as is" in laboratory or hatchery conditions for bivalve larvae counts in a rapid manner.

Bachiller et al. (2012) recommended an internal control mechanism to check the quality of the procedure used for counting and classifying zooplankton (or bivalve larvae in this case) given all of the rapid development of imaged-based methods. We set up an internal control method by establishing a standard set of 9-d-old *C. virginica* larvae to be classified weekly by a previously established training set (Fig. 3.2). This system proved to be very useful to gauge hardware consistency with a performance based metric (classification). In addition, alignment protocols were established to ensure accurate counts of bivalve larvae.

Camera settings were an important determinant of classification accuracy for this method. Training sets used to classify unknown sets imaged under the same camera setting were more accurate than training sets used to image unknowns under

different settings (Table 3.4). The training sets taken under each of the five settings resulted in high classification accuracies of the unknown groups imaged under the corresponding five settings, despite differences between settings (Fig. 3.4), which suggests that the ShellBi technique is robust even when camera settings vary. The tests also indicate that different settings may be optimal at identifying different species (Table 4A-C). Therefore, we recommend that settings should be tested for target species so that optimal classification performance can be achieved.

Thompson et al. (2012) have shown that the ShellBi technique may be more accurate than quantitative PCR and much faster than traditional light microscopy techniques (Carriker 1996) although the latter may still be the most accurate way to identify bivalve larvae to date. The initial set up of ShellBi requires the establishment of known training sets composed of larvae that were reared in similar conditions to the larvae being sampled and identified from the field which can be labor intensive (Thompson et al. 2012, Goodwin et al. 2014). After a specimen library is established, capturing images with our automated image acquisition system and classifying them with ShellBi software is the fastest way to identify and measure *C. virginica* in the Choptank River to date.

Comments and recommendation

We recommend that protocols be established for maintaining classification accuracy over time, which include: 1) systematic sample preparation, 2) repeated checks of the alignment of the camera and stage, 3) monitoring of color channel light intensity, and 4) repeated classification of a standard.

In keeping with previous assessments of this method (Thompson et al. 2012, Goodwin et al. 2014), we recommend that unknown larvae be imaged using the same microscope and camera settings as those for the training sets. We also recommend that validation studies (similar to those in this manuscript) be conducted when using this technique in different systems and with different species of interest. The validation experiments showed that *C. virginica* larvae could be identified with accuracies >85% on average for the ShellBi software and >92% on average for the trained technicians. Therefore, as suggested in Goodwin et al. (2014), the speed of the ShellBi classification technique could be augmented by the high accuracies of a trained technician if a technician checks and corrects the images classified by ShellBi. Because the ShellBi software sorts images into folders for each category of the training set, a trained technician can quickly scan the images to determine if any are out of place.

Future directions for ShellBi involve using a random forest algorithm and online training sets for faster identification (Gallager, pers comm.). In addition, the automated image acquisition system is being tested for imaging copepods (North and J. Pierson, pers. comm.) and the technique could be used to image pteropods as well (Goodwin, pers. obs.). ShellBi (for organisms that exhibit birefringence) and the automated image acquisition system (for plankton in general) could advance our understanding of eutrophic and coastal systems around the world by allowing rapid image acquisition and classification of species that require magnification for identification.

Literature cited

Bachiller, E., J.A. Fernandes, and X. Irigoien. 2012. Improving semi automated zooplankton classification using an internal control and different imaging devices. Limnol. Oceanogr. Methods. 10:1-9. [doi:10. 4319/ lom. 2012. 10. 1].

Benfield, M.C., P. Grosjean, P.F. Culverhouse, X. Irigoien, M.E. Sieracki, A. Lopez-Urrutia, H.G. Dam, Q. Hu, C.S. Davis, A. Hansen, C.H. Pilskaln, E.M. Riseman, H. Schultz, P.E. Utgoff, and G. Gorsky. 2007. RAPID: Research on Automated Plankton Identification. Oceanogr. 20(2):172–187. http://dx.doi.org/10.5670/oceanog.2007.63.

Carriker, M.R. 1996. The Shell and Ligament, *In* V.S. Kennedy, R.E. Newell, and A. F. Eble (eds.), The Eastern oyster *Crassostrea virginica*. Maryland Sea Grant. p. 75-159.

Chanley, P., and J.D. Andrews. 1971. Aids for identification of bivalve larvae of Virginia. Malacol.11:45–119.

Cowan, R.K., and Guigand, C.M. 2008. *In situ* ichthyoplankton imaging system (ISIIS): system design and preliminary results. Limnol. Oceangr. Methods. 6:126-132.

Davis C.S., S.M. Gallager, M. Marra, and W.K. Stewart. 1996. Rapid visualization of plankton abundance and taxonomic composition using the Video Plankton Recorder. Deep Sea Res. Part II. 43(7-8):1947-1970.

Gaines, S., and J. Roughgarden. 1985. Larval settlement rate: A leading determinant of structure in an ecological community of the marine intertidal zone. Proc. Natl. Acad. Sci. USA. Ecology. 82:3707-3711.

Gallager, S., and S. Tiwari. 2008. Optical method and system for rapid identification of multiple refractive index materials using multiscale texture and color invariants. *United States Patent 7,415,136*. Washington, DC: U.S.

Garland, E.D., and C.A. Zimmer. 2002. Techniques for the identification of bivalve larvae. Mar. Ecol. Prog. Ser. 225:299-310 [doi:10. 3354/ meps225299].

Goodwin, J.D., E.W. North, and C.M. Thompson. 2014. Evaluating and improving a semi-automated image analysis technique for identifying bivalve larvae. Limnol. Oceanogr. Methods 12:548-562.

Gorsky, G., M.D. Ohman, M. Picheral, S. Gasparini, L. Stemmann, J. Romagnan, A. Caweood, S. Pesant, C. Garcia-Comas, and F. Prejge. 2010. Digital zooplankton image analysis using the ZooScan integrated system. J. of Plank. Res. 32(3):285-303.

Grosjean, P., M. Picheral, C. Warembourg, and G. Gorsky. 2004. Enumeration, measurement, and identification of new zooplankton samples using the ZOOSCAN digital imaging system. J. Mar. Sci. 61:518-525.

Hare, M.P., S.R. Palumbi, and C.A. Butman. 2000. Single-step species identification of bivalve larvae using multiplex polymerase chain reaction. Mar. Biol. 137:953-961 [doi:10.1007/ s002270000402].

Hendriks, I.E., L.A. Van Duren, and P. M. J. Herman. 2005. Image analysis techniques: a tool for the identification of bivalve larvae? J. Sea Res. 54:151-162. [doi:10. 1016/ j. seares.2005. 03. 001].

Henzler, C.M., E.A. Hoaglund, and S.D. Gaines. 2010. FISHCS—a rapid method for counting and sorting species of marine zooplankton. Mar. Ecol. Prog. Ser. 410:1-11 [doi:10.3354/ meps08654].

Kennedy, V.S. 1996. *In:* V.S. Kennedy, R.E. Newell, and A.F. Eble (eds.), The eastern oyster *Crassostrea virginica*. Maryland Sea Grant p. 371-421.

Larsen, J.B., M.E. Frischer, L.J. Rasmussen, and B.W. Hansen. 2005. Single-step nested multiplex PCR to differentiate between various bivalve larvae. Mar. Biol. 146:1119-1129. [doi:10.1007/s00227-004-1524-2]

Lutz R, J. Goodsell, M. Castagna, S. Chapman, R. Newell, H. Hidu, R. Mann, D. Jablonski, V. Kennedy, S. Siddall, R. Goldberg, H. Beattie, C. Falmagne, A. Chestnut, A. Partridge. 1982. A Preliminary observation on the usefulness of hinge structure for identification of bivalve larvae. J. Shell. Res. 2:65–70.

MacLeod, N., M. Benfield, and P. Culverhouse. 2010. Time to automate identification. Nature, 467:154-155.

Molder, A., S. Drury, N. Costen, G. M. Hartshorne and S. Czanner. 2015. Semiautomated analysis of embryoscope images: Using localized variance of image intensity to detect embryo developmental stages. Cytometery. 87A(2):119-128.

O'Meara, S., D. Holser, S. Brenimer, and S.F. Pucherelli. 2013. Effect of pH, ethanol concentration, and temperature on detection of quagga mussel (*Dreissena bugensis*) birefringence. Manag. of Biol. Invas. 4(2):135-138.

Steele, J.H. 1989. The ocean 'landscape'. Landscape Ecol. 3:185-192.

Tiwari, S., and Gallager, S. 2003. Machine learning and multiscale methods in the identification of bivalve larvae. Proceedings of the Ninth IEEE International Conference on Computer Vision, Nice, France, October 14-17, 2003. [doi:10. 1109/].

Thompson, C.M., S.M. Gallager, and M. Hare. 2012. Semi-automated analysis for the identification of bivalve larvae from a Cape Cod estuary. Limnol. Oceanogr. Methods. 10:538-554 [doi:10. 4319/ lom. 2012. 10. 538].

Vishrutha, V., and M. Ravishankar. 2015. Early detection and classification of breast cancer. Proc. of 3rd international conference of Frontiers of Intelligence Computing: Theory and Applications. 327:413-419. 10.1007/978-3-319-11933-5_45.

Wiens, J.A. 1989. Spatial scaling in ecology. Functional Ecol. 3:385-397.

Zetsche, E. M., A.E. Mallahi, F. Dubois, C. Yourassowsky, J.C. Kromkamp, and F J. Meysman. 2014. Imaging-in-Flow: Digital holographic microscopy as a novel tool to detect and classify nanoplankton organisms. Limnol. Oceanogr. Methods. 12:757-775.

Tables and Figures

Table 3.1. The components, company, model and price (United States dollar) of the automated image acquisition system in 2012. The automated stage and Semprex software is available with several options and the price here includes all components needed to run the stage in the x, y, and z planes. ShellBi software is sold separately and is available from Scott Gallager at Woods Hole Oceanographic Institute.

Component	**Company**	**Model**	**Price**
Digital camera with software	Lumenera/Infinity	2-3C Need stage model number with AMICron	$2,300
Automated stage with software	Semprex	3.2 software	$11,663.9
ShellBi software			
Trinocular polarizing microscope	microscope.net	M837PL	$1,299.99
SDK Lumenera software	Lumenara/Infinity	SDK 2011	$695
Desktop computer	Dell	Optiplex 7010	$917.73
Sedgwick Rafter gridded/ungridded	Cole-Parmer	1801-A10/G20	$135/48 each
Total			**$17,059.62**

Table 3.2. The percent classification accuracy for four 'unknown' bivalve species when images in training and 'unknown' sets were captured under different microscope magnifications and when image resolution was reduced prior to classification. Each training set was composed of 200 images of shells of *Crassostrea virginica* (CV), *Ischadium recurvum (IR), Rangia cuneata* (RC), and *Mytilopsis leucophaeata* (DF)) for a total of 800 images. The training sets were then used to classify 25 images of shells of CV, IR, RC, and DF as 'unknowns'. For each test, the training set images and 'unknown' images were captured under the same magnification and software reduction setting. The different magnifications were applied by changing the objective lenses on the hardware. Image resolution was reduced within the ShellBi software.

			Percent accuracy			
Test	**Percent reduction in image resolution (software)**	**Magnification (hardware)**	CV	DF	IR	RC
1	40	7 x	98	98	100	100
2	40	21 x	97	95	99	100
3	40	41 x	94	88	98	96
4	20	7 x	98	98	100	100
5	20	21 x	96	95	99	100
6	20	41 x	94	88	99	96
7	0	7 x	98	98	100	100
8	0	21 x	97	96	99	100
9	0	41 x	94	89	98	95

Table 3.3. Software configurations of five different settings for the digital camera. The five settings 1-5 were created by changing attributes in Infinity Analyze software including exposure, gain, gamma, light source, saturation, brightness, contrast and the red and green hues. Note: the actual light source was kept constant but the setting choice for "Light source" in the software program was adjusted. The configuration of blue light (1.0), averaging (1), subsampling (1), interval (1 s), and duration (10 s) were held constant across settings.

Setting name	Exposure	Gain	Gamma	Light source	Saturation	Brightness	Contrast	Red	Green
1	151.0	10.6	0.82	fluorescent	1.31	4	4	1.0	1.0
2	151.0	15.2	0.82	fluorescent	1.31	4	4	1.0	1.0
3	89.1	21.4	0.82	Incandescent	1.00	0	0	1.0	1.0
4	84.5	15.2	0.82	Incandescent	1.31	4	4	1.3	1.3
5	270.8	4.4	1.4	fluorescent	1.00	5	28	1.0	1.0

Table 3.4. Classification accuracies for images of shells of A) *C. virginica*, B) *I. recurvum*, C*) R. cuneata*, and D) all three bivalves classified under five different camera settings (1-5). Training sets (rows) were used to classify 'unknown' sets (columns). Each group was imaged under different camera settings (1-5, details in Table 3). The sixth training set, "All1-5", was composed of images captured at all five settings.

		Unknown set				
A) *C. virginca*	**Training set**	**1**	**2**	**3**	**4**	**5**
	1	92	94	84	88	26
	2	84	94	66	66	94
	3	88	82	96	96	42
	4	4	80	52	84	18
	5	4	92	32	16	94
	All(1-5)	96	88	96	88	88
B) *I. recruvum*		**1**	**2**	**3**	**4**	**5**
	1	90	82	90	72	88
	2	70	88	82	80	88
	3	84	74	90	74	84
	4	98	54	54	94	60
	5	98	66	90	44	82
	All(1-5)	88	84	86	84	84
C) *R. cuneata*		**1**	**2**	**3**	**4**	**5**
	1	100	98	100	2	92
	2	48	98	78	0	12
	3	90	96	96	4	76
	4	0	0	0	100	6
	5	40	94	50	38	100
	All(1-5)	100	84	100	84	84
D) All species		**1**	**2**	**3**	**4**	**5**
	1	94	91	91	54	69
	2	67	93	75	49	65
	3	87	84	94	58	67
	4	34	45	35	93	28
	5	47	84	57	33	92
	All(1-5)	95	85	94	85	85

Table 3.5. Classification accuracies for images of shells of *C. virginica* from two validation experiments. Each validation experiment contained multiple tests that were designed to compare classification accuracies by trained technicians with the ShellBi classification software. In each test, 100 images of shells of one-seven species of bivalve larvae, with varying numbers of *C. virginica* shells, were classified. For the tests of the ShellBi software, three different training sets (COM700, COM1000, and COM1700) were used which contained images captured under different microscope settings. The image capture settings for COM1000 matched the settings at which the 'unknown' images in experiment One were captured. The image capture settings for COM700 matched those of the 'unknown' images in experiment Two (corresponding to setting 1 in Table 3.3 and Fig. 3.4). The COM1700 training set was composed of images from both COM700 and COM1000. A '.' indicates that no *C. virginica* larvae were present. 'Cumulative accuracy' was calculated as the total number of true positive classifications for C. *virginica* divided by the total number of *C. virginica* images in all tests combined, multiplied by 100.

A) Validation experiment One

	Images of	Trained technician		ShellBi softwar	
Test	*C. virginica*	**Goodwin**	**Wingate**	**COM700**	**COM1000**
1	41	98	98	46	93
2	1	100	100	0	0
3	0	.	.	.	.
4	8	100	38	75	75
5	20	100	90	65	95
6	0	.	.	.	.
7	16	100	100	38	94
8	19	100	100	74	95
9	5	100	80	80	80
10	0	.	.	.	.
11	16	100	100	100	88
12	26	88	96	88	96
13	7	100	100	100	86
14	10	100	100	80	100
15	5	100	100	100	80
16	0	.	.	.	.
17	19	100	84	95	95
18	7	100	100	100	100
	mean	**99**	**92**	**74**	**84**
	std	3	16	28	24
	cumulative accuracy	**98**	**94**	**73**	**92**

B) Validation experiment Two

	Images of	Trained technician		ShellBi softwar	
Test	*C. virginica*	**Goodwin**	**Wingate**	**COM700**	**COM1000**
1	15	100	100	93	60
2	44	100	75	84	86
3	5	40	80	100	80
4	26	100	100	88	96
5	5	100	100	100	60
6	0	.	.	.	.
7	15	100	100	100	47
8	37	86	100	100	84
9	13	100	100	100	77
10	15	100	100	93	93
11	35	100	100	86	60
12	19	100	100	95	47
13	4	100	100	100	25
14	16	100	100	81	69

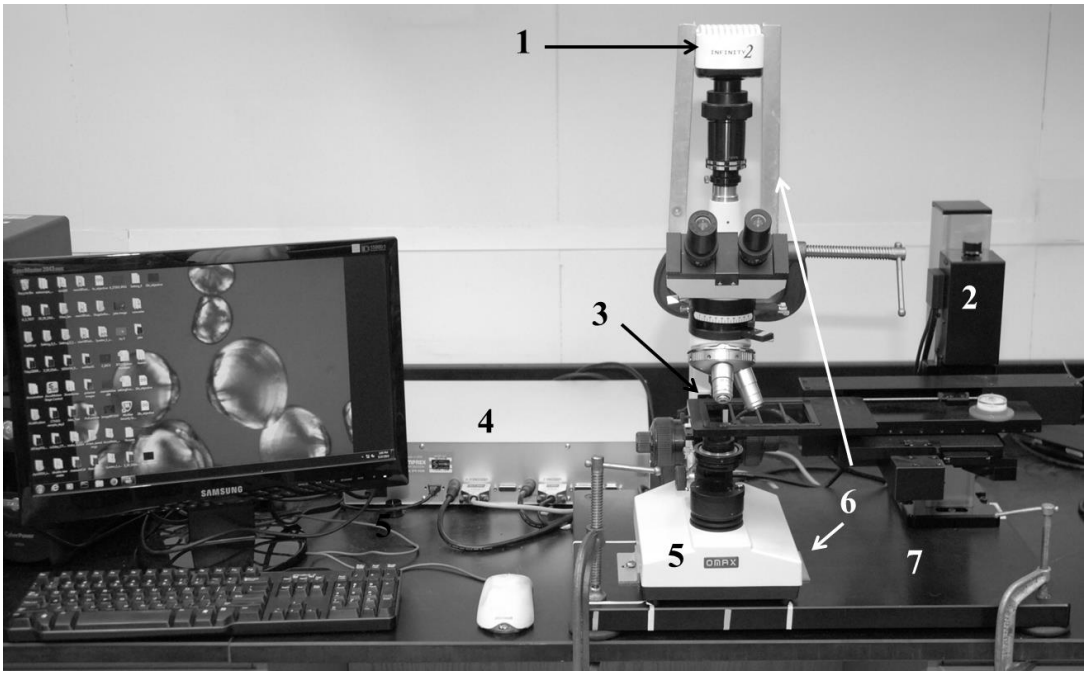

Fig. 3.1. Automated imaging acquisition system composed of 1) Infinity 2-3C digital microscope camera with metal braces on each side, 2) Semprex automated stage motor, 3) Semprex automated stage with Sedgwick Rafter slide in well plate holder, 4) stage motor controller hub, 5) Omax inverted polarizing microscope with metal braces on each side of base, 6) four metal braces (two on each side), and 7) aluminum baseplate clamped to benchtop.

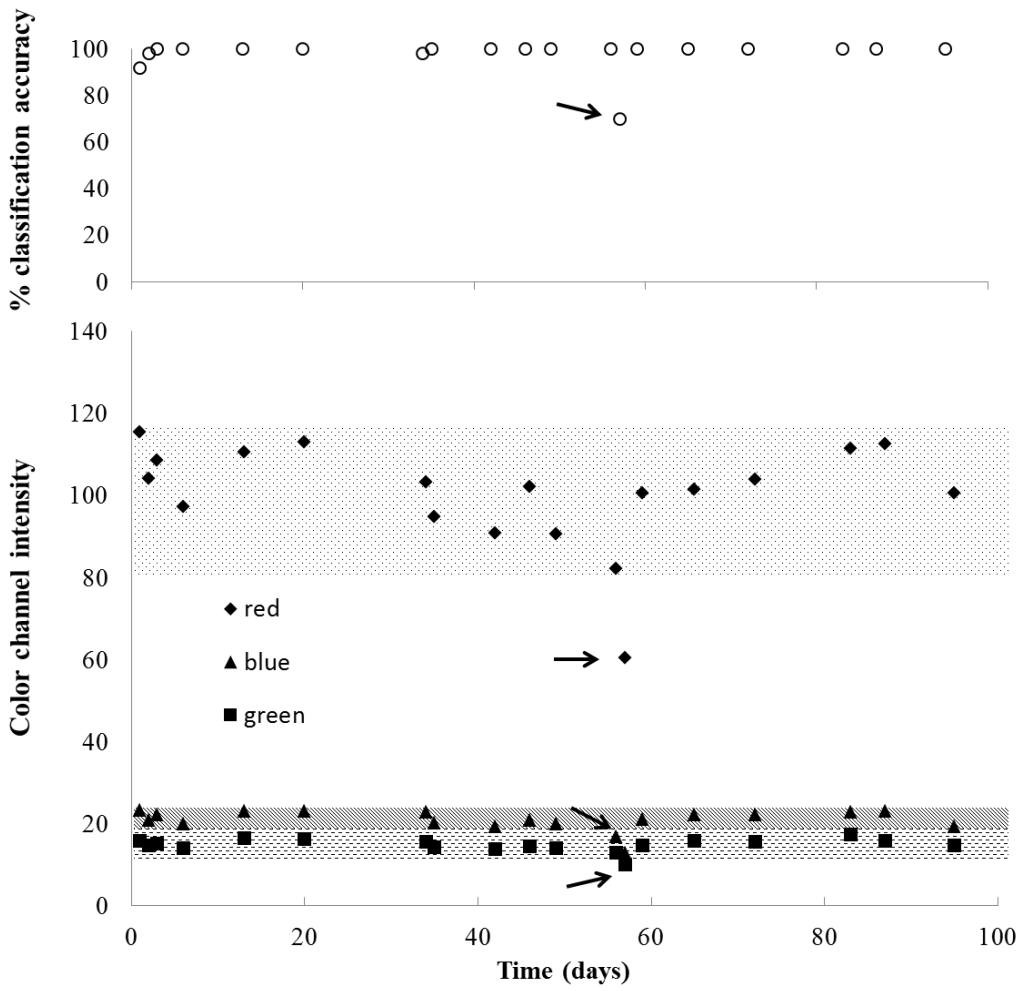

Fig. 3.2. Percent classification accuracy of 9-d- old *C. virginica* larvae (upper panel) and concurrent color channel intensity measurements (bottom panel) taken over a span of 100 days. Each data point for classification accuracy was the result of classifying 50 images of 9-d-old *C. virginica* using a three species training set (*C. virginica, I. recurvum, and R. cuneata*). The color channel intensity values were calculated using five blanks captured from the automated stage and were compared to the acceptable range (hatched regions) (see Procedures section). Arrows indicate the time when color channel intensity values dropped below the acceptable range due to a microscope light bulb malfunction, and when percent classification accuracies also dropped (from an average of 98 to 70%).

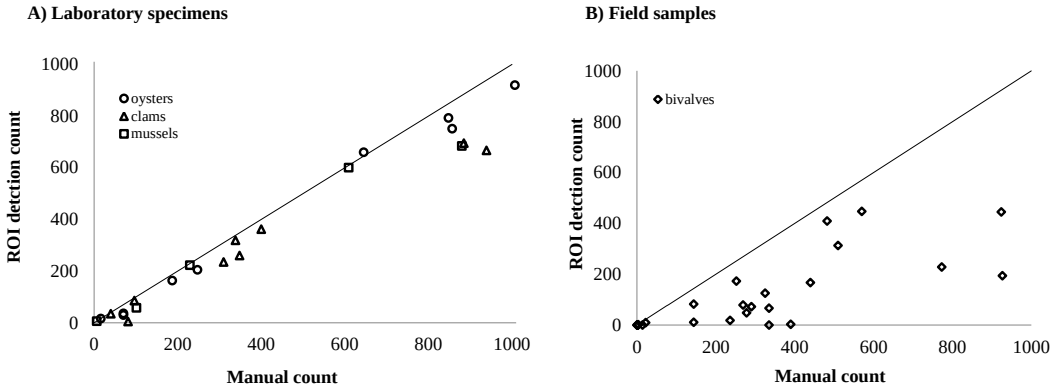

Fig. 3.3. The number of shells of bivalve larvae in A) samples containing laboratory specimens (n = 23), and B) field samples (n = 30) which were detected by the automated ROI detection software (y-axis) versus those counted by a trained technician (x-axis). The line indicates a 1:1 ratio between counts of bivalve shells by trained technicians and the automated ROI detection software. Both the laboratory specimens and field samples contained species of oyster, clams, and mussel larvae.

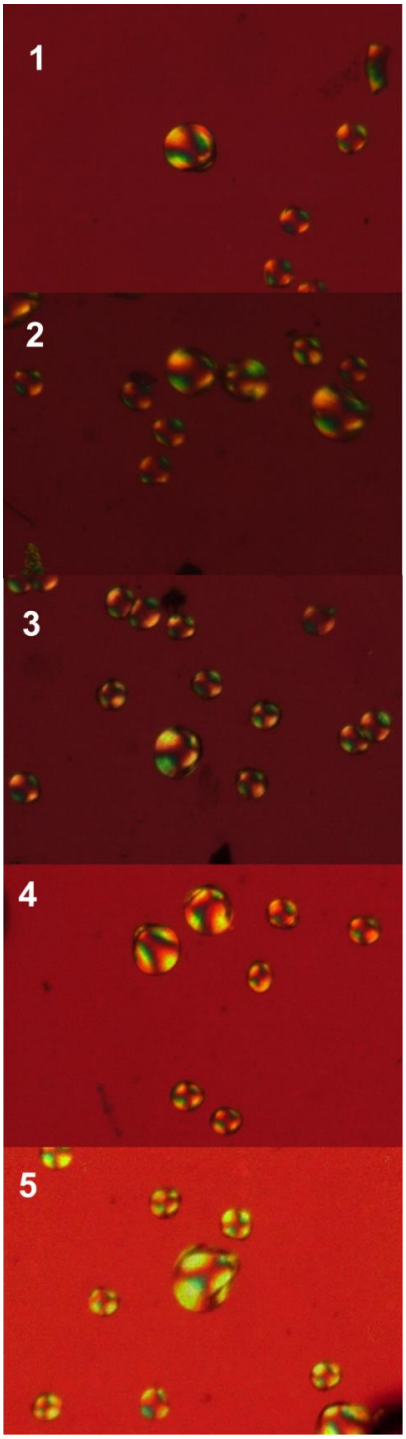

Fig. 3.4. Images 1-5 contain four- and nine-d-old larvae of *C. virginica* and correspond to the camera settings 1-5 (details in Table 3.3) which were used for tests reported in Table 3.4. Setting differences were created by altering attributes in the camera software Infinity Analyze.

A. B.

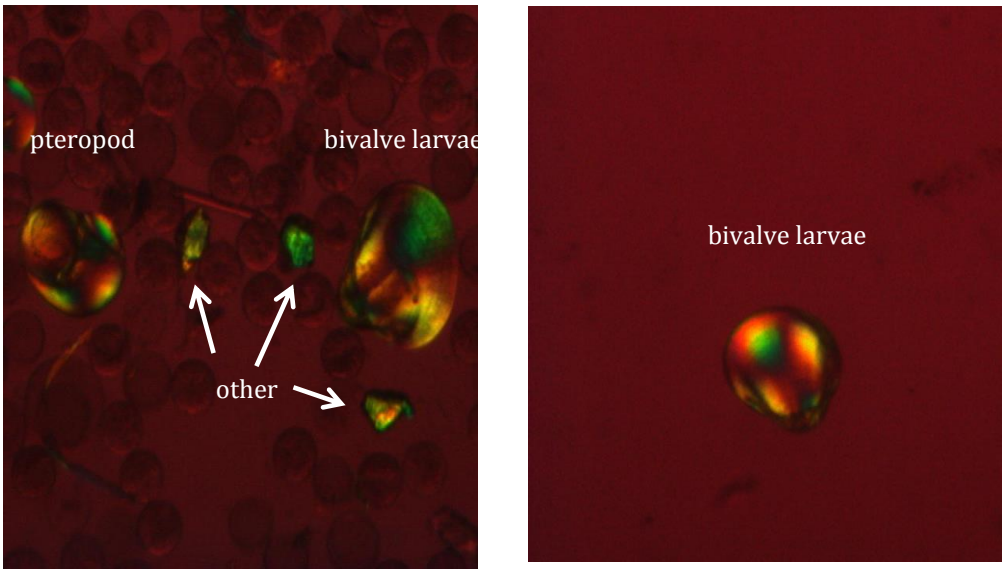

Fig. 3.5. Images from A) a field sample and B) laboratory-reared bivalves which were imaged at 7 x magnification. The field sample contained small birefringent materials or other birefringent organisms like pteropods which made it difficult to automate cropping of ROIs.

Supplementary material

Table S.3.1. Information on the taxonomy and ages of the 8 species of bivalve larvae whose images were used to construct training sets for the validation experiments. The age groups represented were evenly distributed (a closely as possible) so that the total number of images for each species would contain an even representation of all ages. Each training set had three categories (Ostreoida (oysters), Mytiloida (mussels), and Veneroida (clams)which contained equal numbers of images. The two training sets (COM1000, COM7000) were bothed created using setting one (Table 3.3). However, color channel intensities for COM1000 were not measured and were different than those for COM7000.

				COM1000 Training Set		COM700 Training Set	
order	**family**	**genus**	**species**	**ages**	**total**	**ages**	**total**
Ostreoida	Ostreidae	*Crassostrea*	*virginica*	2, 4, 9, 12, 14, 16	1000	2, 4, 9, 12, 14, 16	1000
Mytiloida	Mytilidae	*Ischadium*	*recurvum*	4, 6, 7, 14	500	4, 6, 7, 14	1000
Mytiloida	Mytilidae	*Geukensia*	*demissa*	8, 10, 13	500	N/A	0
Veneroida	Tellinoidea	*Macoma*	*mitchelli*	4, 6, 8, 10	200	4,8	200
Veneroida	Mactridae	*Mulinia*	*lateralis*	2, 6, 8, 10, 13	200	2 ,8, 10,13	200
Veneroida	Dreissenida	*Mytilopsis*	*leucophaeata*	2, 4, 6, 8, 10	200	2, 4, 6, 8, 10	200
Veneroida	Mactridae	*Rangia*	*cuneata*	2, 4, 6, 8	200	2,4,8	200
Veneroida	Solecurtida	*Tagelus*	*plebeius*	1, 3, 8, 13	200	3, 8, 13	200

3.S.2. Results from the two validation tests using three ShellBi training sets (COM1000, COM700, and COM1700) and two humans (Goodwin and Wingate to manually classify images of *C. virginica* of various ages and quantities within 18 folders. Each folder had 100 images of different haphazardly picked bivalve larvae chosen from table S.3.1. Tables A and C show the actual number of *C. virginica* images "actual CV" in each of the 18 folders as well as how many were classified by ShellBi, Goodwin, and Wingate. Tables B and D show the classification accuracy (percent correctly classified). Blank values mean there were no *C. virginica* in those particular folders.

A) validation test one (actual number of *C. virginica* vs. classified *C. virginica*)

folder	actual CV	COM1000	Goodwin	Wingate	COM700	COM1700
1	41	38	40	40	19	39
2	1	0	1	1	0	1
3	0	0	0	0	0	0
4	8	6	8	3	6	6
5	20	19	20	18	13	18
6	0	0	0	0	0	0
7	16	15	16	16	6	15
8	19	18	19	19	14	18
9	5	4	5	4	4	4
10	0	0	0	0	0	0
11	16	14	16	16	16	16
12	26	25	23	25	23	25
13	7	6	7	7	7	7
14	10	10	10	10	8	9
15	5	4	5	5	5	5
16	0	0	0	0	0	0
17	19	18	19	16	18	18
18	7	7	7	7	7	6

B) Classificaiton accuracies for *C. virginica*

folder	COM1000	Goodwin	Wingate	COM700
1	93	98	98	46
2	0	100	100	0
3				
4	75	100	38	75
5	95	100	90	65
6				
7	94	100	100	38
8	95	100	100	74
9	80	100	80	80
10				
11	88	100	100	100
12	96	88	96	88
13	86	100	100	100
14	100	100	100	80
15	80	100	100	100
16				
17	95	100	84	95
18	100	100	100	100

C) validation test two (actual *C. virginica* vs. classified *C. virginica*)

folder	actual CV	COM1000	Goodwin	Wingate	COM700	COM1700
1	15	14	15	15	9	9
2	44	37	44	33	38	35
3	5	5	2	4	4	5
4	26	23	26	26	25	23
5	5	5	5	5	3	5
6	0	0	0	0	0	0
7	15	15	15	15	7	13
8	37	37	32	37	31	33
9	13	13	13	13	10	12
10	15	14	15	15	14	14
11	35	30	35	35	21	26
12	19	18	19	19	9	15
13	4	4	4	4	1	2
14	16	13	16	16	11	15
15	10	10	10	10	2	5
16	4	4	4	4	2	4
17	25	23	25	25	9	15
18	20	17	20	20	5	14

D) Classificaiton accuracies for *C. virginica*

folder	COM1000	Goodwin	Wingate	COM700
1	93	100	100	60
2	84	100	75	86
3	100	40	80	80
4	88	100	100	96
5	100	100	100	60
6				
7	100	100	100	47
8	100	86	100	84
9	100	100	100	77
10	93	100	100	93
11	86	100	100	60
12	95	100	100	47
13	100	100	100	25
14	81	100	100	69
15	100	100	100	20
16	100	100	100	50
17	92	100	100	36
18	85	100	100	25

Chapter 4: Identifying factors that influence vertical distributions of *C. virginica* larvae and estimating their mortality

Abstract

The eastern oyster *Crassostrea virginica* disperses solely during the larval stage when swimming behavior influences transport and mortality affects population dynamics. Yet, obtaining information on swimming behavior and mortality has been hindered by the difficulty in distinguishing *C. virginica* larvae from other bivalves. The objective of this study was to apply ShellBi, a new approach for identifying bivalve larvae, to infer factors that cue *C. virginica* larval swimming behavior and estimate their mortality rates. A combination of mapping and fixed station sampling strategies were employed in the Choptank River, a subestuary of Chesapeake Bay, to collect *C. virginica* larvae which were identified and measured using ShellBi. A length-to-age relationship based on hatchery data and laboratory experiments was applied to estimate mortality rates for 8-16 d-old larvae collected in the field. Analysis of field samples suggest that *C. virginica* vertical distributions were influenced by the halocline, because> 90% of larvae that were < 200 μm in shell height were found above a salinity gradient of 1.2 m^{-1}. Estimated instantaneous daily mortality rates of 8-16 d-old larvae ranged 0.37 d^{-1} to 0.58 d^{-1}, with the most reliable rates being 0.37-0.38 d^{-1} when most assumptions of the analysis were met. These results advance understanding of the larval ecology of *C. virginica* by providing

quantitative estimates of mortality and by inferring physical conditions that cue larval behavior.

Introduction

The eastern oyster *Crassostrea virginica* (Gmelin 1791) is an important commercial (Stevenson 1894) and ecological (Newell 1988, Kennedy 1996) species that is in decline worldwide (Beck et al. 2011). Specifically, in Chesapeake Bay, populations are estimated to be less than 1% of historic levels (Wilberg et al. 2011). Improved knowledge of factors that affect the larval stage is essential for understanding the relationship between reproductive output and population growth (Botsford et al. 1998). Unfortunately, due to the lack of a rapid identification and measuring technique, identifying and measuring large numbers of *C. virginica* larvae has been difficult. This has resulted in the larval stage of *C. virginica* being the least understood aspect of its life history. Yet, this stage is important to understand because it influences population connectivity and gene flow (Pineda et al. 2007, Dame 2012). The goal of this research is to expand knowledge of two aspects of the early life of *C. virginica* larvae: to identify factors that influence the vertical distribution of *C. virginica* larvae, and thereby infer swimming behavior and to estimate their mortality rates.

Swimming behavior and vertical distributions

The combination of both physical processes (e.g., currents and wind) and swimming behavior has been suggested as the primary explanation for advection and/or retention of invertebrate larvae in estuarine and coastal systems (Boicourt

1982, Wood and Hargis 1971, Andrews 1983, Mann 1988, Shanks and Brink 2005). For example, Shanks and Brink (2005) showed that the physical effect of upwelling and downwelling on larval vertical distributions varied for particular species in the same area and was not a result of passive behavior. North et al. (2008) showed that different swimming behavior between two oysters (*C. virginica* and *Crassostrea ariakensis*) resulted in different simulated dispersal distances and connectivity patterns in Chesapeake Bay. Various stages of C. *virginica* larvae were observed to have different distributions based on tidal phase and stratification (Carriker 1951, Kennedy 1996). Kim et al. (2010) found that although biological movement increased larval retention in some areas, it caused little changed in the overall patterns of larval transport which they suggested was due to destratification of the shallow Mobile Bay system. Puckett et al. (2014) reported that physical forces, like wind, were the dominant influence on transport in shallow coastal areas near North Carolina (Puckett et al. 2014). The relative contribution of behavior may depend on the depth of the estuary, role of wind mixing and the existence of two-layer circulation.

Although the actual swimming behavior of *C. virginica* larvae has not been observed in the field, many studies have inferred swimming behavior based laboratory studies and on the vertical distributions of larvae found in the field. The life cycle of *C. virginica* begins with externally fertilized eggs that form gametes and after 5-6 hours a girdle of cilia form and the larvae swim upward (Galtsoff 1964). There is an ontogenetic migration where smaller (early-stage) larvae are found in the upper water column and older (late-stage) larvae are found near the bottom (Carriker 1951, Andrews 1983). As the larvae develops, both the swimming and sinking speeds

increase (Galtsoff 1964). Although horizontal currents are too great for larvae to swim against, they can still swim vertically (Hidu and Haskin 1978, Mann 1986). Specifically, smaller (75 μm) larvae can swim at a rate of 0.01 cm s^{-1} up the water column and large (300 μm) *C. virginica* larvae can swim at 0.08-0.31 cm s^{-1} (Hidu and Haskin 1978, Mann and Rainer 1990). If the larvae cease to swim however, the sinking speed of smaller larvae is 0.02 cm s^{-1} and 0.08 cm s^{-1} for the larger larvae (Hidu and Haskin 1978). These smaller and larger stage larvae could sink between 7-18 m in 6 hours if they are dead or not swimming. Therefore it is likely that larvae found in the upper part of the water column are actively swimming.

To understand the factors that influence the vertical distribution of *C. virginica* larvae, and thereby infer swimming behavior, both field and laboratory studies have been conducted. Salinity appeared to be the dominant factor that cued swimming behavior (Nelson 1927, Wood and Hargis 1971, Carriker 1951). Younger stage larvae were frequently found above the halocline in stratified conditions during periods of low wind and mixing (Nelson 1927, Nelson and Perkins 1931), which supported the hypothesis that those larvae were active swimmers when cued by a salinity gradient. Wood and Hargis (1971) found that the highest numbers of *C. virginica* larvae were found when salinity increased in the accompanying flood tide, they concluded that larvae were responding actively to salinity cues because they behaved differently than observed passive inert particles of similar buoyancy. Laboratory studies have also shown that in the presence of a halocline, *C. virginica* larvae changed behavior and swam upward (Hidu and Haskin 1978). However, the laboratory-induced halocline may not be reflective of those experienced in the field

and additional observations are needed to determine how larvae of different stages respond to salinity gradients *in situ*.

Although salinity has been observed as a dominant cue for *C. virginica* larval swimming behavior, the effect of dissolved oxygen (D.O.) on the vertical distributions of *C. virginica* larvae is not well known. Hypoxia occurs in Chesapeake Bay during summer (Officer et al. 1984) when *C. virginica* spawn (Kennedy and Krantz 1982, Kennedy 1986). Mann and Rainer (1990) showed that the swimming rate of larvae decreased with lower levels of oxygen. The tolerance of *C. virginica* larvae to low oxygen levels increases with developmental stage and body size (Widdows et al. 1989). Widdows et al. (1989) showed that median mortality times in anoxic conditions (created by bubbling N_2 gas) were 11, 51, and 150 hours for *C. virginica* larvae of length 82 μm, 312 μm, and newly settled spat, respectively. It is not clear whether D.O. cues *C. virginica* swimming behavior in the field.

Although previous research has provided information on the factors that could influence *C. virginica* vertical distributions, many of the field studies lacked identification and measuring techniques that would allow for large numbers of bivalve larvae to be enumerated, identified, and measured. Therefore more information is needed, especially field observations, to identify whether salinity, D.O., and other physical and biological conditions influence larval swimming behavior. One of the goals of this research program was to observe what factors appear to influence the vertical distributions of *C. virginica* larval and thereby infer what cues their swimming behavior.

Mortality

Understanding the mortality in pelagic early life stages of marine organisms has been a major goal in marine and fisheries ecology (Houde 2002). Mortality estimates for planktonic larvae are difficult to obtain because larvae are small and concentrations are patchy (Vaughn and Allen 2010). Yet, understanding larval mortality is important because it can influence population dynamics (Fassler et al. 2011). The estuarine environment presents unpredictable risks to planktonic organisms including *C. virginica* larvae. Predation (Nelson 1925, Burrell and Von Engel 1976, Steinberg and Kennedy 1979), food quality, salinity, temperature (Davis 1958, Davis and Calabrese 1964), and even the condition of the gametes from the previous generation (Loosanoff 1965) can influence larval mortality. However, larval mortality calculations for bivalves are scarce. Instantaneous daily mortality rates were calculated, from field data, to be 0.10 to 0.32 d^{-1} for several species of bivalves (Pedersen et al. 2008). Rumrill (1990) calculated an average rate of 0.22 d^{-1} based on several marine invertebrate larvae. Furthermore, there are very few estimates of larval mortality calculated in the field for *C. virginica*. Drinnan and Stallworthy (1979) estimated that *C. virginica* larvae mortality rates ranged between between 0.05 - 0.30 d^{-1} in Bidford River, Canada. However, the mortality rates of *C. virginica* larvae have not been estimated in Chesapeake Bay. Because mortality can fluctuate over space and time (Aksnes and Ohman 1996, Pedersen 2008, Tapia and Pineda 2007), multiple estimates are needed to better understand the factors that control mortality of *C. virginica* larvae in the plankton.

There are multiple approaches for calculating mortality rates in the plankton. Mortality rates for some invertebrate can be calculated using stage-specific estimates, such as the vertical life table (VLT) approach (Aksnes and Ohman 1996). Traditionally this method has used a snapshot of an organism's stage ratios (e.g. copepodite stage compared to adult copepods). Tapia and Pineda (2007) used this approach across horizontal sampling sites to estimate instantaneous rates of mortality for barnacle species. The VLT approach has several assumptions including the assumptions that recruitment to the stage, stage duration, and mortality for a stage is constant (Aksnes and Ohman 1996). The method is useful when at least 10 samples have been collected, when horizontal techniques are likely to fail due to advective influence, or when there is a lack of adequate time-series (i.e. tracking a particular cohort through time and space).

Another method to calculate mortality rates is the catch curve approach that applies age instead of stage to estimate mortality. Like the VLT approach, the catch curve approach focuses on a snap shot of the population in time. However, the catch curve approach uses age frequency to calculate mortality based on the slope of the natural-log-frequency-at-age (Ricker 1975). This method has the assumption that all of the age classes in the calculation are 'equally catchable' by the gear used. It also assumes that mortality is constant across ages and that recruitment for each observed age is constant (Chapman and Robson 1960). The catch curve approach offers an estimate of uncertainty from the standard error of the slope of the natural-log-frequency plot.

Quantifying mortality rates and improving knowledge of the physical factors that influence vertical distributions of *C. virginica* larvae will improve our fundamental understanding of the early life of this species. The main objectives of this research were to: 1) investigate how salinity, temperature, dissolved oxygen, total suspended solids (TSS), chlorophyll *a*, and current velocities influence the vertical distribution of *C. virginica* larvae in the Choptank River, 2) infer factors that may cue oyster larval behavior, and 3) calculate mortality rates for *C. virginica* larvae. These objectives were addressed with a field sampling campaign that included a mapping and fixed station cruise during which the horizontal and vertical distributions of oyster larvae were determined in relation to physical and biological factors.

Methods

Data were collected from the Choptank River, a subestuary of Chesapeake Bay, at several locations during one 'mapping' cruise and one 'fixed station' cruise (Fig. 4.1). The mapping cruise was conducted on the 8-m *R/V Terrapin* and consisted of 15 stations from the mouth of the river to the low salinity (< 5) region. Stations were all sampled in a 12 hour period on July 5, 2012. The fixed station cruise was conducted on the 46-m *R/V Hugh R. Sharp* and consisted of two stations that were occupied from July 10-14, 2012.

Mapping cruise

The mapping cruise was conducted on July 5, 2012 to determine the horizontal and vertical distribution of oyster larvae in relation to physical and

biological factors, and to provide spatial context for the fixed station cruise which occurred 5 d later. Fifteen stations across the Choptank River were occupied. The timing of the cruise was chosen to focus effort on the peak period of *C. virginica* larval spawning in this region (Kennedy and Krantz 1982, Kennedy 1986). During the cruise, station locations (Fig. 4.1) were selected to map bivalve larvae in Choptank River from the mouth to a station upstream with low salinity (~5). The *R/V Terrapin* was equipped with a CTD and pump system to measure water properties and collect plankton samples. Sensors on the CTD measured temperature, conductivity, pressure, fluorometery, dissolved oxygen, optical backscatter and photosynthetically active radiation. The CTD was deployed to measure water properties on the down-cast. In addition, hoses attached to the CTD frame were used to pump water that was filtered through a plankton net (64-μm net mesh) to collect bivalve larvae. Collections were made above and below the highest salinity gradient that was observed in plots generated during the initial CTD downcast at each of the 15 stations. At each station ~ 200 l of seawater was pumped with two sets of hoses and pumps from below and above the highest observed salinity difference by slowly moving the CTD up through the water column continuously. The actual amount of water pumped varied slightly from 200 l and was measured with digital flowmeters (Great Plains Industries model RG45-B). The actual volume of water pumped was used to calculate concentrations of *C. virginica* larvae for each sample. A total of 30 samples were collected and fixed in 4% buffered formalin (the formalin was buffered by adding sodium borate until pH was $\geq$ 8.0). Water samples were collected to measure chlorophyll *a* pigments (using a

syringe/filter apparatus) to calibrate the fluorometer and to measure total suspended solids (TSS) to calibrate the optical backscatter sensor.

Fixed station cruise

One four-day-long 'fixed station' cruise aboard the 45-m *R/V Hugh R. Sharp* was conducted on July 10-14, 2012 to enhance understanding of physical and biological factors that influenced the vertical distributions of *C. virginica*. A time series of plankton collections were made at two stations while the ship was at anchor. The water column was highly stratified at one station (station One) and was more mixed at the other station (station Two) (Fig. 4.1). CTD casts and larval collections were conducted every 1.5 hours at each station. On the CTD downcast, measurements of water properties were conducted and included salinity, temperature, depth, D.O., turbidity, and fluorescence. On the CTD up-cast, a bellows pump was used to pump ~ 200 l of seawater per sample. Seawater was pumped through a 64-μm net contained in a 55 gallon drum that was half-filled with seawater to minimize damage to the plankton. Plankton samples were collected from five (station One) or four (station Two) 1.5-m targeted depth intervals by pumping water below, through, and above the mid-point depth interval. The targeted mid-point depths were 0.9, 2.7, 4.5, 6.3, and 8.1 m at station One and 0.6, 2.3, 4.0, 5.7, and 7.4 m at station Two. The flow rate of the bellows pump was measured regularly and was used with the duration of each sample collection to calculate the volume filtered for each sample. A total of 307 samples were collected and fixed in 4% buffered (sodium borate) formalin.

Current velocity was measured at both stations of the fixed station cruise. An RDI Workhorse Sentinel 1200 KHz with mode 12 (high ping rate) Acoustic Doppler Profiler (ADCP) was moored at each station. The ADCP was deployed on an upward looking bottom landing frame with the ADCP mounted 0.5 m above the seabed and placed within 0.4 - 0.6 km of the ship.

Plankton sample processing

All plankton samples were returned to the laboratory and processed using a semi-automated image analysis technique that was optimized to identify and measure *C. virginica* larvae (Goodwin et al. 2014, Chapter 3). Each sample was poured through a 333 μm filter, bleached for 20 minutes to remove tissue and break apart shells, and then rinsed with distilled water buffered with sodium borate and placed on two Sedgewick Rafter slides. Each Sedgewick Rafter slide was placed on an automated image acquisition system that was comprised of an automated stage, a polarized microscope, a digital camera, and custom software that automatically captured images of half of one slide in 23 min (Chapter 3). Imaging half of each slide resulted in a 50% sub-sample of the shells. Because each bivalve has two shells, the number of shells imaged approximated the number of bivalves in the sample. After the images of bivalve larvae were captured and masked (Chapter 3), the larvae that were *C. virginica* were identified to species using the ShellBi software with an estimated accuracy of 80-93% (Chapter 3).

All images were used to estimate the shell height of larvae. For D-stage larvae, the minor axis (shortest distance across the shell) was the best approximation of their true shell height whereas the major axis (the longest distance across the shell)

best represented the shell height of later stage larvae. To determine the major axis size of D-stage larvae, 300 images of *C. virginica* D-stage larvae were selected haphazardly from field samples of the mapping and fixed stations. The longest axis was measured and a mean of 106 μm was determined to be the average major axis length of D-stage larvae. Therefore, the minor axis length was used as an estimate of shell height for all larvae with a major axis length < 106 μm (i.e., all larvae < 106 were assumed to be D-stage). The major axis length was used as an estimate of shell height for larvae > 106 μm.

Data analysis

Interpolated maps of physical factors and *C. virginica* larvae abundances (no m^{-2}) in three size classes (< 106, 106-200, and ≥ 200 μm) were created with data from the mapping cruise. The three size classes were chosen because of their distinct morphology and shell patterns under polarized light (Fig. 4.2). It is likely that the ≥ 200 μm size class included both late stage veliger and pediveliger larvae. Abundances of larvae (no. m^{-2}) were calculated by multiplying the concentration of larvae (no. m^{-3}) by the sample depth interval (m).

Contour plots of the time series of vertical distributions of physical factors and *C. virginica* larval concentrations (no m^{-3}) for the three size classes (< 106, 106-200, and ≥ 200 μm) were generated for station One and Two of the fixed station cruise. All contour plots for mapping and fixed station cruises were created using Golden Software Surfer (v. 10.0). The gridding method was kriging with assumed isotropy. The grid-line geometry was no finer than half the distance between measurements in the X (time) or Y (depth) directions. Because the CTD casts were between 0.5-2.0 m

shallower than the bottom, the data were not interpolated below the depth of the CTD cast.

The data collected during the downcasts of the CTDs were processed in 0.25 m depth intervals using SeaBird software (v. 7.13). The maximum salinity gradient (the most rapid change in salinity over depth) was calculated for each CTD cast of the fixed station cruise. The maximum salinity gradient (m^{-1}) was calculated by determining the location where the largest change in salinity occurred in the water column during each cast, then dividing that change in salinity by the depth from one salinity measurement to the next. The 2 mg l^{-1} oxycline was calculated by linear interpolation between D.O. measurements.

The ADCP data was processed by Steven Suttles and rotated to derive along-channel current velocity profiles. The average along channel current velocity in each 1 m bin was calculated for two blocks of time that corresponded to approximately one tidal period at both station One and station Two. At station One, the duration of the averaging interval was 24.72 hrs at the beginning of the station occupation and 24.48 hrs near the end. For station Two, the duration of the averaging interval was 24.60 hrs at the beginning and 24.74 hrs near the end. The average current velocity during each of these tidal periods was multiplied by the number of seconds in the averaging interval to estimate the average displacement (km) of water.

Statistical analysis

Nonparametric analyses were conducted on data from the mapping and fixed station cruises. Potential associations between *C. virginica* larvae of different size classes and depth, current velocities, temperature, salinity, D.O., TSS, chlorophyll,

and current velocities during the mapping and fixed station cruises were investigated using a correlation analysis (JMP pro v. 11). Spearman rank-order correlation coefficients were calculated. A Kruskal Wallis test was conducted (JMP pro v. 11) to test whether the mean concentration larvae above and below the maximum salinity gradient were significantly different during the fixed station cruises (data from station One and Two were pooled). A nonparametric test was necessary because concentrations were not normally distributed even after transformation. The analysis was conducted for each size class of larvae < 106, 106-200, ≥ 200 μm.

Calculating mortality estimates for larval stages of *C. virginica*

Mortality calculations were conducted using the VLT and catch curve approaches. Before these methods were applied, the age of each larva was estimated. An age-length relationship was determined from larvae reared in hatchery and laboratory conditions (26.3-27.7 ^{o}C, and salinity of 9.0-12.1) that closely matched those in the Choptank River when the larvae were sampled. At least 30 larvae were measured in each of the following age classes: 2, 4, 8, 12, 14, and 16 days. Hatchery observations indicated that larvae were "eyed" and ready to settle after 16 days in these conditions. The natural log of the larval age (days) vs. length (μm) was plotted and a linear regression line was fit to the data (Fig. 4.3A). The regression equation was rearranged to solve for age in order to estimate the age of *C. virginica* larvae caught in the field based on length measurements. The length (μm) of each larvae measured in the field was converted to age using equation (1) where *A* is age in days and L is length (shell height) in μm:

$$A = \frac{[(Ln(L) - 4.2)]}{0.075}$$

Equation 1

An additional regression line (Fig. 4.3B) was created that included measurements of larvae that were reared in cooler conditions (temperature ranges 22.0 – 22.3 ^{o}C and salinities 9.0-21). This line could be used to estimate ages for a different range of sampling conditions not observed in this study.

Mortality estimates were calculated for 8 to 16 d-old larvae, a time window which was based on the sizes of larvae that were effectively caught by the plankton nets and would have been expected to be present in the plankton. To ensure that all larvae in the analysis were collected effectively, the analysis was limited to 8-16 d old larvae. Larvae calculated as 8 d-old larvae under Equation 1 (~121μm shell height) were likely collected effectively because their minor axis was sufficiently larger than the diagonal across the 64 μm net mesh. Larger larvae over 16-d-old were assumed to be settled because the conditions of salinity and temperature, known to affect settlement (Medcof 1939, Stallworthy 1979, Loosanoff and Davis 1963), were similar between hatchery and field conditions and 16-d-old larvae were observed to be "eyed" in samples from the hatchery. .

Once the age of each larva was calculated, a vertical life table approach was used to calculate mortality based on Aksnes and Ohman (1996). The iterative equation designed for copepod mortality calculations was applied to the age groups of 8 and 16 d for *C. virginica* larvae (Asknes and Ohman 1997):

$$\frac{e^{d_i a_i} - 1}{1 - e^{d_l a_l + 1}} = f_i$$

Equation 2

where d_i = instantaneous death rate for stage i and a_i = stage duration for stage i (which was 8 d). The ratio of observed stages (age 8 and age 16 d larvae in this case) was $f_i = n_i/n_{i+1}$ where n_i is the number of individuals in development stage i. The calculation for this iterative equation was conducted using MATLAB (v. 2012b) after Pierson et al. (2007). Mortality rates using all stations of the mapping cruise as well as stations One and Two of the fixed sampling cruise were calculated.

Mortality estimates also were made using the catch curve approach. A regression line was fit to the frequencies of the natural log of daily age groups (8-16 d) and the slope of the curve was used to estimate the instantaneous daily mortality rate (Ricker 1975). The standard error of the slope provided an estimate of uncertainty. This calculation was completed with data from the mapping cruise, from station One, and from station Two in order to calculate mortality rates for each of these locations and times.

Sensitivity analysis. A sensitivity analysis was conducted to better understand how the procedure for estimating larval age from length measurements could influence calculated mortality rates. Hypothetical "maximum" and "minimum" growth equations were constructed using larvae reared in hatchery and laboratory conditions. Instead of using all data (as in the analysis described above), regression equations were constructed with the maximum and minimum length values within

each age class (dashed lines in Fig. 4.3A). The ages calculated from these regression equations were then used to estimate mortality rates based on hypothetical "high" and "low" growth scenarios.

Results

The overall average concentration of oyster larvae in Choptank River for all cruises and samples combined was 1,292 larvae m^{-3}, which is 10 times less than historical concentrations from the early 1900s (13,307 larvae m^{-3}) (Nelson 1913) (Table 4.1). Maximum concentrations of larvae during mapping and fixed station cruises ranged from 89 to 9190 m^{-3} (Table 4.2). Larvae sampled during the mapping cruise were collected five days prior to station One of the fixed station cruise and seven days prior to larvae from station Two. It is possible that the same cohort of larvae < 106 μm sampled during the mapping cruise also could have been sampled as larger individuals during the fixed station cruise.

Mapping cruise

During July 2012, river flow into the Chesapeake Bay was lower than average (USGS station 01570500, http://waterdata.usgs.gov/usa/nwis/uv?site_no=01570500) but surface salinity and temperatures in the Choptank were within the long term mean (MDNR, station ET5.2, www.eyesonthebay). The average surface salinity and temperature for July 2012 in the Choptank River were 11.54 +/- 0.16 s.t.d. and 27.8 +/- 0.01 s.t.d. ^{o}C respectively (MDNR, station ET5.2, www.eyesonthebay). During the mapping cruise, observed surface salinity ranged from 8.1 - 14.7 and temperature

ranged from 25.5 - 30.8 ^{o}C (Fig. 4.4) which were within the long term average for that time period in the Choptank (MDNR, station ET5.2, www.eyesonthebay). Contour plots of physical factors for the mapping cruise show that salinity was 12 near the mouth and decreased upstream (Fig. 4.4A,B). Temperatures were about 1 ^{o}C cooler on the bottom than at the surface (Fig. 4.4C,D). Hypoxic water was present near the mouth of the Choptank at the bottom but hypoxia was not observed within the river (Fig. 4.4E,F). Chlorophyll *a* increased upriver and was higher in surface waters (Fig. 4.4G,H).

Concentrations and abundances of larvae in the Choptank River varied by size class and location (Fig. 4.5). Smaller size classes (< 106 μm) of larvae had concentrations ranging 0-8,005 larvae m^{-3} and abundances ranging from 0-48,274 larvae m^{-2}. These smaller larvae were most abundant near Broad Creek (Fig. 4.1,4.5A) with lower abundances in the middle of the river (Fig. 4.5A). The 106-200 μm sized larvae had concentrations ranging from 0-8,380 larvae m^{-3} and abundances ranging from 0-60,622 larvae m^{-2}. These larvae were most abundant mid-river (Fig. 4.5B). The larger (≥ 200 μm) larvae were rare compared to the other size classes and had concentrations and abundances that ranged from 0-795 larvae m^{-3} and 0-5,168 larvae m^{-2}, respectively. Higher abundances of larvae ≥ 200 μm were observed near the mouth of Harris Creek (Fig. 4.5C). There were no significant correlations between larval abundances and depth, temperature, salinity, density, D.O., TSS, or Chlorophyll *a* for samples collected during the mapping cruise (Table 4.3). The smallest size class < 106 μm had significant correlations with the 106-200 μm size class but not the largest > 200 μm size class (Table 4.4). These results indicate that *C.*

virginica spawning had taken place in multiple areas prior to sampling and that smaller larvae were more abundant than larger larvae.

Fixed station cruises

Station One. Station One was characterized by cooler, saltier, hypoxic, turbid water during flood tide, by warmer fresher water during ebb tide, and by high stratification, especially during flood tides (Fig. 4.6A-C, and Fig. 4.7A). Temperature and salinity ranged from 25.2 - 29.2 ^{o}C and 12.5 - 17, respectively (Fig. 4.8). As found during the mapping cruise near the mouth of the river on July 5 (Fig. 4.4F), hypoxic water was present on July 12 at station One where it was found during both tidal cycles and occurred within 4-5 m of the surface during flood tide (Fig. 4.6B). Chlorophyll *a* peaked in surface and bottom waters (Fig. 4.6D). The maximum along channel current velocity was 0.45 m s^{-1} during ebb tide and 0.35 m s^{-1} during flood tide (Fig. 4.7A). The average displacement of water was between 5-7 km out of the estuary in the surface layers and between 3-4 km up-estuary in the lower layers during each of the ~24 hour tidal periods (Fig. 4.9).

Larval concentrations at station One varied by size class. The maximum concentration for size classes < 106, 106-200, and ≥ 200 μm were 4,745, 3,867, and 89 m^{-3}, respectively (Table 4.2). Concentrations of larvae of all stages were highest during ebb tides at station One (Fig. 4.10). Earlier stage (< 106, 106-200 μm) larvae were observed in greater concentrations than later stage (≥ 200 μm) larvae (Table 4.2). Larvae of all size classes at station One were positively correlated with depth, temperature, D.O., and Chlorophyll *a*, and negatively correlated with salinity and TSS (Table 4.3). Salinity had the highest correlation with concentrations of larvae in each

size class (r = 0.66, 0,53, 0.50 for 106, 106-200, and ≥ 200 μm size classes, respectively) (Table 4.3). In addition, larval size classes were significantly correlated with one another (Table 4.4).

Station Two. Station Two had fairly well mixed conditions across tidal cycles with lower salinity, temperature, and D.O. gradients than station One (Fig. 4.11A-C). The ranges of temperature and salinity were 27.2 - 28.8 ^{o}C and 12.4 - 14.4, respectively (Fig. 4.12). Hypoxic water was present throughout tidal cycles in the deeper (below 5 m) part of the water column (Fig. 4.11B). Concentrations of TSS were higher in deeper water below the 13 isohaline (Fig. 4.11C) and chlorophyll *a* was abundant above and below the 13 isohaline (Fig. 4.11D). The maximum along channel current velocity was 0.34 m s^{-1} during ebb tide and 0.22 m s^{-1} during flood tide (Fig. 4.7B). The average displacement of water in both the upper and lower layers was < 1.5 km during each of the ~24 tidal periods (Fig. 4.13).

Larval concentrations varied by size class and were present throughout both ebb and flood tides. The maximum concentration for size classes < 106, 106-200, and ≥ 200 μm were 6,460, 3,780, and 180 m^{-3}, respectively (Table 4.2). Larvae were present during both flood and ebb tide (Fig. 4.14). The larvae also were present across the range of temperatures and salinities measured at station Two (Fig. 4.12). Smaller (< 106, 106-200 μm) larvae were observed in greater concentrations than larger larvae (≥ 200 μm). Larval concentrations were positively correlated with depth, temperature, and D.O. and negatively correlated with salinity, and TSS (Table 4.3). Larvae < 200 μm had the highest correlations with salinity and 1arvae ≥ 200 μm had

the highest correlation with D.O (Table 4.3). All concentrations of the three different size classes of larvae were significantly correlated with each other (Table 4.4).

Maximum salinity gradient and *C. virginica* vertical distributions

Most larvae < 200 μm were observed above the maximum salinity gradient during all CTD casts (Fig. 4.10A,B, 4.14A,B). At station One where stratification was relatively high, maximum salinity gradients ranged between 0.1 and 6.9 m^{-1} with only 4 out of 29 CTD casts having maximum salinity gradients < 1.1 m^{-1}. The majority of larvae were found above the maximum salinity gradient: 95, 93, and 89% percent of larval concentrations were above the maximum salinity gradient for the 106, 106-200, and > 200 μm size classes, respectively. Station Two had much lower maximum salinity gradients (0.1 - 1.5 m^{-1}) and the percent of larval concentrations above the maximum salinity gradient was 93, 85, and 74% for the 106, 106-200, and > 200 μm size classes, respectively.

Median concentrations of all size classes of larvae were significantly higher above the maximum salinity gradient. The median concentration of larvae < 106 μm above the maximum salinity gradient (1017 m^{-3} +/- 2220 s.t.d.) was significantly higher than the median concentration below it (48 m^{-3} +/- 203 s.t.d.) when data from both station One and Two were pooled (Kruskal Wallis, $p = 0.0001$, $Z = -8.26$, $\alpha = 0.05$, $n = 59$). The median concentration of larvae 106-200 μm above the maximum salinity gradient (510 m^{-3} +/- 1136 s.t.d.) was significantly higher than the median concentration below it (30 m^{-3} +/- 161 s.t.d.) when data from both station One and Two were pooled (Kruskal Wallis, $p = 0.0001$, $Z = -7.85$, $\alpha = 0.05$, $n = 59$). The median concentration of larvae ≥ 200 μm above the maximum salinity gradient (30

m^{-3} +/- 25 s.t.d.) was significantly higher than the median concentration below it (0 m^{-3} +/-11.5 s.t.d.) when data from both station One and Two were pooled (Kruskal-Wallis, $p = 0.0001$, $Z = -7.16$, $\alpha = 0.05$, $n = 59$). Based on these observations, the majority of larvae from all size classes appear to remain above salinity gradients > 1.2 m^{-1}, except larger larvae which were found deeper in the water column when salinity gradients < 1.2 m^{-1} were observed.

Four locations in time and space had salinity gradients that exceeded 3.1 m^{-1} and had D.O. levels < 2 mg l^{-1} at the same depth. One hundred percent of larvae of all size classes were found above these depths (Fig. 4.15A-C), suggesting that D.O., in addition to salinity, may influence the vertical distributions of larvae.

Mortality rates

Mortality rates of larvae 8-16 d-old varied for each cruise and for each method used to calculate them. Using the VLT approach, instantaneous daily mortality rates were estimated to be 0.48, 0.51, and 0.37 d^{-1} for the mapping cruise, station One, and station Two, respectively (Table 4.5). The instantaneous daily mortality rates and confidence intervals derived with the catch curve approach were 0.50 (95% CI 0.37-0.63), 0.58 (95% CI 0.45-0.71), and 0.38 (95% CI 0.28-0.48) d^{-1} for the mapping cruise, station One, and station Two, respectively (Table 4.5). The VLT estimates fell within the 95% confidence interval of the continuous catch curve estimates for all cruises (Figure 16B). In other words, both methods used to calculate mortality rates were not statistically different. In summary, the instantaneous daily mortality rates for *C. virginica* larvae between 8-16 days old in Choptank River were estimated to be 0.37-0.58 d^{-1}.

The sensitivity analysis which was conducted to examine the effect of age-length estimates on mortality rates indicated that the rates calculated using the "minimum" growth equation (0.15-0.23 d^{-1}) were substantially different, approximately 50% lower, than those predicted with all data (0.37-0.58 d^{-1}), whereas rates calculated with the "maximum" growth equation (0.44-0.63 d^{-1}) were slightly higher than those calculated with all data (Table 4.5, Fig. 4.16). Estimated daily mortality using the VLT approach under both the 'minimum' and maximum' growth scenarios were within the 95% CI interval of the catch curve approach for all cruises and differed by no more than 0.07 d^{-1} from the catch curve estimate. When a different time window was chosen, 10-16 d-old larvae (all 'catchable' under the minimum growth conditions), the "minimum" growth equation yielded higher mortality rates for the mapping, and stations One and Two using the VLT (0.31, 0.18, and 0.28 d^{-1}, respectively) and catch curve (0.52, 0.42, and 0.32 d^{-1} respectively) approaches. Therefore, this sensitivity analysis suggests that both the data used to estimate the age of larvae in the field as well as the time window used to estimate mortality rates could strongly influence mortality rate calculations. Furthermore, these results show that both the VLT and catch curve approaches offer similar estimates of *C. virginica* larval mortality.

Discussion

The overall concentration of larvae in the Choptank River found in this study was ten times lower than those in Barnegat Bay during the early 1900s (Nelson 1913, Nelson 1927) and ~5 times lower than some concentrations reported in the James

River and the Choptank River during the 1980s (Andrews 1983, Seliger 1982) (Table 4.1). Despite the uncertainty in estimates due to differences in sampling gear and identification techniques, these studies still show the general downward trend of larval concentrations over time. This downward trend in larvae is most likely a result of the downward trend in the recruitment of *C. virginica* since 1940 in the Maryland portion of the Chesapeake Bay (Kimmel and Newell 2007). This study shows that, despite the depressed abundances of *C. virginica* currently in Chesapeake Bay, enough larvae were present in the Choptank River during this study to advance understanding of larval ecology of *C. virginica*.

This study also indicates that there could be different source locations and/or transport patterns for *C. virginica* larvae in Choptank River based on the high abundances of larvae < 200 μm in two separate areas of the river (Fig 5A-C). The presence of larvae in July is consistent with previous spawning at these locations in previous years (Kennedy and Krantz 1982, Kennedy 1986). The high abundance of all stages of larvae in the northwest (Fig. 4.5A-C) may indicate that multiple spawning events could have occurred several days to a few weeks prior to sampling.

Swimming behavior and vertical distributions

The location of the maximum salinity gradient appeared to influence the vertical distributions of *C. virginica*. The majority of larvae in all size classes were found above the maximum salinity gradient at station One (89 to 95%) and at station Two (74 to 93%). Fewer larvae ≥ 200 μm were found above the maximum salinity gradient than larvae < 200 μm, which supports the observations that late stage

veligers and pediveligers depth distributions tend to shift toward bottom (Carriker 1951, Andrews 1983). Higher percentages of larvae were found above the salinity gradient at station One compared to station Two, perhaps the result of higher salinity gradients at station One compared with those at station Two. These observations support previous findings (Nelson 1913, Carriker 1951, Hidu and Haskin 1978) that indicated that salinity appears to be a dominant driver of vertical distributions of *C. virginica* larvae.

In addition to salinity, advection of different water masses also may have influenced the vertical distribution of *C. virginica* larvae. Station One was characterized by hypoxic water with higher salt content during flood tide with very low concentrations of larvae (< 833 m^{-3}) compared to more oxygenated ebb tides that contained high concentrations of larvae at the same depths (> 6730 m^{-3}) (Fig 6, 10). The influx of salty hypoxic water during each flood tide at station One may provide evidence that an upwelling event had occurred. Intrusions of hypoxic water into the Choptank River can occur due to upwelling from the mainstem of the Bay (Sanford et al. 1990). This could explain the sharper gradients and lower numbers of larger ≥ 200 μm larvae below the maximum salinity gradient compared with station Two. It also could explain why the majority of all sizes of larvae were only present during ebb tide.

Dissolved oxygen also may have influenced the vertical distribution of *C. virginica* larvae. Although most larvae were found above the salinity gradient at stations One and Two (Fig. 4.10,4.14), some larvae ≥ 200 μm larvae were found below it at station Two (Fig. 4.14C). Most of these larvae were not present in hypoxic

waters (Fig. 4.6B, 4.14C), indicating that these larvae may have avoided hypoxia. At station One, salinity gradients > 3.1 m^{-1} and the 2 mg l^{-1} oxycline were located at the same time and depth (n=4). Although 100% of all larvae were found above this depth during these casts (Fig 4.15A-C), there was not enough information to discern whether salinity or hypoxia may have cued upward swimming behavior, or whether the absence of larvae in deep waters was simply the result of advection of hypoxic water with no larvae in it. Nevertheless, results provide some support for the idea that hypoxia could cue upward swimming of *C. virginica* larvae, but further studies would be needed to better characterize the response of *C. virginica* larvae to hypoxic conditions in the field.

In summary, larvae observed in the upper part of the water column were likely there as a result of their swimming behavior that could have been stimulated by both salinity gradients and oxygen levels. Distributions of larvae at station One were likely a result of both swimming and advective forces which reinforces the idea that both physical factors and biological factors play a role in the vertical distributions of *C. virginica* larvae (Carriker 1951, Andrews 1983, Arnold et al. 2005, North et al. 2008, Kim et al. 2010, Puckett et al. 2014).

Mortality

Mortality rates differed between cruises. The vertical life table approach yielded instantaneous daily mortality rates that were similar to the catch curve approach for all growth scenarios and cruises (Table 4.5, Fig. 4.16A-C). Rates calculated with all growth data (Equation 1) are consistent with the upper ranges of previous studies for *C. virginica* larvae (0.05-0.30 d^{-1}) (Drinnan and Stalworthy

1979). Mortality estimates using the VLT approach were within the 95% confidence intervals of the catch curve approach (Fig. 4.16). Therefore, the VLT and catch curve approaches generate similar values that are not statistically different.

The mortality estimates were based on the observed growth of larvae that were reared in salinity and temperature conditions similar to those sampled in the field (Fig. 4.3A) which was important because temperature and salinity have an important influence on larval growth (Davis and Calabrese 1964). However, other factors like food (e.g., species of algae ingested) and synergistic effects of temperature and salinity can also influence growth (Lough 1975, Davis and Calabrese 1964). Results of the sensitivity analysis to examine the influence of length-age regressions on mortality estimates indicate that mortality rates can differ by as much as 0.45 d^{-1} when different length-age regressions are used. However, the mortality estimates calculated under the minimum growth scenario account for most of this difference as mortality estimates were less than 0.10 d^{-1} between estimates based on the maximum growth conditions and growth predicted with all data. The large difference between mortality rates based on the "minimum" growth equation and the "all data" and "maximum" growth equations likely was due to the fact that the minimum size of larvae caught by the gear was estimated to be 121 μm which translated to 6, 8, and 10 d-old larvae under minimum, all data, and maximum growth regressions (Fig. 4.3A). Larvae considered 6 d-old under the minimum growth scenario were excluded from the analysis because they were not within the 8-16 d window, causing lower estimates for both the catch curve and VLT approaches. The estimates are still useful because they offer a comparison between the VLT and catch

curve approaches using the same data although they may not reflect mortality accurately.

Advection may have influenced mortality calculations by transporting different larval stages in different directions. Specifically, mortality estimates at station One likely violated assumptions of equal sampling for all larval stages within a cohort. The along channel current velocities in shallower water (< 5 m), (where smaller larvae were found) were moving in a different direction than larvae in lower layers (where larger larvae were found). Furthermore, the net displacement of water over a tidal cycle was on the order of several kilometers which was larger than the patch sizes observed five days previously during the mapping cruise (Fig. 4.5). Thus the larvae collected at station One may not have been from the same larval patch or cohort.

The net flow of water at Station Two was in the same direction (up-estuary) in the upper and lower layers of the water column. The net displacement was less than 1.5 km which was smaller than observed patch sizes from the mapping cruise (Fig. 4.5). Therefore, mortality estimates at Station Two may be more accurate. The advection effects are less likely to influence mapping cruise mortality estimates because stations were sampled on the same day over the entire system. However, it is likely that the mapping cruise was reflective of multiple cohorts (Fig. 4.5) that would violate assumptions. Based on these observations, Station Two instantaneous daily mortality estimates are likely the most accurate and ranged from 0.37-0.38 d^{-1}.

In conclusion, results of this study support the idea that the swimming behavior of *C. virginica* larvae is influenced by salinity gradients and possibly by low

oxygen, and provides a quantitative estimate of the strength of the salinity gradient that may cue larval swimming (> 1.2 m^{-1}). In addition, the mortality rates, calculated for the first time for oyster larvae in Chesapeake Bay, help provide fundamental knowledge of the ecology of *C. virginica* larvae and could be used in future studies aimed at understanding their population dynamics and transport.

Literature cited

Aksnes, D.L. and M.D. Ohman. 1996. A vertical life table approach to zooplankton mortality estimation. Limnol. Oceanogr. 41(7):1461-1469.

Andrews, J.D. 1983. Transport of bivalve larvae in James River, Virginia. J. Shell. Res. 3:29-49.

Beck, M.W., R.D. Brumbaugh, L. Airoldi, A. Carranza, L.D. Coen, C. Crawford, O. Defeo, G.J. Edgar, B. Hancock, M. Kay, H. Lenihan, M.W. Luckenbach, C.L. Toropova, G. Zhang & X. Guo. 2011. Oyster reefs at risk and recommendations for conservation, restoration, and management. Bioscience, 61:107–116.

Boicourt, W.C. 1982. Estuarine larval retention mechanisms on two scales. *In*: Kennedy (ed), Estuarine Comparisons. Academic Press, New York, pp 445-458.

Botsford, L.W., J.C. Castilla, C.H. Peterson. 1997. The management of fisheries and marine ecosystems. Science. 277:509-515.

Burrell, V.G. and W.A. Van Englel. 1976. Predation by and distribution of a ctenophore, *Mnemiopsis leidyi* A. Agassiz, in the York Estuary. Estuar. Coast. Mar. Sci. 4:235-242.

Carriker, M.R. 1951. Ecological observations on the distribution of oyster larvae in New Jersey estuaries. Ecol. Monogr. 21:19-38.

Chapman, D.G., and D.S. Robson. 1960. The analysis of a catch curve. Biometrics 16(3):354-368.

Dame, R.F. 2012. Population processes, *In*: P. Petrailia, and H. Linna (eds.) Ecology of marine bivalves an ecosystem approach, 2nd ed. CRC Press Taylor Frances Group. pp. 75-103.

Drinnan, R.E. and Stallworthy. 1979. Oyster larval populations and assessment of spatfall, Bidford River, P.E.I. 1961. Fish. Mar. Serv. Tech. Report. No 792.

Davis, H.C. and A. Calabrese 1964. Combined effects of temperature and salinity on development of eggs and growth of larvae of *M. mercenaria* and *C. virginica*. Fish. Bull. 63:643-655.

Fassler, S.M., M.R. Payne, T. Brunel and M. Dickey-Collas. 2011. Does larval mortality influence population dynamics? An analysis of North Sea herring (*Clupea harengus*) time series. Fish. Oceanogr. 20(6):530-543.

Galtsoff, P.S. 1964. The American oyster, *Crassostrea virginica* (Gmelin) Fishery Bull. Fish Wildl. Serv. U.S. 64:1-480.

Goodwin, J.D., E.W. North and C.M. Thompson. 2014. Evaluating and improving a semi-automated image analysis technique for identifying bivalve larvae. Limnol. Oceanogr. Meth. 12:548-562.

Hidu, H. and H. Haskin. 1978. Swimming speeds of oyster larvae *Crassostrea virginica* in different salinities and temperatures. Estuaries. 1(4):252-255.

Houde, E.D. 2002. Mortality. *In*: Werner, R.G. and Fuiman, L.A. (Eds), Fishery Science. The Unique contributions of early life stages. Blackwell Publishing, Oxford, pp.64-87.

Kennedy, V.S. 1996. Biology of larvae and spat. *In*: V.S. Kennedy, I.E. Newell, and E.F. Eble (eds). The eastern oyster *Crassostrea virginica* xChapter 10. Maryland Sea Grant pp. 371-421.

Kennedy, V.S. 1986. Expected seasonal presence of Crassostrea virginica (Gmelin) larval populations, emphasizing Chesapeake Bay. Amer. Malacol. Bull. Spec. Edit. 3:25-29.

Kennedy, V.S., and L.B. Krantz. 1982. Comparative gametogenic and spawning patterns of the oyster *Crassostrea virginica* (Gmelin) in central Chesapeake Bay. J. Shellfish Res. 9:133-140.

Kim, C.-K., K. Park, S. P. Powers, W.M. Graham and K.M. Bayha. 2010. Oyster larval transport in coastal Alabama: Dominance of physical transport over biological behavior in a shallow estuary.J. Geophys. Res.,115, C10019, doi:10.1029/2010JC006115.

Kimmel, D.G., and R.I.E. Newell. 2007. The influence of climate variation on eastern oyster (*Crassostrea virginica*) juvenile abundance in Chesapeake Bay. Limnol. Oceanogr. 52(3):959-965.

Loosanoff, V.L. 1965. The American or eastern oyster. United States Dept. of the Interior Circular 205:1-36.

Loosanoff, ,V.L. and H.C. Davis 1963. Rearing of bivalve molluscs. Adv. Mar. Biol. 1:1-136.

Mann, R. 1988. Distribution of bivalve larvae at a frontal system in the James River, Virginia. Mar. Ecol. Prog. Ser. 50:29-44.

Mann, R. 1988. Distribution of bivalve larvae at a frontal system in the James River, Virginia, Mar. Ecol. Prog. Ser., 50,29–44.

Mann, R., and J.S. Rainer. 1990. Effect of decreasing oxygen tension on swimming rate of *Crassostrea virginica* (Gmelin, 1791) larvae. J. Shell. Res. 9:323-327.

Medcof, J.C. 1939. Larval life of the oyster (*Ostrea virginica*) in Bideford River. J. Fish. Res. Board Can. 4:287-301.

Nelson, T.C. 1911. Report of the biologist. Oyster culture studies in 1910. In: Ann. Rep. Agric. Exp. Sta. New Brunswick New Jersey. 1926. pp. 103-113.

Nelson, T.C. 1913. Report of the biologist. Observations of natural propogation data of 1912. Pages 281-345 in Ann. Rep. N.J. Agric. Exp. Sta. for 1912, New Brunswick, N.J.

Nelson, T.C. 1925. On the occurrence and food habits of ctenophores in New Jersey inland coastal waters. Biol. Bull. 48:92-111.

Nelson, T.C. 1927. Report of the department of biology. In: Ann. Rep. Agric. Exp. Sta. New Brunswick New Jersey. 1926. pgs103-113.

Nelson, T.C. and E.B. Perkins. 1931. Annual report of the department of biology, July 1, 1929-June 30, 1930. N. J. Agrric. Exp. Stn. Bull. 522:3-47.

Newell, R.I.E. 1988. Ecological Changes in Chesapeake Bay: Are they the result of the American oyster, *Crassostrea virginica*?, p. 536-546. *In:* M.P. Lynch and E.C. Krome (eds), Understanding the estuary: Advances in Chesapeake Bay research. Chesapeake Research Consortium, Gloucester Point, Virginia.

North, E.W., Z. Schlag, R.R. Hood, M. Li, L. Zhong, T. Gross, and V.S. Kennedy. 2008. Vertical swimming behavior influences the dispersal of simulated oyster larvae in a coupled particle-tracking and hydrodynamic model of Chesapeake Bay. Mar. Ecol. Prog. Ser. 359:99-115.

Officer, C.B., R.B. Biggs, J.L. Taft, L.E. Cronin, M.A. Tyler, and W.R. Boynton. 1984. Chesapeake Bay anoxia: Origin, development, and significance. Science 223:22-27.

Pedersen T.M., J.L.S. Hansen, A.B. Josefson, B.W. Hansen. 2008. Mortality through ontogeny of soft-bottom marine invertebrates with planktonic larvae. J. Mar. Syst. 73:185-207.

Pierson, J.J., Frost, B.W., and A.W. Leising. 2007. The lost generation of *Calanus pacificus*: Is the diatom effect responsible? Limnol. Oceanogr. 52(5):2089-2098.

Pineda, J., J.A. Hare, S. Sponaugle. 2007. Larval dispersal and transport in the coastal ocean and consequences for population connectivity. Oceanogr. 20, 22–39.

Puckett, B.J., D.B. Eggleston, P.C. Kerr and R.A. Luettich Jr. 2014. Larval dispersal and population connectivity among a network of marine reserves. Fish. Ocenogr. 23(4):342-361.

Ricker, W.E. 1975. Computation and interpretation of biological statistics of fish populations. Fish. Res. Bd. Canada Bull. 191.

Rumrill, S.S. 1990. Natural mortality of marine invertebrate larvae. Ophelia 32:163-198.

Sanford, L.P., K.G. Sellner, and D.L. Breitburg. 1990. Covariability of dissolved oxygen with physical processes in the summertime Chesapeake Bay. J. of Mar. Res. 48:567-590.

Seliger, H.H. Boggs, J.A. Rivkin, R.B. Biggley, W.H. Aspden, K.R.H. 1982. The transport of oyster larvae in an estuary. Mar. Biol. 71:57-72.

Shanks, A.L. and L. Brink. 2005. Upwelling, downwelling, and cross-shelf transport of bivalve larvae: test of a hypothesis. Mar. Ecol. Prog. Ser. 302:1-12.

Steinberg, P.D., and V.S. Kennedy. 1979. Predation upon *Crassostrea virginica* (Gmelin) larvae by two invertebrate species common to Chesapeake Bay oyster bars. The Veliger 22(1):78-84.

Stevenson, C.H. 1894.The oyster industry in Maryland. U.S. Fish Commission Bulletin for 1892 12: 205-297.

Tapia F.J., J. Pineda. 2007. Stage-specific distribution of barnacle larvae in nearshore waters: potential for limited dispersal and high mortality rates. Mar. Ecol. Prog. Ser. 342:177-90.

Vaughn, D. and Allen, J.D. 2010. The peril of the plankton. Integr. Comp. Biol. 50(4):552-570.

Widdows, J., R.I.E. Newell and R. Mann. 1989. Effects of hypoxia and anoxia on survival, energy metabolism, and feeding of oyster larvae (*Crassostrea virginica*, Gmelin). Biol. Bull. 177:154-166.

Wilberg, M.J., M.E. Livings, J.S. Barkman, B.T. Morris, and J.M. Robinson. 2011. Overfishing, disease, habitat loss, and potential extirpation of the oysters in upper Chesapeake Bay. Mar. Ecol. Prog. Ser. 436:131-144.

Wood, L. and W.J. Hargis, Jr. 1971. *In:* D.J. Crisp (eds.). Transport of bivalve larvae in a tidal estuary. Fourth European marine biology symposium. Cambridge University Press, New York. pp. 29-44.

Tables and Figures

Table 4.1. Summary of previous field efforts focused on *C. virginica* larvae. The study, location, gear, mesh size, number of samples, and total volume of water filtered are all reported. The concentrations are the estimated number of larvae collected in studies divided by the total volume sampled for each study * Denotes studies that only measured late stage larvae.

Study	Location	Mesh size	capture mechanism	No. of samples	Total volume filtered (l)	Concentration of larvae (no. m^{-3})	Sub sample size
Nelson (1911)	Barnegat Bay, NJ, USA	Lautenschlager paper	pump	212	318	26,170	20%
Nelson (1913)	Barnegat Bay, NJ USA	Lautenschlager paper	pump	1026	1,539	13,307	20%
Carriker (1951)	Barneget and Great Bays NJ, USA	18 XXX silk bolting cloth	pump	248	2,480	5,880	no
Drinnan and Stalworthy (1958)	Bidford River Prince Edward Island, Canada	No. 18 plankton net	pump/transects	114	44,436	26,200	1%
Wood & Hargis (1971)	James River VA, USA	No. 18 plankton net	pump	24	2,400	242	10%
Andrews (1983)	James River VA, USA	No. 20 plankton net	pump	90	9,000	4,500	10%
Seliger et al. (1982)*	Choptank River, MD, USA	44 µm	pump	64	6,400	7,400	33%
Mann (1988)*	James River VA, USA	80 um	pump	23	18,230	500	no
Kim et al. (2010)	Mobile Bay AL, USA	35 µm	pump	20	200	22,300	25%
This study (2015)	Choptank River, MD, USA	64 µm	pump	316	64,124	1,292	50%

Table 4.2. The minimum, maximum, mean, and standard deviation of the mean concentration (m^{-3}) of larvae from samples collected on the A) mapping cruise and on the fixed station cruise at stations B) One, and C) Two for three size classes of *C. virginica* larvae (< 106, 106-200, and ≥ 200 µm).

	Minimum m^{-3}	Maximum m^{-3}	Mean	s.t.d.
A. Mapping				
< 106 µm	0	9,195	490	773
106-200 µm	0	8,380	545	675
≥ 200 µm	0	795	11	14
B. One				
< 106 µm	0	4,745	615	1,043
106-200 µm	0	3,867	657	734
≥ 200 µm	0	89	32	39
C. Two				
< 106 µm	0	6,460	279	346
106-200 µm	0	3,780	153	190
≥ 200 µm	0	185	10	26

Table 4.3. The results of a correlation analysis for concentrations of *C. virginica* larvae (no. m^{-3}) and physical parameters at stations One and Two of the fixed station cruise. The same analysis was conducted for the abundances of larvae (m^{-2}) for the mapping cruise. Physical parameters were measured with a CTD and averaged within the depth intervals of the plankton samples (D.O. = dissolved oxygen, TSS = total suspended solids, Chl-a = Chlorophyll *a*). Significant correlations are listed in the table (* = P < 0.01, ** = P < 0.01, *** = P <0.001, n.s. = not significant. 'n/a' indicated that no physical information was available).

Station	Size (µm)	Depth (m)	Temperature (^{o}C)	Salinity	D.O. (mg l^{-1})	TSS (µm l^{-1})	Chl-*a* (µm l^{-1})	Current (m s^{-1})
One	< 106	- 0.55***	0.62***	- 0.66***	0.62***	-0.44**	0.39***	n.s.
One	106-200	- 0.57***	0.54***	-0.53***	0.53***	-0.40**	0.28**	n.s.
One	≥ 200	- 0.40 ***	0.28**	-0.52***	0.50***	-0.51***	0.29***	n.s
Two	< 106	- 0.52***	0.54***	-0.61***	0.48***	-0.41***	n.s	n.s
Two	106-200	- 0.56***	0.53***	-0.56***	0.50***	-0.40**	n.s	n.s
Two	≥ 200	- 0.22**	0.24**	-0.21**	0.25**	- 0.17**	n.s.	n.s.
Mapping	< 106	n.s.	n.s.	n.s.	n.s.	n.s.	n.s.	n/a
Mapping	106-200	n.s.	n.s.	n.s.	n.s.	n.s.	n.s.	n/a
Mapping	≥ 200	n.s.	n.s.	n.s.	n.s.	n.s.	n.s.	n/a

Table 4.4. Results of correlation analysis between three size classes < 106, 106-200, and > 200 µm of *C. virginica* larvae during the mapping cruise (m^{-2}) and at stations One and Two of the fixed station cruise (no. m^{-3}). (* = P < 0.01, ** = P < 0.01, *** = P <0.001, n.s. = not significant).

Station	**Size (µm)**	**< 106 µm (m^{-3})**	**106-200 µm (m^{-3})**	**≥ 200 µm (m^{-3})**
One	< 106 µ	1.00	0.79***	0.425***
One	106-200	0.79***	1.00	0.51***
One	≥ 200	0.43***	0.51***	1.00
Two	< 106	1.00	0.85***	n.s
Two	106-200	0.85***	1.00	0.37***
Two	≥ 200	n.s.	0.37***	1.00
Mapping	< 106	1.00	0.87***	n.s.
Mapping	106-200	0.87***	1.00	0.70***
Mapping	≥ 200	n.s.	0.70***	1.00

Table 4.5. Instantaneous mortality rates (d^{-1}) of 8-16 d old *C. virginica* larvae during the mapping cruise and fixed stations One and Two using all length-age data. Mortality rates were calculated with the vertical life table (VLT) and catch curve (CC) approaches, the latter of which provided 95% confidence intervals (95% CI). A sensitivity analysis was conducted to examine the effect of age-length estimates on mortality rates were estimated using different regression equations of age (A) versus length (L, shell height in μm) that were calculated assuming average, maximum and minimum growth conditions.

		Mapping			One			Two		
Length-age-data	**Regression equation**	**VLT**	**CC**	**95% CI**	**VLT**	**CC**	**95% CI**	**VLT**	**CC**	**95% CI**
All data	A = 0.075L + 4.2	0.48	0.50	(0.37-0.63)	0.51	0.58	(0.45-0.71)	0.37	0.38	(0.28-0.48)
Minimum	A = 0.077L + 4.0	0.19	0.23	(0.09-0.33)	0.18	0.19	(0.00-0.40)	0.15	0.16	(0.06-0.26)
Maximum	A = 0.077L + 4.3	0.44	0.45	(0.35-0.55)	0.60	0.63	(0.53-0.73)	0.47	0.45	(0.35-0.55)

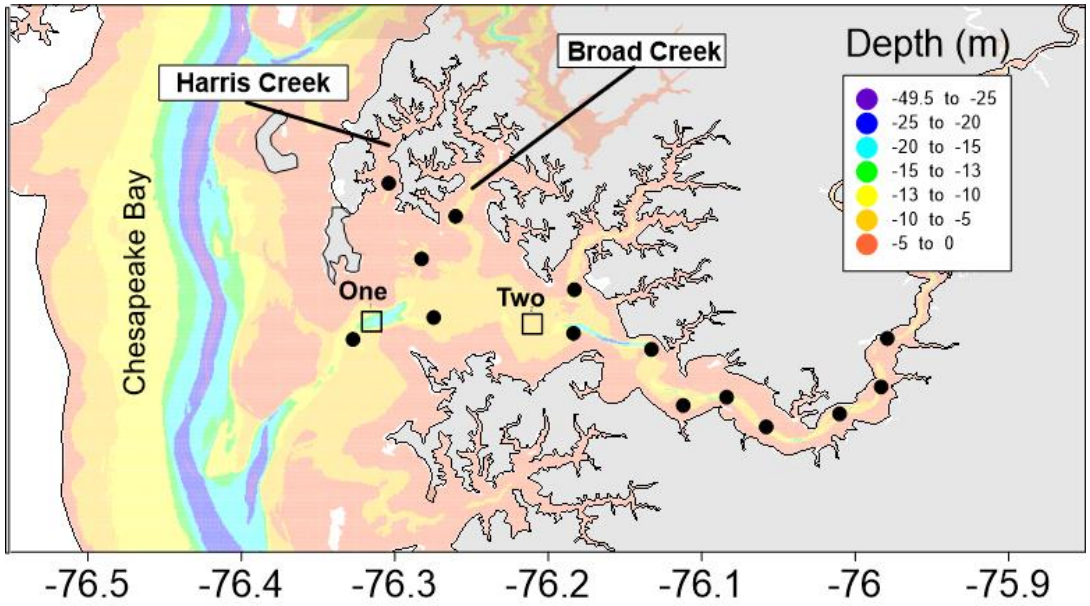

Fig. 4.1. Locations of the stations during the fixed station (labeled "One" and "Two" squares) and mapping (circles) cruises in the Choptank River, a tributary of Chesapeake Bay. The mapping cruise and fixed station cruises were conducted on July 5, 2012 and July 12-15, 2012, respectively. Shaded contours indicated depth (m).

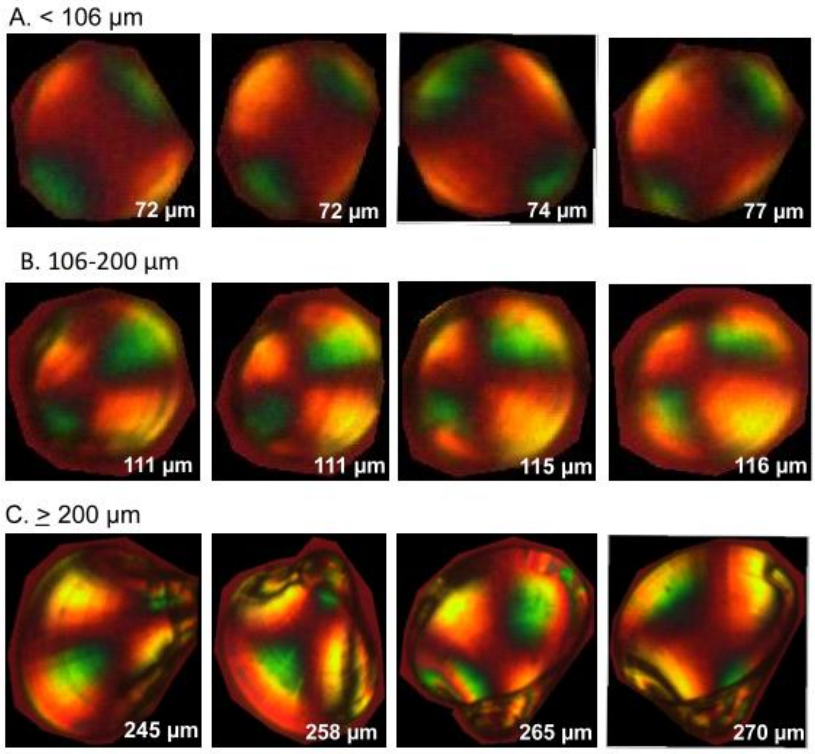

Fig. 4.2. Example images of three size classes of *C. virginica* larvae under polarized light which correspond to the size classes chosen for analysis: A) < 106 µm, B) 106-200 µm, and C) ≥ 200 µm). The number indicates the shell height (shortest axis for the smallest size class and longest axis for the larger two size classes).

A.

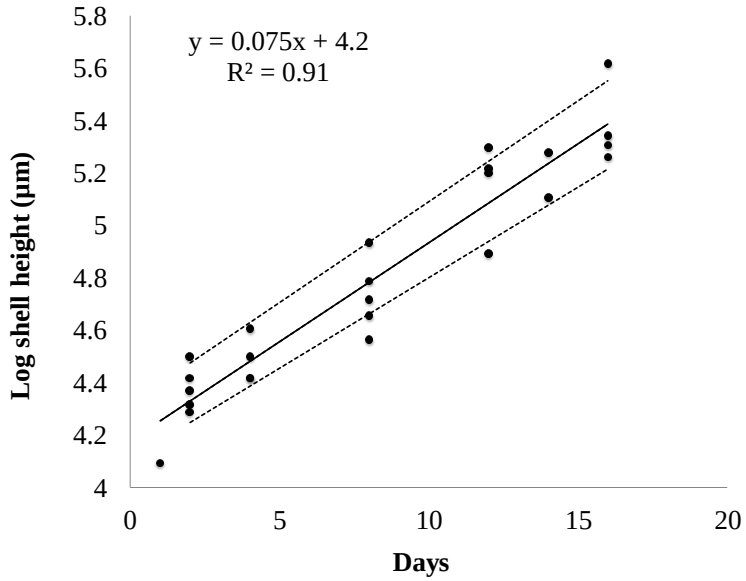

B.

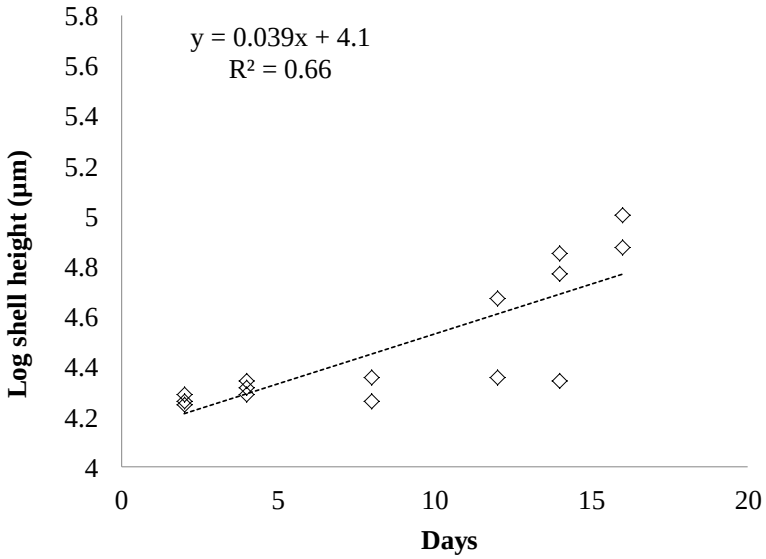

Fig. 4.3. Length-age regression line based on known shell heights and ages for larvae reared in laboratory conditions that were A) representative of temperatures and salinities during July, 2012 when field collections occurred and B) cooler conditions. The regression equation fit to all data in panel A (solid line in center) was used to estimate larval age for field-collected specimens. The two other regression lines on panel A were used to estimate age under both maximum (top dotted line) and minimum (lower dotted line) growth conditions. Panel B contains a regression line suitable for cooler (22^{o}C) temperatures which were not observed in the field during this research program.

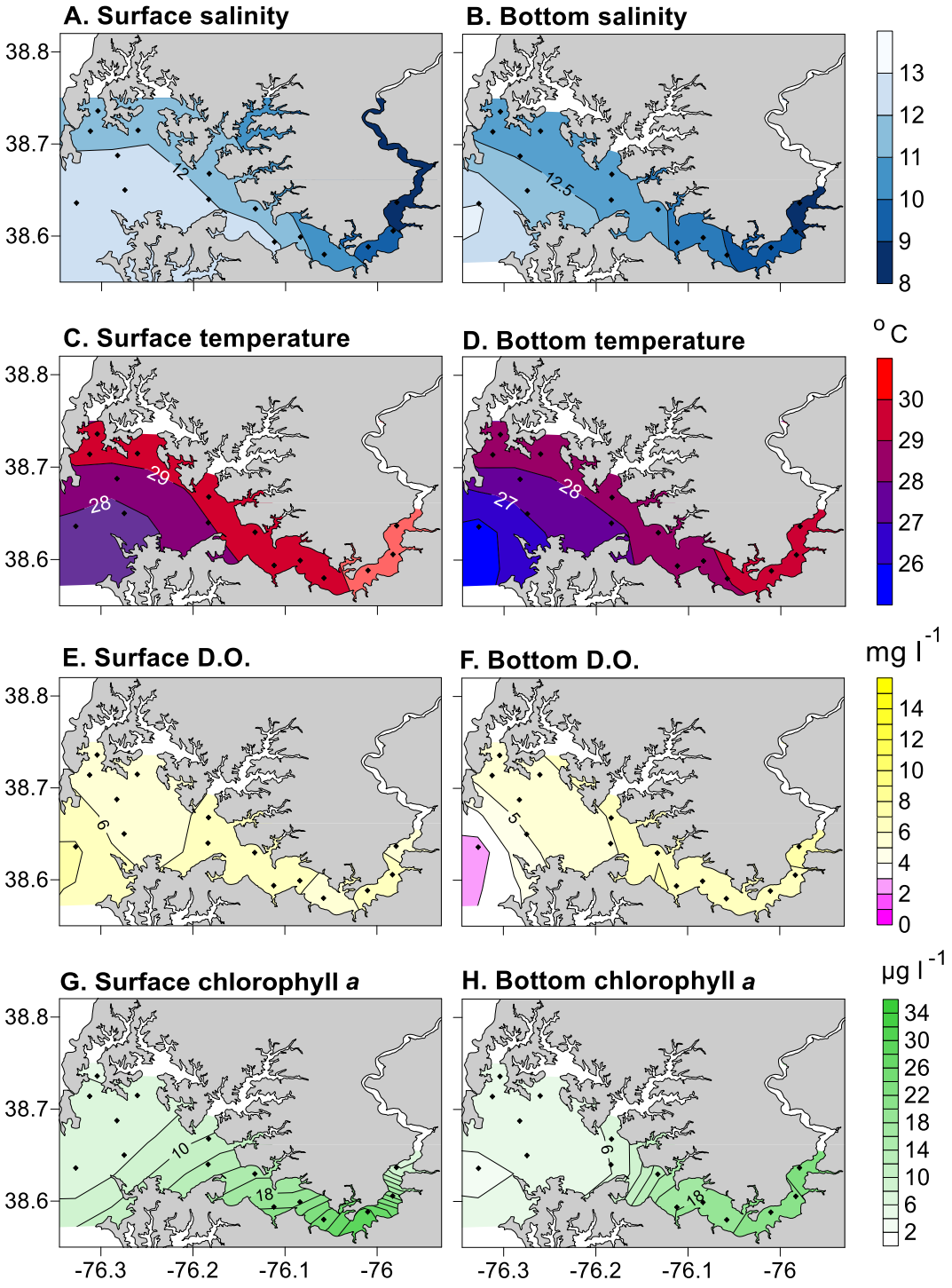

Fig. 4.4. Physical conditions near surface (left panels) and near bottom (right panels) during the mapping cruise on July 5th, 2012: A,B) salinity, C,D) temperature, E,F) dissolved oxygen (DO), and G,H) chlorophyll *a* concentrations.

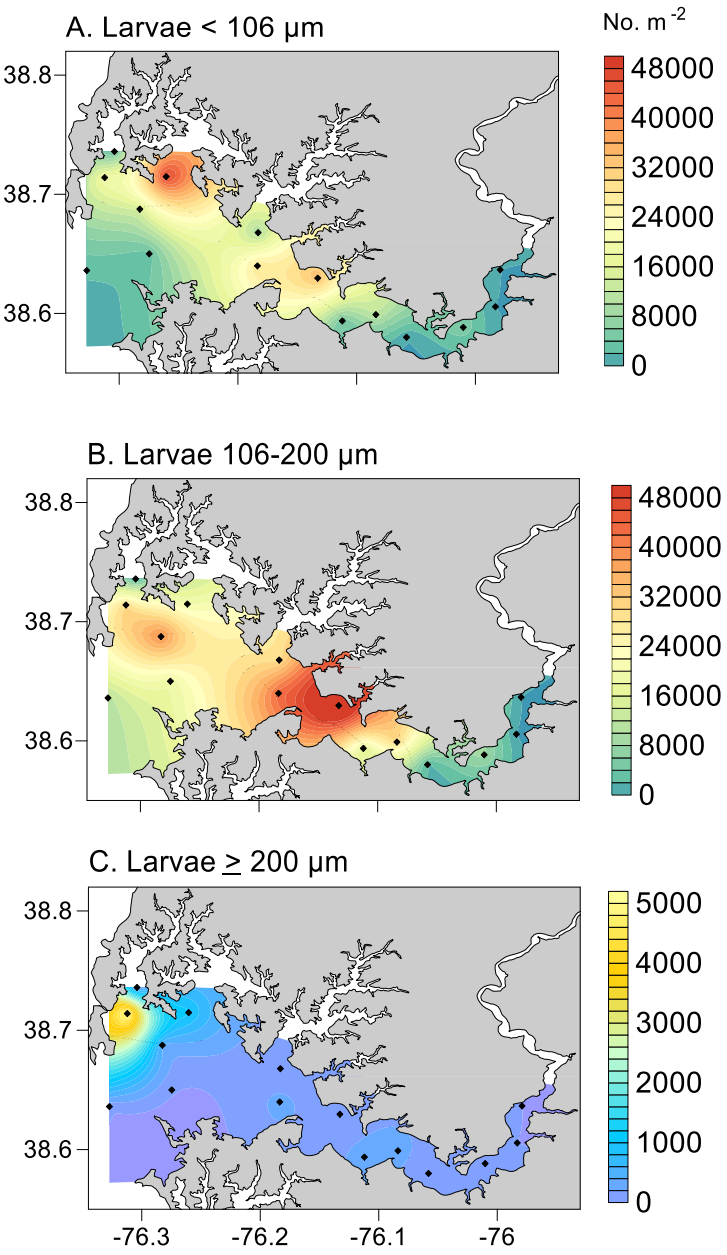

Fig. 4.5. Abundances of *C. virginica* larvae (no m^{-2}, color contours) with shell heights of A) < 106 µm, B) 106-200 µm, and C) ≥ 200 µm during the mapping cruise on July 5, 2012. Stations locations are indicated by black diamonds. Contour lines of surface salinity in intervals of one are also depicted.

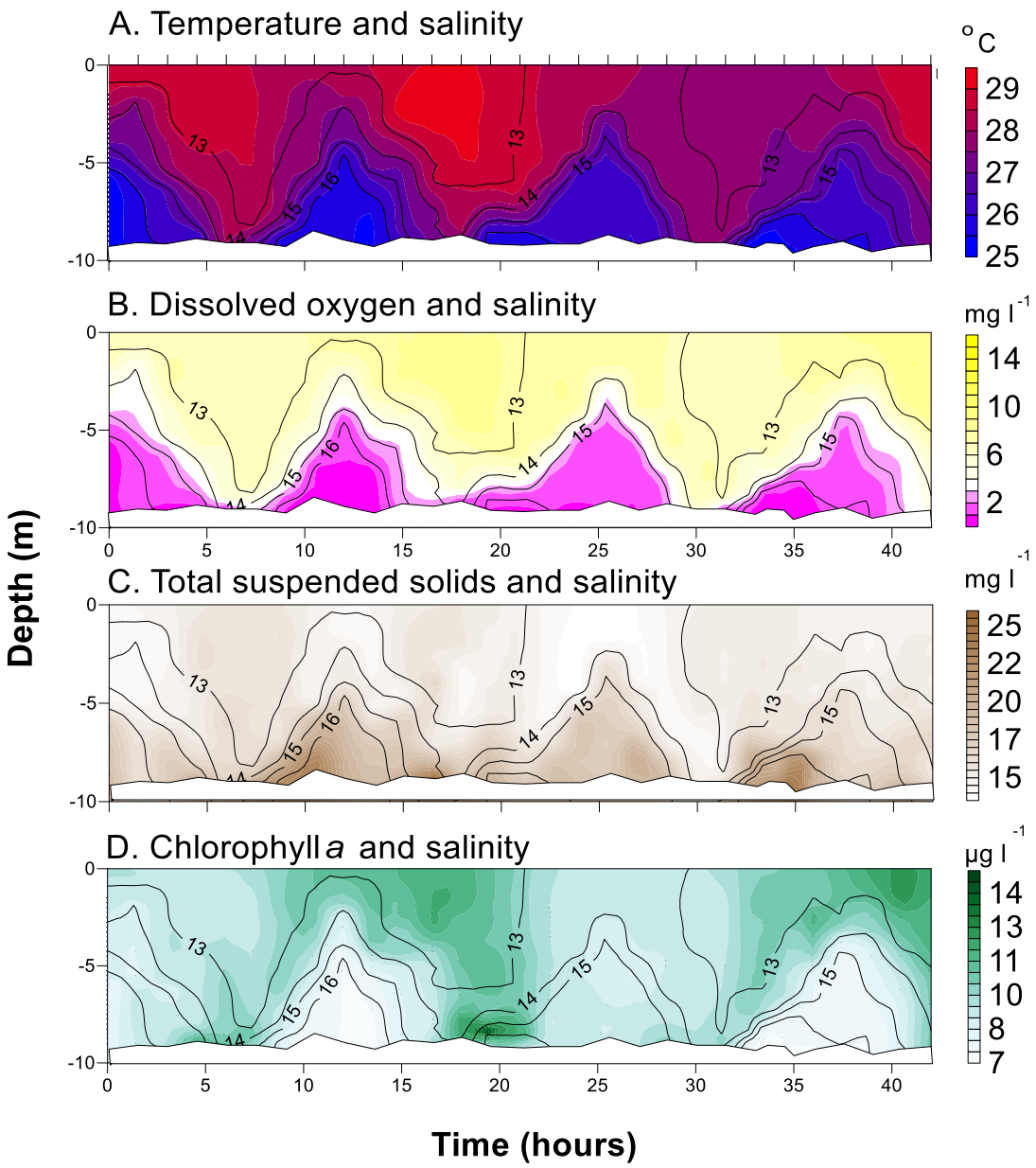

Fig. 4.6. Color contour plots of temperature (^{o}C) with the salinity gradient (black line), dissolved oxygen (mg l^{-1}), total suspended solids (mg l^{-1}), and chlorophyll-a (µg l^{-1}) with salinity contour lines (black) taken at station One of the fixed station cruise (July 10-12, 2015). CTD casts (indicated by tick marks top of panel A) were conducted every 1.5 hours for 45 hours. Salinity contour lines are in intervals of 1.

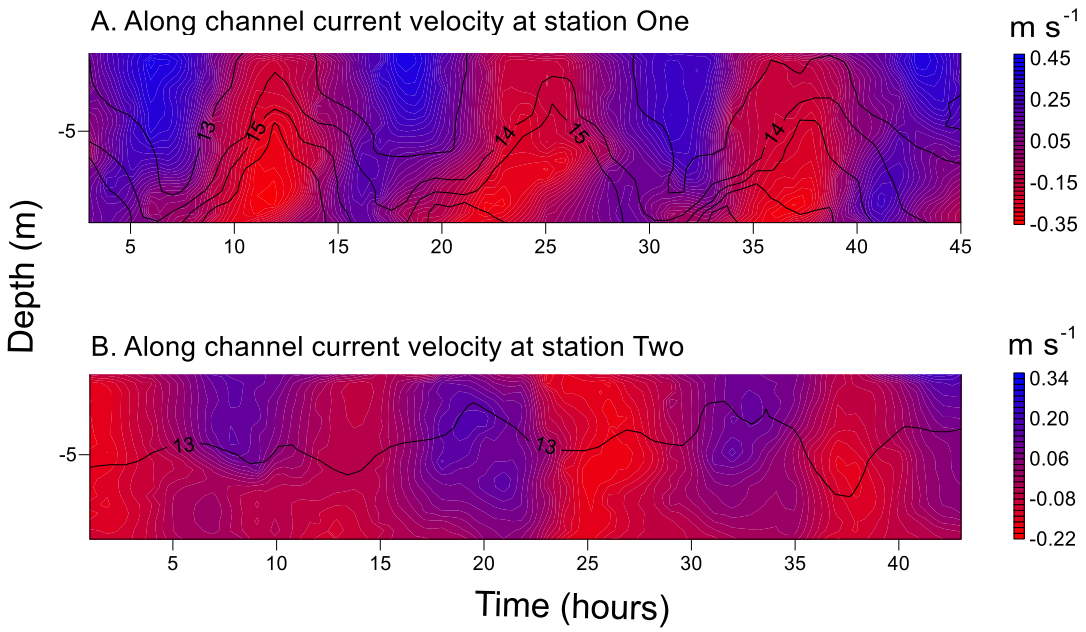

Fig. 4.7. Along-channel current velocities (m s^{-1}) measured by an Acoustic Doppler Current Profiler at station A) One and B) Two of the fixed station cruise. Red indicates flooding tides from Chesapeake Bay into the Choptank River, while blue indicates ebbing water flowing downstream.

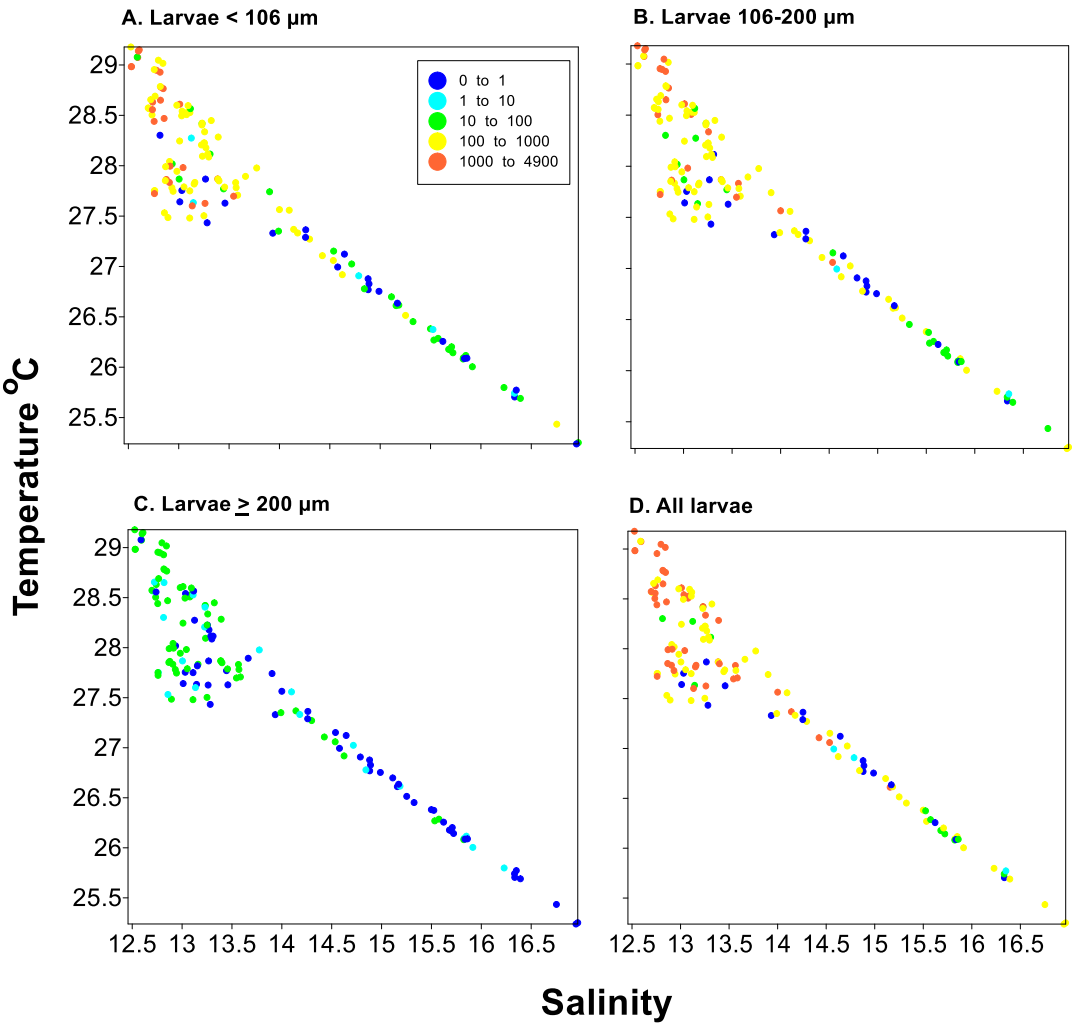

Fig. 4.8. Temperature (°C), salinity and concentration (no. m^{-3}) of *C. virginica* larvae (colored circles, see legend in panel A) at Station One July 12-14, 2012. Panels correspond to larvae with shell heights of A) < 106 µm, B) 106-200 µm, C) ≥ 200 µm, and D) all larvae.

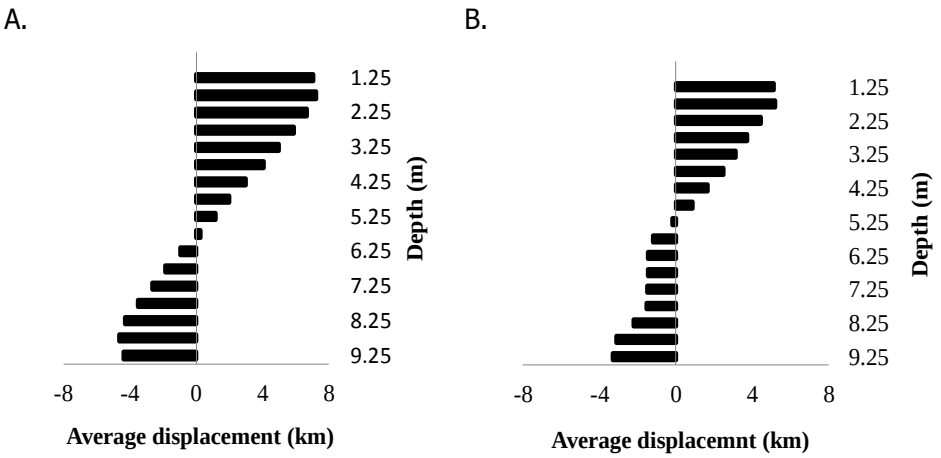

Fig. 4.9. The average displacement of water (km) at fixed station One over the A) initial tidal cycle of 24.72 hours and B) the ending tidal cycle of 24.48 hours. Calculations were based on along-channel current velocities that were averaged within 1-m. Negative values correspond to movement up estuary while positive corresponds to movement down estuary.

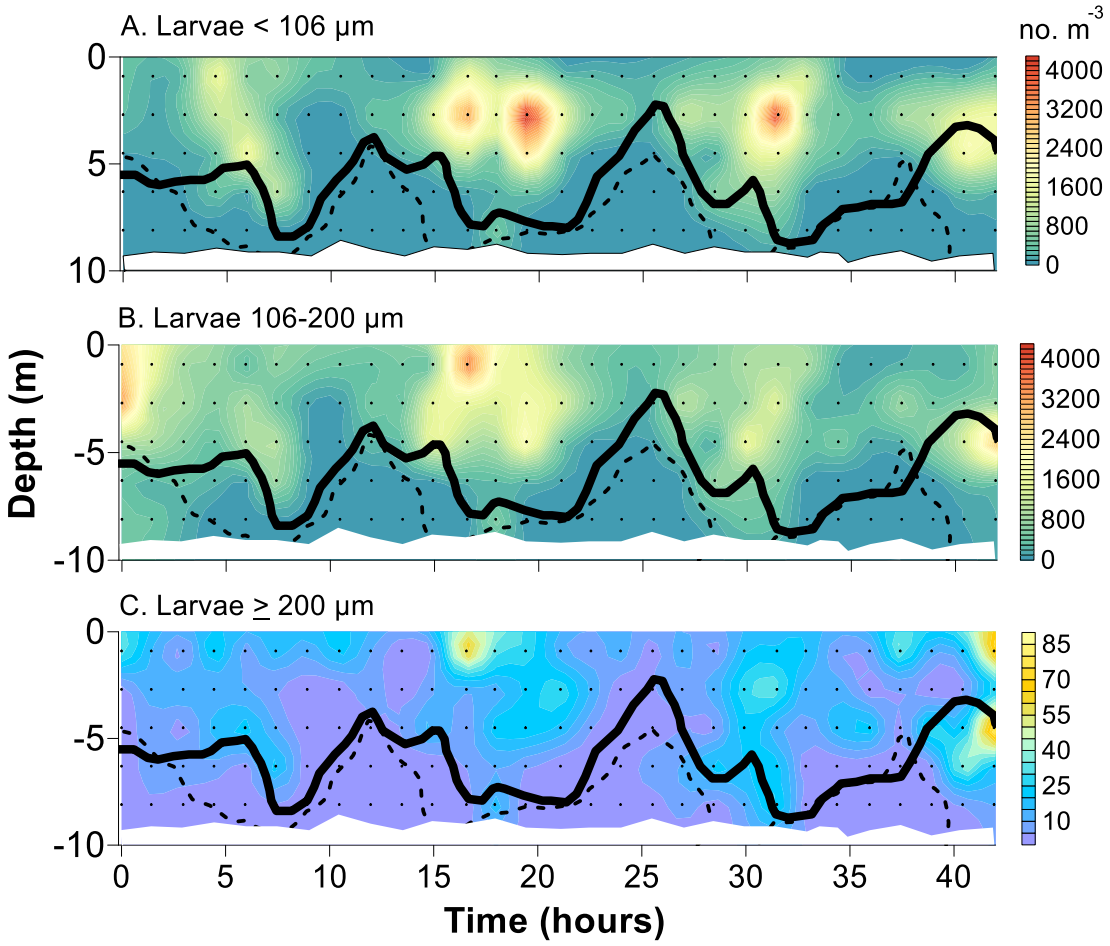

Fig. 4.10. Concentrations of *C. virginica* larvae with shell heights A) < 106 µm, B) 106-200 µm, and C) ≥ 200 µm collected at station One during the fixed station cruise on July 10-12, 2012. The targeted midpoint depth of sample collection (black dots), maximum salinity gradient (solid line), and the 2 mg l^{-1} oxycline (dotted line) are also depicted. Note that larvae with shell heights ≥ 200 µm (panel C) were plotted with a different color scale due to their lower concentrations.

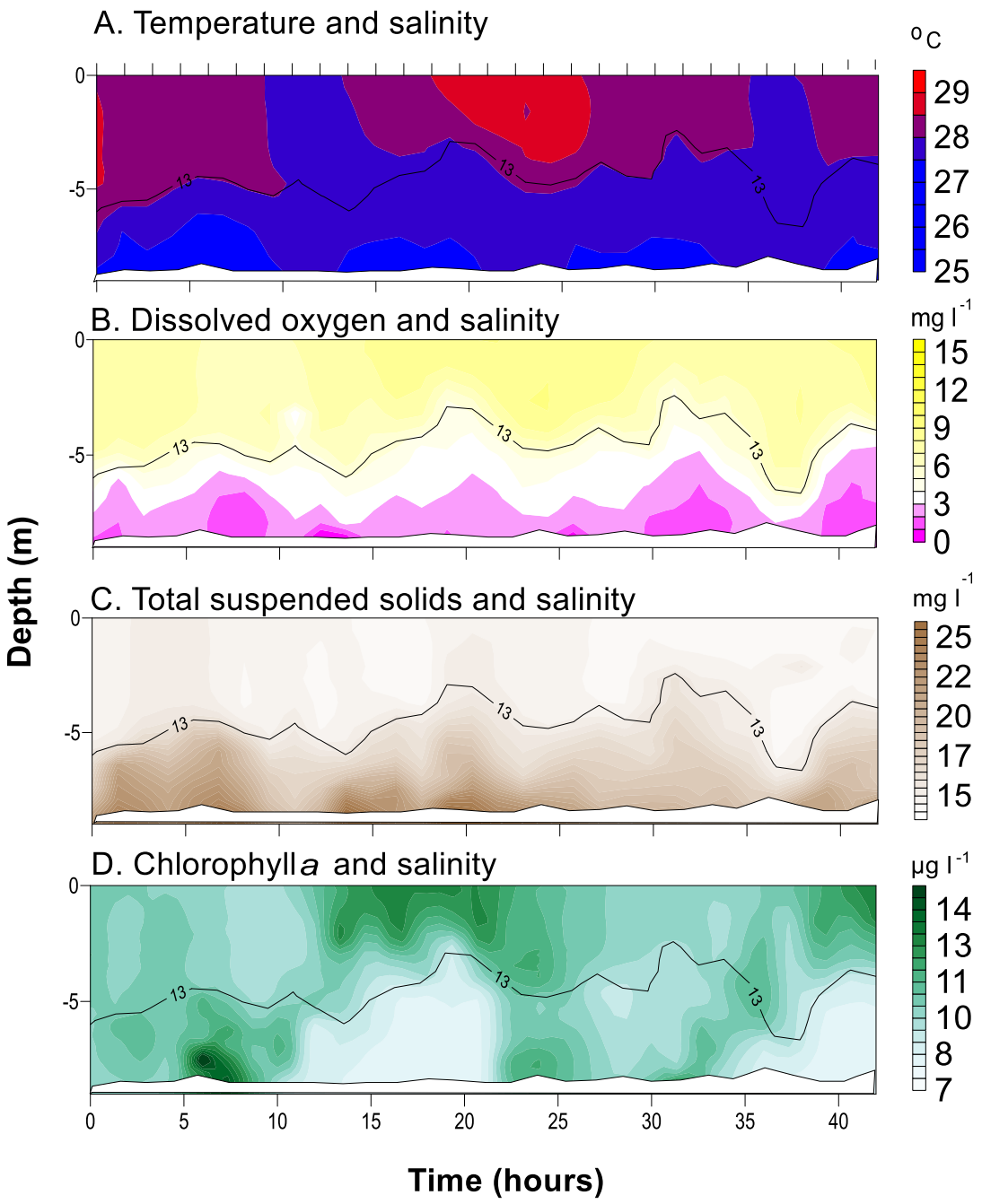

Fig. 4.11. Color contour plots of temperature (^{o}C) with the salinity gradient (black line), dissolved oxygen (mg l^{-1}), total suspended solids (mg l^{-1}), and chlorophyll *a* (µg l^{-1}) with salinity contour lines (black) taken at station Two of the fixed station cruise (July 12-14, 2015). CTD casts (indicated by tick marks top of panel A) were conducted every 1.5 hours for 45 hours. Salinity contour lines are in intervals of 1.

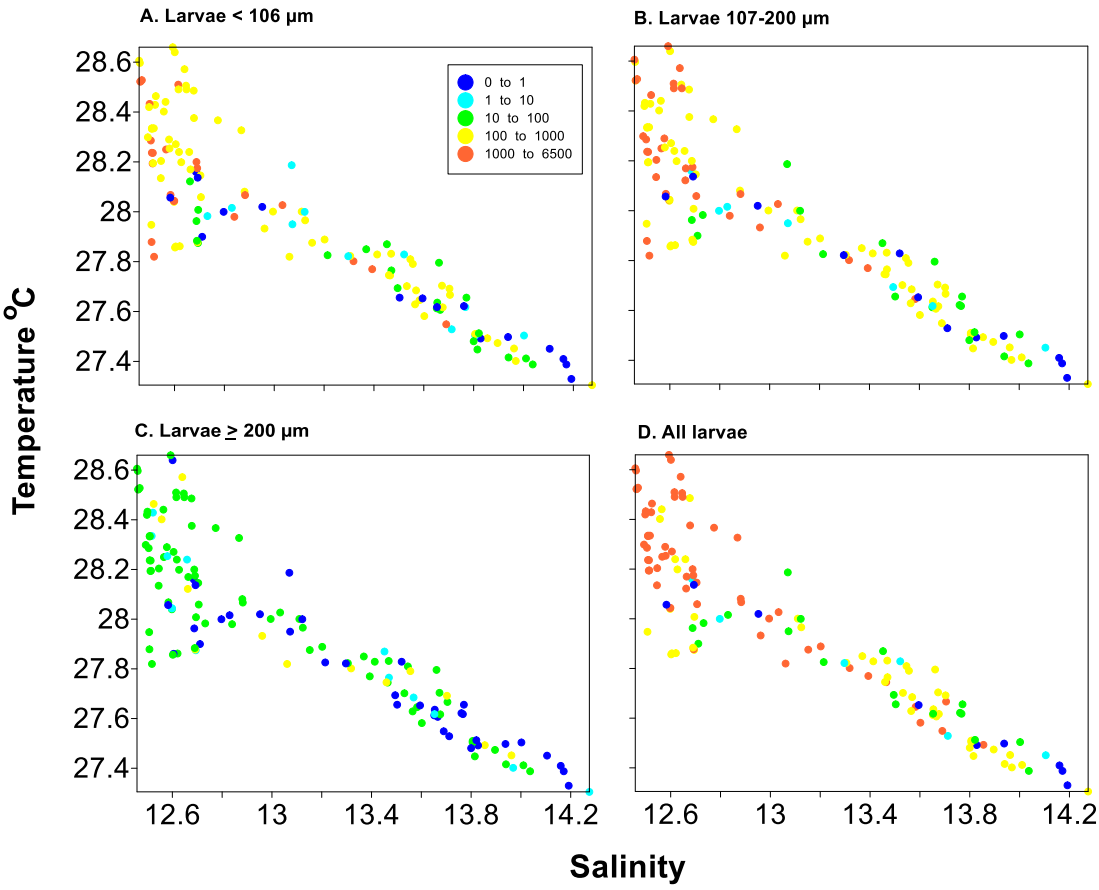

Fig. 4.12. Temperature (^{o}C), salinity and concentration (no. m^{-3}) of *C. virginica* larvae (colored circles, see legend in panel A) at fixed station Two on July 12-14, 2012. Panels correspond to larvae with shell heights of A) < 106 µm, B) 106-200 µm, C) ≥ 200 µm, and D) all larvae.

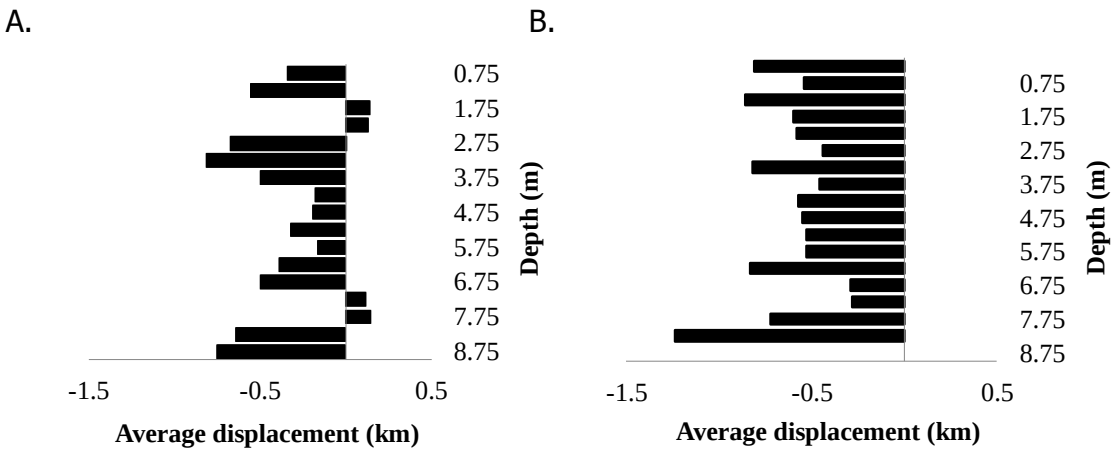

Fig. 4.13. The average displacement of water (km) at fixed station Two over the A) initial tidal cycle of 24.60 hours and B) ending tidal cycle of 24.74 hours. Calculations were based on along-channel current velocities that were averaged within 1-m. Negative values correspond to movement up estuary while positive corresponds to movement down estuary.

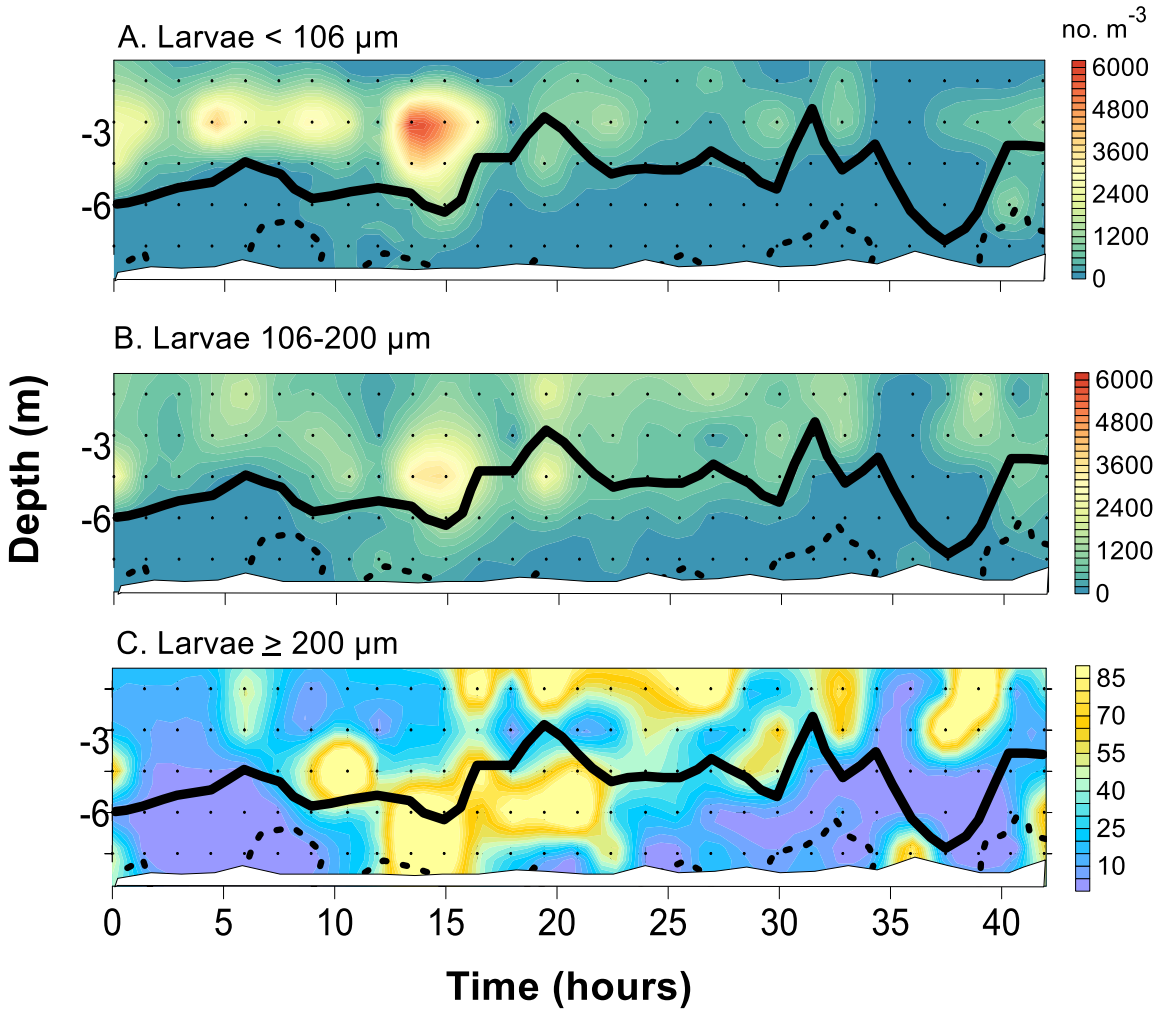

Fig. 4.14. Concentrations of *C. virginica* larvae with shell heights A) < 106 µm, B) 106-200 µm, and C) ≥ 200 µm collected at station Two during the fixed station cruise on July 12-14, 2012. The targeted midpoint depth of sample collection (black dots), maximum salinity gradient (solid line), and the 2 mg l^{-1} oxycline (dotted line) are also depicted. Note that larvae with shell heights ≥ 200 µm (panel C) were plotted with a different color scale due to their lower concentrations.

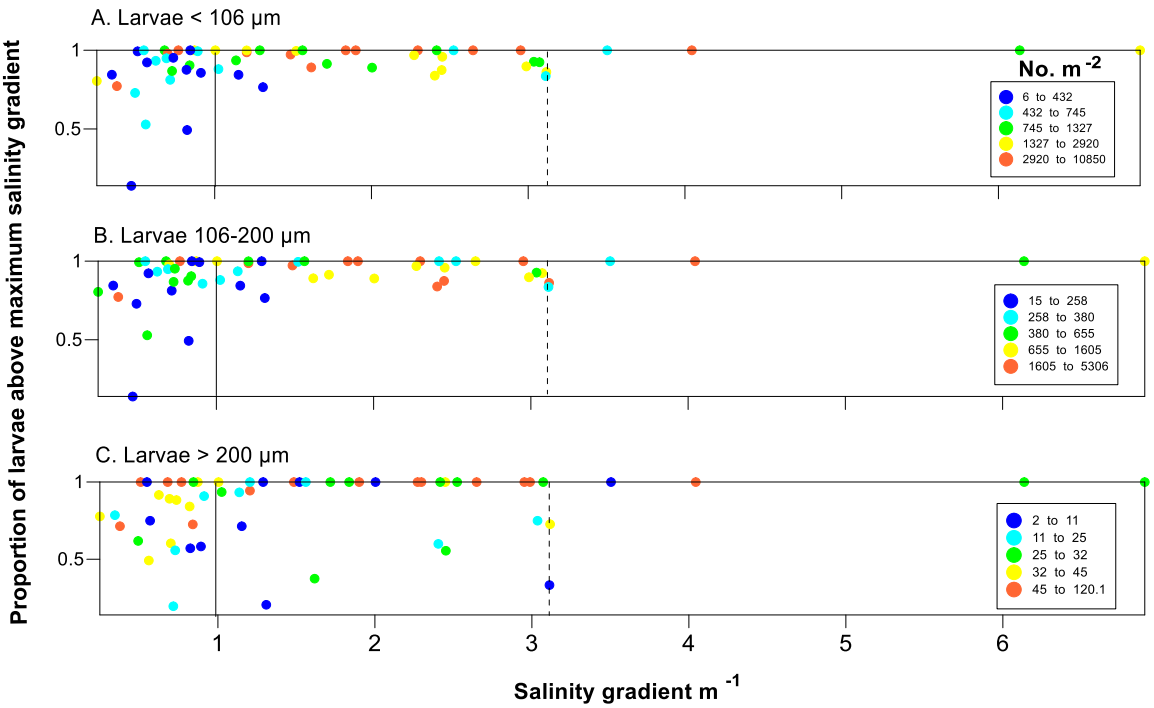

Fig. 4.15. The proportion of *C. virginica* larvae with shell heights A) < 106 µm and B) 106-200 µm, C) > 200 µm that were found above the salinity gradient (m^{-1}) during the fixed station cruise at both station One and Two. The salinity gradient was defined as the largest change in salinity during each CTD cast. The leftmost vertical line (solid) indicates a gradient of 1.0 above which 90% of all larvae were found. The rightmost vertical line (dashed) indicates an MSG of 3.1, above which 100% of all larvae were found. The color of the symbol corresponds to the abundance of larvae per CTD cast (no. m^{-2}).

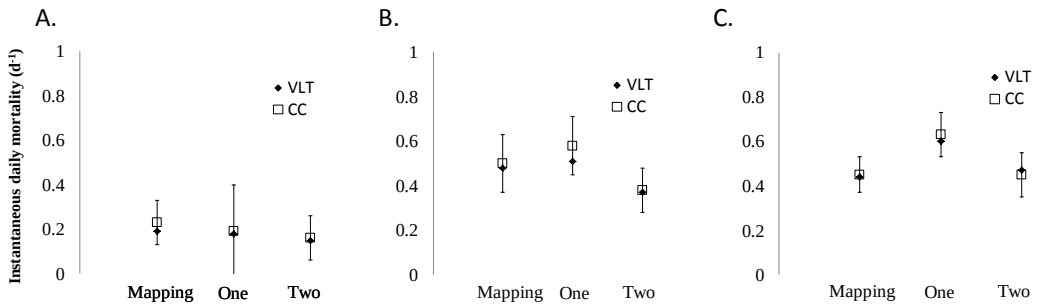

Fig. 4.16. The instantaneous daily mortality rates (d^{-1}) plotted for the mapping cruise and Stations One and Two of the fixed station cruises under A) minimum, B) all data, and C) maximum estimated growth rates (see Figure 3A and Table 5). Black diamonds represent mortality calculations made using the vertical life table (VLT) approach and open squares represent values for the catch curve (CC) approach. The whiskers are the 95% confidence intervals calculated using the catch curve approach.

Chapter 5: Synthesis

The work of this dissertation helped to fill knowledge gaps by 1) creating a visual guide and key that enhanced the identification of *Crassostrea virginica* (eastern oyster) larvae in the Choptank River, 2) testing and improving ShellBi, a novel supervised image classification method that uses pattern recognition software to identify images of bivalve larvae taken under cross-polarized light, 3) developing a benchtop automated image acquisition system to rapidly capture images for use with ShellBi, and 4) applying these advances to identify factors that influence the vertical distribution of *C. virginica* larvae and to estimate their mortality rates in the field.

Summary

Highly accurate techniques for the identification of bivalve larvae exist (Lutz et al. 1982) but are time consuming. More rapid molecular techniques (Hare et al. 2000, Wight et al. 2009, Henzler et al. 2010, Sanchez et al. 2014) also provide some insight into the identity and quantity of bivalve larvae. However, this research offers a rapid identification technique that identifies, quantifies, and measures the sizes of larvae.

This research indicates that the use of cross-polarized light can enhance detection of bivalve larvae in samples, increase speed of identification, and maintain

high accuracies. The birefringent shells of bivalves are much easier to see under cross-polarized light making identification much easier when looking at them through the microscope. In addition, the ShellBi software applied and advanced in this research provides classification accuracies ranging 81-100% for a targeted species (*C. virginica*).

Automated image acquisition, like the system developed as part of this research program, has the potential to greatly advance understanding of the larval ecology of bivalves. Although we have been studying the larval stage of *C. virginica* for over three centuries, previous research has been limited due to the lack of automated and rapid identification. The development of automated imaging system was essential for imaging field samples. Field samples were imaged over a 46-day period but without this technology, it could have taken over 350 days. This technology could allow increased sampling sizes and processing times for future studies aimed at understanding factors that influence the distribution and abundance of bivalve larvae.

Results from field collections reported in Chapter 4 can be used to enhance models of larval transport and better understand population dynamics. Specifically, the transient larval stage of bivalves is important to understand because it influences population connectivity and gene flow (Pineda et al. 2007; Dame 2012). The swimming behavior of larvae in particle tracking models that incorporate hydrodynamics is extremely important (e.g. North et al. 2008), and this research indicates that a salinity gradient of 1.2 m^{-1} should be used to cue stimulated vertical swimming behavior. Furthermore, the mortality estimates could be used in

fundamental models aimed to understand the basic ecology of *C. virginica* populations.

Future research

This research program helped develop an accurate rapid way to identify oyster larvae but improvements and the potential to develop it for other targeted bivalves or organisms exists. Accuracies could be improved with further software developments (e.g. using random Forrest in the program "R" (Liaw and Wiener 2002), instead of a Support Vector machine in MATLAB software) or experimenting with different camera and light source settings (e.g. Chapter 3). The automated cropping program developed in Chapter 3 could be utilized for hatchery applications in its current state or improved for better accuracy with field samples.

Although the research conducted in this dissertation has helped advance the field of bivalve larval identification and the understanding of their ecology, more studies are needed to fully understand the complexities of the larval stage of these organisms. The ShellBi software coupled with the automated image acquisition system (for plankton in general) could have a substantial impact on our understanding of eutrophic and coastal systems around the world by allowing for rapid image acquisition and classification of species that require magnification for identification.

Future applications of ShellBi could be used to identify other organisms (e.g. pteropods) as well as bivalves in other systems. In addition, ShellBi could help detect dissolution of calcium carbonate shells of marine plankton. Studies are needed to determine if ShellBi could be used to detect dissolution due to pH changes for certain species. Preliminary studies conducted in lab show that the birefringence patterns of

C. virginica larvae are affected by low levels of pH (Fig. 5.1). Shells of 9-d old *C. virginica* larvae stored at low pH (4.0) for 1 month experienced dissolution which affected their birefringence patterns compared to larvae that were stored in pH of 8 or higher. The automated image acquisition system has application for rapidly imaging other planktonic organisms at high magnification and should be tested on other organisms (e.g. copepods, pteropods and other plankton). More effort is needed to automate post processing of the bivalve images *in situ* to improve automatic ROI detection.

This research suggests the swimming behavior of *C. virginica* larvae is influenced by salinity gradients and possibly by low oxygen, and provides a quantitative estimate of the strength of the salinity gradient that cues larval swimming ($> 1.2\ m^{-1}$). However, future studies are needed in the field that can tease out how *C. virginica* larvae respond to low oxygen levels. Furthermore, multiple mapping cruises should be conducted to identify spawning areas and source populations, dispersal, and transport of bivalve larvae.

The mortality rates calculated help provide fundamental knowledge of the ecology of *C. virginica* larvae and could be used in future studies aimed at understanding their population dynamics and transport. Fisheries catch curve and vertical life table mortality estimations were used for the first time to estimate mortality for *C. virginica* (or any bivalve) larvae. Future studies are needed to enumerate *C. virginica* larvae < 106 μm shell height, so that mortality rate calculations could be made for larvae < 8 d old. Furthermore, future studies are

needed to test the variability of growth conditions of *C. virginica* larvae in the field because growth conditions can influence mortality rate calculations.

This research program had a large focus on the development of technology that could be used to support long-term monitoring programs for bivalve larvae. Monthly monitoring of larvae could provide improved knowledge of spawning trends in various systems and aid in enhanced understanding of the factors that cause inter-annual fluctuations in recruitment. In addition, these tools could also be used to track changes in larval concentrations near projects aimed at restoring adult populations.

Literature cited

Dame, R.F. 2012. Population processes, *In*: Ecology of marine bivalves an ecosystem approach P. Petrailia, and H. Linna (eds.), 2nd ed. CRC Press Taylor Frances Group. pp. 75-103.

Hare, M. P., S. R. Palumbi, and C. A. Butman. 2000. Single-step species identification of bivalve larvae using multiplex polymerase chain reaction. Mar. Biol. 137:953-961.

Henzler, C. M., E. A. Hoaglund, and S. D. Gaines. 2010. FISH-CS - a rapid method for counting and sorting species of marine zooplankton. Mar. Ecol. Prog. Ser. 410:1-11.

North, E.W., Z. Schlag, R.R. Hood, M. Li, L. Zhong, T. Gross, and V.S. Kennedy. 2008. Vertical swimming behavior influences the dispersal of simulated oyster larvae in a coupled particle-tracking and hydrodynamic model of Chesapeake Bay. Mar. Ecol. Prog. Ser. 359:99-115.

Liaw, A., and M. Wiener. 2002. Classification and regression by random forrest. R news. (2/3):18-22.

Lutz, R. J., and others. 1982. Preliminary observations on the usefulness of hinge structures for identification of bivalve larvae. J. Shell. Res. 2(1): 65-70.

Pineda, J., J.A. Hare, S. Sponaugle. 2007. Larval dispersal and transport in the coastal ocean and consequences for population connectivity. Oceanogr. 20, 22–39.

Sanchez, A., J. Quinteiro, M. Rey-Mendez, R.I. Perez-Martin, and C.G. Sotelo. 2014. Identificaiton and quanitificaiton of two species of oyster larvae using real-time PCR. Aquatic living resources. 27(3-4):135-145.

Wight, N. A., J. Suzuki, B. Vadopalas, and C.S. Friedman. 2009. Development and optimization of quantitative PCR assays to aid *Ostrea lurida* Carpenter 1984 restoration efforts. J. Shell. Res. 28(1): 33-41.

Figure

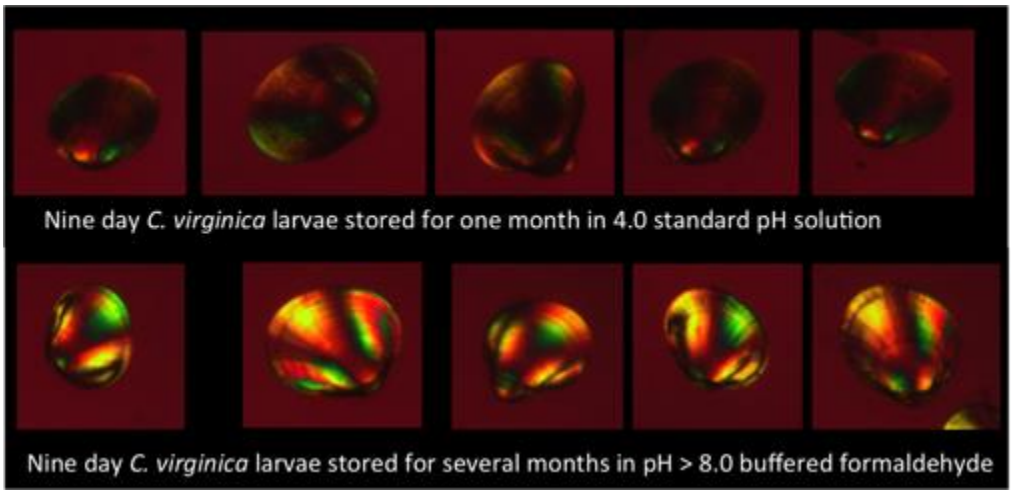

Fig. 5.1. Nine-day-old *C. virginica* larvae stored for one month in low (4.0) pH conditions (upper panel) and higher (8.0) pH (lower panel). Dissolution had an effect on the birefringence patterns in the lower pH.

Literature Cited (all)

Chapter 1

Allen, J.F. 1962. Gonad development and spawning of *brachidontes recurvus* in Chesapke. Bay. Naut. 75(4):149-156.

Andrews, J.D. 1979. Pelecypoda: Ostreidae. *In:* A.C. Giese and J.S. Pearse (eds). Reproduction of marine invertebrates, vol. 5. Academic Press, New York. Pages 293-341.

Baker, S. and R. Mann. 2003. Late stage bivalve larvae in a well-mixed estuary are not inert particles. Estuaries. 26(4A):837-845.

Beck, M.W., R.D., Brumbaugh, L. Airoldi, A. Carranza, L.D. Coen, C. Crawford, O. Defeo, G.J. Edgar, B. Hancock, M.C. Kay, H.S. Lenihan, M.W. Luckenbach, C.L. Toropova, G. Zhang, and X. Guo. 2011. Oyster reefs at risk and recommendations for conservation, restoration, and management. BioScience, 61:107-116.

Berlin, A. 2008. Foraging values of *Mulinea lateralis* and *Ischadium recurvum*: energetics of surf scoters wintering in the Chesapeake Bay. MEES Dissertation University of Maryland. 2008.

Bertness, M.D. and E. Grosholz. 1985. Population dynamics of the ribbed mussel, *Geukensia demissa*: The costs and benefits of an aggregated distribution. Oecologia 67:192-204.

Blundon, J.A. and V.S. Kennedy. 1982. Refuges for infaunal bivalves from blue crab, *Callinectes sapidus* (Rathbun), and predation on Chesapeake Bay bivalves. J. Exp. Mar. Biol. Ecol. 65:67-81.

Borrero, F.J. 1987. Tidal height and gametogenesis: reproductive variation among populations of *Geukensia demissa*. Biological Bulletin 173:160-168.

Breuer, J.P. 1957. An ecological survey of Baffin and Aluzan Bay Tx. Publ. Inst. Marine. Sci. 4:134-155.

Brousseau, D.J. 1984. Age and growth rate determinations for the Atlantic ribbed mussel, *Geukensia demissa* Dillwyn (Bivalvia: Mytilidae). Estuaries and Coasts 7:233-241.

Cain, T.D. 1975. Reproduction and recruitment of the brackish water clam *Rangia cuneata* in the James River, Virginia. Fish. Bull. 73:412-430.

Calabrese, A. 1969. The early life history and larval ecology of the coot clam, *Mulinia lateralis* (Say) (Mactridae: Pelecypoda). Dissertation, Univ. of Connecticut, 1969. 101 pp.

Calabrese, A., and E.W. Rhodes 1974. Culture of *Mulinia lateralis* and *Crepidula fornicate* embryos and larvae for studies of pollution effects. Thal. Jugoslavica 10:89-102.

Carriker, M.R., and Gaffney P.M. 1996. A catalogue of selected species of living oysters (Ostreacea) of the world. *In*: V.S. Kennedy, I.E. Newell, and E.F. Eble (eds). The eastern oyster *Crassostrea virginica* Chapter 1. Maryland Sea Grant pp 1-18.

Carriker, M.R. 1996. Chapter 3. The shell and ligament. *In*: Kennedy, V.S., R.I. E. Newell, and A.F. Eble (eds). The eastern oyster *Crassostrea virginica*. Maryland Sea Grant, College Park, Maryland.
Carriker, M.R. 1986. Influence of suspended particles on biology of oyster larvae in estuaries. Amer. Malcol. Bull., spec. ed. 3:41-49.
Carriker M.R. and R.E. Palmer. 1979. A new mineralized layer in the hinge of the oyster. Science 206:691-693.
Chang, L.L.Y., R.A. Howie, and J. Zussman 1996. Rock-forming minerals, (2nd edition), v. 5B, non-silicates, 108–135.
Chanley, P. 1965. Larval development of the brackish water mactrid clam, *Rangia cuneata*. Chesapeake Sci. 6(4):209-213.
Chanley, P. 1970. Larval development of the hooked mussel, *Brachiodontes recurves* Rafineque (Bivalvia: Mytilidae) including a literature review of larval characteristics of the Mytilidae. Proc. Natl. Shell. Assoc. 60:86-94.
Chanley, P., and M. Castagna. 1971. Larval Development of the Stout Razor Clam, *Tagelus plebeius* Chesapeake Sci. 12(3):167-172.
Checa, A.G., T. Okamoto, and J. Ramirez. 2006. Organization pattern of nacre in Pteriidae (Bivalvia:Mollusca) explained by crystal competition. Proc. Biol. Sci. 273(1592):1329-1337.
Darnell, R.M. 1958. Food habits of fishes and large invertebrate of Lake Pontchartrain, Louisiana, an estuarine community. Publ. Inst. Mar. Sci. Univ. Tex. 5:353-416.
Davis, H.C., and A. Calabrese. 1964. Combined effects of temperature and salinity on development of eggs and growth of larvae of *M. mercenaria* and *C. virginica*. U.S. Fish Wildl. Serv., Fish. Bull. 63:643-655.
Dungan, C.F., R.M. Hamilton, K.L. Hudson, C.B. McCollough, and K.S. Reece. 2002. Two epizootic diseases in Chesapeake Bay commercial clams, *Mya arenaria* and *Tagelus plebeius*. Dis. Aquat. Org. 50:67-78.
Eyster, L.S. 1983. Ultrastructure of early embryonic shell formation in the opisthobranch gastropod *Aeolidia papillosa*. Biol. Bull. 165:394-408.
Eyster, L.S. 1986. Shell inorganic composition and onset of shell mineralization during bivalve and gastropod embryogenesis. Biol. Bull. 170:211-231.
Fogarty, M.J., and L.W. Botsford. 2007. Population Connectivity and Spatial Management of Marine Fish. Oceanogr. 20:112-123.
Franz, D. 2001. Recruitment, survivorship, and age structure of a New York ribbed mussel population (*Geukensia demissa*) in relation to shore level-A nine year study. Estuaries, 24(3):319-327.
Fulford, R.S., D.L Breitburg, M. Luckenbach, and R.E. Newell. 2010. Evaluating ecosystem response to oyster restoration and nutrient load reduction with a multispecies bioenergetics model. Ecol. Applications, 20, 915-934.
Gallager, S., and S. Tiwari. 2008. Optical method and system for rapid identification of multiple refractive index materials using multiscale texture and color invariants. *United States Patent 7,415,136*. Washington, DC: U.S.
Galtsoff, P.S. 1964. The American oyster, *Crassostrea virginica* (Gmelin) Fishery Bull. Fish Wildl. Serv. U.S. 64:1-480.

Garland, E.D., and C.A. Zimmer. 2002. Techniques for the identification of bivalve larvae. Mar. Ecol. Prog. Ser. 225:299-310.

Chapter 2

Bachiller, E., J. A. Fernandes, and X. Irigoien. 2012. Improving semiautomated zooplankton classification using an internal control and different imaging devices. Limnol. Oceanogr. Methods. 10:1-9.

Baldi, P., and S. Brunak. 2001. Bioinformatics-the machine learning approach, MIT Press, Cambridge, MA.

Boicourt, W. C. 1988. Recruitment dependence on planktonic transport in coastal waters, p. 183-202. *In* B.J. Rothschild (ed.), Toward a theory on biological-physical interactions in the world ocean. Kluwer Academic Publishers.

Bland, J. M., and D. G. Altman. 1995. Multiple significance tests: the Bonferroni method. BMJ 310:170.

Calabrese, A. 1969. *Mulinia lateralis*: Molluscan fruit fly? Proceedings of the National Shellfisheries Association 59:65-66.

Calabrese, A., and E. W. Rhodes. 1974. Culture of *Mulinia lateralis* and *Crepidula fornicate* embryos and larvae for studies of pollution effects. Thalassia Jugosl. 10:89-102.

Cawley, G. C. 2000. (MATLAB) Support vector machine toolbox (v0.55\beta). University of East Anglia, School of information systems, Norwich, Norfolk, U.K. NR4 7TJ. http://theoval.cmp.uea.ac.uk/svm/toolbox/

Chanley, P. 1970. Larval development of the hooked mussel, *Brachiodontes recurves* Rafinesque (Bivalvia: Mytilidae) including a literature review of larval characteristics of the Mytilidae. Proceedings of the National Shellfisheries Association 60:86-94.

Chanley, P., and J. D. Andrews. 1971. Aids for identification of bivalve larvae of Virginia. Malacol. 11:45-119.

Chanley, P., and M. Castagna. 1971. Larval development of the stout razor clam, *Tagelus plebeius* solander (solecurtidae: Bivalvia). Ches. Sci. 12:167-172.

Dame, R. F. 2012. Population processes p. 75-103. *In*: (eds) P. Petrailia, and H. Linna. Ecology of marine bivalves an ecosystem approach 2nd edition. CRC Press Taylor Frances Group. Boca Raton, FL.

Davis, C. S., Q. Hu, S. M. Gallager, X. Tang, and C. J. Ashjian. 2004. Real-time observation of taxa-specific plankton distributions: an optical sampling method. Mar. Ecol. Prog. Ser. 284:77-96.

Fernandes, F. A., X. Irigoien, G. Boyra, J. A. Lozano, and I. Inza 2009. Optimizing the number of classes in automated zooplankton classification. J. Plankton Res. 31(1):19-29.

Fogarty, M. J., and L.W. Botsford. 2007. Population connectivity and spatial management of Mar. Fish. *Oceanogr.* 20(3):112–123,http://dx.doi.org/10.5670/oceanog.2007.34.

Fukunaga, K., and D. M. Hummels. 1989. Leave-one-out procedures for nonparametric error estimates. IEEE Trans. Pattern Anal. Mach. Intellig. 11:421-423.

Garland, E. D., and C. A. Zimmer. 2002. Techniques for the identification of bivalve larvae. Mar. Ecol. Prog. Ser. 225: 299-310.

Grosjean, P., M. Picheral, C. Warembourg, and G. Gorsky. 2004. Enumeration, measurement, and identification of new zooplankton samples using the ZOOSCAN digital imaging system. J. Mar. Sci. 61:518-525.

Hare, M. P., S. R. Palumbi, and C. A. Butman. 2000. Single-step species identification of bivalve larvae using multiplex polymerase chain reaction. Mar. Biol. 137:953-961.

Helm, M., N. Bourne, and A. Lovatelli. 2004. Hatchery culture of bivalves: A Practical manual, FAO Fisheries Technical Paper 471, Rome.

Hendriks, I. E., L. A. van Duren, and P. M. J. Herman. 2005. Image analysis techniques: a tool for the identification of bivalve larvae? J. Sea Res. 54:151-162.

Henzler, C. M., E. A. Hoaglund, and S. D. Gaines. 2010. FISH-CS - a rapid method for counting and sorting species of marine zooplankton. Mar. Ecol. Prog. Ser. 410:1-11.

Hu, Q., and C. Davis. 2006. Accurate automatic quantification of taxa-specific plankton abundance using dual classification with correction. Mar. Ecol. Prog. Ser. 306:51-61.

Kennedy, V.S., R. A. Lutz, and C. A. Fuller. 1989. Larval and early postlarval development of *Macoma mitchelli* Dall (Bivalvia: Tellinidae). The Veliger 32:29-38.

Kennedy, V. S. 1996. Biology of larvae and spat. p. 371-421. *In* (eds.) V. S. Kennedy, R. E. Newell, and A. F. Eble. The Eastern Oyster *Crassostrea virginica.* Maryland Sea Grant.

Kennedy, V. S. 2011a. The invasive dark false mussel *Mytilopsis leucophaeata* (Bivalvia: Dreissenidae): A literature review. Aqua. Ecol. 45:163-183.

Kennedy, V. S. 2011b. Biology of the uncommon dreissenid bivalve *Mytilopsis leucophaeata* (Conrad 1831) in central Chesapeake Bay. J. Mull. Stud. 77:154-164.

Langdon, C. J. and I. E. Newell. 1996. Digestion and Nutrition in Larvae and Adults. p. 231-269. *In* (eds.) V. S. Kennedy, R. E. Newell, and A. F. Eble. The Eastern Oyster *Crassostrea virginica.* Maryland Sea Grant.

Lin, Y., Y. Lee and G. Wahba. 2002. Support Vector Machines for classification in nonstandard situations. Mach. Learn. 46(1-3):191-202.

Loosanoff, V. L., H. C. Davis, and P. E. Chanley. 1966. Dimensions and shapes of larvae of some marine bivalve mollusks. Malacol. 4:351-435.

Lou, T., K. Kramer, D. Goldgof, L.O. Hall, S. Samson, A. Remsen, and T. Hopkins. 2003. Learning to recognize plankton, p. 888-893. In Proceedings of the IEEE International Conference on Systems, Man and Cybernetics. Washington C.C. October 2003.

Lutz, R. J., and others. 1982. Preliminary observations on the usefulness of hinge structures for identification of bivalve larvae. J. Shell. Res. 2(1): 65-70.

(MDNR) Maryland Department of Natural Resources 2012. Fixed station monthly monitoring buoy EE1.1 http://mddnr.chesapeakebay.net/bay_cond/bay_cond.cfm?param=wt&station=EE11

Munroe, D. M., J. M. Klinck, E. E. Hofmann, and E. N. Powell. 2012. The role of larval dispersal in metapopulation gene flow: local population dynamics matter. J. of Mar. Res. 70:441-467.

North, E., Z. Schlag, R. Hood, M. Li, L. Zhong, T. Gross, and V. S. Kennedy. 2008. Vertical swimming behavior influences the dispersal of simulated oyster larvae in a coupled particle tracking and hydrodynamic model of Chesapeake Bay. Mar. Ecol. Prog. Ser. 359: 99-115.

Pineda, J., J. A. Hare, and S. Sponaugle. 2007. Larval transport and dispersal in the coastal ocean and consequences for population connectivity. Oceanogr. 20(3):22-39.

Provost, F. 2000. Machine learning from imbalanced data sets 101, p. 1-3. *In* Proceedings of the AAAI,00 workshop on learning from imbalanced data sets, Austin, TX. AAAI.

Shanks, A. L., and L. Brink. 2005. Upwelling, downwelling, and cross-shelf transport of bivalve larvae: test of a hypothesis. Mar. Ecol. Prog. Ser. 302:1-12.

Sokal, R., and J. Rohlf. 1987. p. 225-227. *In* Sokal, R. and J. Rohlf (eds). Non parametric methods *in lieu* of ANOVA Introduction to biostatistics. W.H. Freeman and Company.

Sun, Y., M. M. Karnel, A. K. C. Wong, and Y. Wang. 2007. Cost-sensitive boosting for classification imbalanced data. Patt. Recogn. 40:3358-3378.

Sundberg, K., and V. S. Kennedy. 1992. Growth and development in larval and post-metamorphic *Rangia cuneata* (Sowerby, 1831). J. Shell. Res. 11:9-12.

Sundberg, K., and V. S. Kennedy. 1993. Larval settlement of Atlantic Rangia, *Rangia cuneata* Bivalvia: Mactridae). Estuaries 16(2):223-228.

Thompson, C. M., M. P. Hare, and S. M. Gallager. 2012a. Semi-automated image analysis for the identification of bivalve larvae from a Cape Cod estuary. Limnol. Oceanogr. Methods: 10:538-554.

Thompson, C. M., R. H. York, and S.M. Gallager. 2012b. Species-specific abundance of bivalve larvae in relation to biological and physical conditions in a Cape Cod estuary: Waquoit Bay, Massachusetts (USA). Mar. Ecol. Prog. Ser. 469:53-69.

Tiwari, S., and S. M. Gallager. 2003a. Optimizing multiscale invariants for the identification of bivalve larvae. Proceedings of the 2003 IEEE International Conference on Image Processing, Barcelona, Spain, September 14-17, 2003.

Tiwari, S., and S. Gallager. 2003b. Machine learning and multiscale methods in the identification of bivalve larvae. Proceedings of the Ninth IEEE International Conference on Computer Vision, Nice, France, October 14-17, 2003.

Wight, N. A., J. Suzuki, B. Vadopalas, and C.S. Friedman. 2009. Development and optimization of quantitative PCR assays to aid *Ostrea lurida* Carpenter 1984 restoration efforts. J. Shell. Res. 28(1): 33-41.

Zhao, F., F. Lin, and H. S. Sea. 2010. Binary SIPPER plankton image classification using random subspace. Neurocomp. 73:1853-1860.

Chapter 3

Bachiller, E., J.A. Fernandes, and X. Irigoien. 2012. Improving semi automated zooplankton classification using an internal control and different imaging devices. Limnol. Oceanogr. Methods. 10:1-9. [doi:10. 4319/ lom. 2012. 10. 1].

Benfield, M.C., P. Grosjean, P.F. Culverhouse, X. Irigoien, M.E. Sieracki, A. Lopez-Urrutia, H.G. Dam, Q. Hu, C.S. Davis, A. Hansen, C.H. Pilskaln, E.M. Riseman, H. Schultz, P.E. Utgoff, and G. Gorsky. 2007. RAPID: Research on Automated Plankton Identification. Oceanogr. 20(2):172–187. http://dx.doi.org/10.5670/oceanog.2007.63.

Carriker, M.R. 1996. The Shell and Ligament, *In* V.S. Kennedy, R.E. Newell, and A. F. Eble (eds.), The Eastern oyster *Crassostrea virginica*. Maryland Sea Grant. p. 75-159.

Chanley, P., and J.D. Andrews. 1971. Aids for identification of bivalve larvae of Virginia. Malacol.11:45–119.

Cowan, R.K., and Guigand, C.M. 2008. *In situ* ichthyoplankton imaging system (ISIIS): system design and preliminary results. Limnol. Oceangr. Methods. 6:126-132.

Davis C.S., S.M. Gallager, M. Marra, and W.K. Stewart. 1996. Rapid visualization of plankton abundance and taxonomic composition using the Video Plankton Recorder. Deep Sea Res. Part II. 43(7-8):1947-1970.

Gaines, S., and J. Roughgarden. 1985. Larval settlement rate: A leading determinant of structure in an ecological community of the marine intertidal zone. Proc. Natl. Acad. Sci. USA. Ecology. 82:3707-3711.

Gallager, S., and S. Tiwari. 2008. Optical method and system for rapid identification of multiple refractive index materials using multiscale texture and color invariants. *United States Patent 7,415,136*. Washington, DC: U.S.

Garland, E.D., and C.A. Zimmer. 2002. Techniques for the identification of bivalve larvae. Mar. Ecol. Prog. Ser. 225:299-310 [doi:10. 3354/ meps225299].

Goodwin, J.D., E.W. North, and C.M. Thompson. 2014. Evaluating and improving a semi-automated image analysis technique for identifying bivalve larvae. Limnol. Oceanogr. Methods 12:548-562.

Gorsky, G., M.D. Ohman, M. Picheral, S. Gasparini, L. Stemmann, J. Romagnan, A. Caweood, S. Pesant, C. Garcia-Comas, and F. Prejge. 2010. Digital zooplankton image analysis using the ZooScan integrated system. J. of Plank. Res. 32(3):285-303.

Grosjean, P., M. Picheral, C. Warembourg, and G. Gorsky. 2004. Enumeration, measurement, and identification of new zooplankton samples using the ZOOSCAN digital imaging system. J. Mar. Sci. 61:518-525.

Hare, M.P., S.R. Palumbi, and C.A. Butman. 2000. Single-step species identification of bivalve larvae using multiplex polymerase chain reaction. Mar. Biol. 137:953-961 [doi:10.1007/ s002270000402].

Hendriks, I.E., L.A. Van Duren, and P. M. J. Herman. 2005. Image analysis techniques: a tool for the identification of bivalve larvae? J. Sea Res. 54:151-162. [doi:10. 1016/ j. seares.2005. 03. 001].

Henzler, C.M., E.A. Hoaglund, and S.D. Gaines. 2010. FISHCS—a rapid method for counting and sorting species of marine zooplankton. Mar. Ecol. Prog. Ser. 410:1-11 [doi:10.3354/ meps08654].

Kennedy, V.S. 1996. *In:* V.S. Kennedy, R.E. Newell, and A.F. Eble (eds.), The eastern oyster *Crassostrea virginica*. Maryland Sea Grant p. 371-421.

Larsen, J.B., M.E. Frischer, L.J. Rasmussen, and B.W. Hansen. 2005. Single-step nested multiplex PCR to differentiate between various bivalve larvae. Mar. Biol. 146:1119-1129. [doi:10.1007/s00227-004-1524-2]

Lutz R, J. Goodsell, M. Castagna, S. Chapman, R. Newell, H. Hidu, R. Mann, D. Jablonski, V. Kennedy, S. Siddall, R. Goldberg, H. Beattie, C. Falmagne, A. Chestnut, A. Partridge. 1982. A Preliminary observation on the usefulness of hinge structure for identification of bivalve larvae. J. Shell. Res. 2:65–70.

MacLeod, N., M. Benfield, and P. Culverhouse. 2010. Time to automate identification. Nature, 467:154-155.

Molder, A., S. Drury, N. Costen, G. M. Hartshorne and S. Czanner. 2015. Semiautomated analysis of embryoscope images: Using localized variance of image intensity to detect embryo developmental stages. Cytometery. 87A(2):119-128.

O'Meara, S., D. Holser, S. Brenimer, and S.F. Pucherelli. 2013. Effect of pH, ethanol concentration, and temperature on detection of quagga mussel (*Dreissena bugensis*) birefringence. Manag. of Biol. Invas. 4(2):135-138.

Steele, J.H. 1989. The ocean 'landscape'. Landscape Ecol. 3:185-192.

Tiwari, S., and Gallager, S. 2003. Machine learning and multiscale methods in the identification of bivalve larvae. Proceedings of the Ninth IEEE International Conference on Computer Vision, Nice, France, October 14-17, 2003. [doi:10. 1109/].

Thompson, C.M., S.M. Gallager, and M. Hare. 2012. Semi-automated analysis for the identification of bivalve larvae from a Cape Cod estuary. Limnol. Oceanogr. Methods. 10:538-554 [doi:10. 4319/ lom. 2012. 10. 538].

Vishrutha, V., and M. Ravishankar. 2015. Early detection and classification of breast cancer. Proc. of 3rd international conference of Frontiers of Intelligence Computing: Theory and Applications. 327:413-419. 10.1007/978-3-319-11933-5_45.

Wiens, J.A. 1989. Spatial scaling in ecology. Functional Ecol. 3:385-397.

Zetsche, E. M., A.E. Mallahi, F. Dubois, C. Yourassowsky, J.C. Kromkamp, and F J. Meysman. 2014. Imaging-in-Flow: Digital holographic microscopy as a novel tool to detect and classify nanoplankton organisms. Limnol. Oceanogr. Methods. 12:757-775.

Chapter 4

Aksnes, D.L. and M.D. Ohman. 1996. A vertical life table approach to zooplankton mortality estimation. Limnol. Oceanogr. 41(7):1461-1469.

Andrews, J.D. 1983. Transport of bivalve larvae in James River, Virginia. J. Shell. Res. 3:29-49.

Beck, M.W., R.D. Brumbaugh, L. Airoldi, A. Carranza, L.D. Coen, C. Crawford, O. Defeo, G.J. Edgar, B. Hancock, M. Kay, H. Lenihan, M.W. Luckenbach, C.L. Toropova, G. Zhang & X. Guo. 2011. Oyster reefs at risk and recommendations for conservation, restoration, and management. Bioscience, 61:107–116.

Boicourt, W.C. 1982. Estuarine larval retention mechanisms on two scales. *In*: Kennedy (ed), Estuarine Comparisons. Academic Press, New York, pp 445-458.

Botsford, L.W., J.C. Castilla, C.H. Peterson. 1997. The management of fisheries and marine ecosystems. Science. 277:509-515.

Burrell, V.G. and W.A. Van Englel. 1976. Predation by and distribution of a ctenophore, *Mnemiopsis leidyi* A. Agassiz, in the York Estuary. Estuar. Coast. Mar. Sci. 4:235-242.

Carriker, M.R. 1951. Ecological observations on the distribution of oyster larvae in New Jersey estuaries. Ecol. Monogr. 21:19-38.

Chapman, D.G., and D.S. Robson. 1960. The analysis of a catch curve. Biometrics 16(3):354-368.

Dame, R.F. 2012. Population processes, *In*: P. Petrailia, and H. Linna (eds.) Ecology of marine bivalves an ecosystem approach, 2nd ed. CRC Press Taylor Frances Group. pp. 75-103.

Drinnan, R.E. and Stallworthy. 1979. Oyster larval populations and assessment of spatfall, Bidford River, P.E.I. 1961. Fish. Mar. Serv. Tech. Report. No 792.

Davis, H.C. and A. Calabrese 1964. Combined effects of temperature and salinity on development of eggs and growth of larvae of *M. mercenaria* and *C. virginica*. Fish. Bull. 63:643-655.

Fassler, S.M., M.R. Payne, T. Brunel and M. Dickey-Collas. 2011. Does larval mortality influence population dynamics? An analysis of North Sea herring (*Clupea harengus*) time series. Fish. Oceanogr. 20(6):530-543.

Galtsoff, P.S. 1964. The American oyster, *Crassostrea virginica* (Gmelin) Fishery Bull. Fish Wildl. Serv. U.S. 64:1-480.

Goodwin, J.D., E.W. North and C.M. Thompson. 2014. Evaluating and improving a semi-automated image analysis technique for identifying bivalve larvae. Limnol. Oceanogr. Meth. 12:548-562.

Hidu, H. and H. Haskin. 1978. Swimming speeds of oyster larvae *Crassostrea virginica* in different salinities and temperatures. Estuaries. 1(4):252-255.

Houde, E.D. 2002. Mortality. *In*: Werner, R.G. and Fuiman, L.A. (Eds), Fishery Science. The Unique contributions of early life stages. Blackwell Publishing, Oxford, pp.64-87.

Kennedy, V.S. 1996. Biology of larvae and spat. *In*: V.S. Kennedy, I.E. Newell, and E.F. Eble (eds). The eastern oyster *Crassostrea virginica* xChapter 10. Maryland Sea Grant pp. 371-421.

Kennedy, V.S. 1986. Expected seasonal presence of Crassostrea virginica (Gmelin) larval populations, emphasizing Chesapeake Bay. Amer. Malacol. Bull. Spec. Edit. 3:25-29.

Kennedy, V.S., and L.B. Krantz. 1982. Comparative gametogenic and spawning patterns of the oyster *Crassostrea virginica* (Gmelin) in central Chesapeake Bay. J. Shellfish Res. 9:133-140.

Kim, C.-K., K. Park, S. P. Powers, W.M. Graham and K.M. Bayha. 2010. Oyster larval transport in coastal Alabama: Dominance of physical transport over biological behavior in a shallow estuary.J. Geophys. Res.,115, C10019, doi:10.1029/2010JC006115.

Kimmel, D.G., and R.I.E. Newell. 2007. The influence of climate variation on eastern oyster (*Crassostrea virginica*) juvenile abundance in Chesapeake Bay. Limnol. Oceanogr. 52(3):959-965.

Loosanoff, V.L. 1965. The American or eastern oyster. United States Dept. of the Interior Circular 205:1-36.

Loosanoff, ,V.L. and H.C. Davis 1963. Rearing of bivalve molluscs. Adv. Mar. Biol. 1:1-136.

Mann, R. 1988. Distribution of bivalve larvae at a frontal system in the James River, Virginia. Mar. Ecol. Prog. Ser. 50:29-44.

Mann, R. 1988. Distribution of bivalve larvae at a frontal system in the James River, Virginia, Mar. Ecol. Prog. Ser., 50,29–44.

Mann, R., and J.S. Rainer. 1990. Effect of decreasing oxygen tension on swimming rate of *Crassostrea virginica* (Gmelin, 1791) larvae. J. Shell. Res. 9:323-327.

Medcof, J.C. 1939. Larval life of the oyster (*Ostrea virginica*) in Bideford River. J. Fish. Res. Board Can. 4:287-301.

Nelson, T.C. 1911. Report of the biologist. Oyster culture studies in 1910. In: Ann. Rep. Agric. Exp. Sta. New Brunswick New Jersey. 1926. pp. 103-113.

Nelson, T.C. 1913. Report of the biologist. Observations of natural propogation data of 1912. Pages 281-345 in Ann. Rep. N.J. Agric. Exp. Sta. for 1912, New Brunswick, N.J.

Nelson, T.C. 1925. On the occurrence and food habits of ctenophores in New Jersey inland coastal waters. Biol. Bull. 48:92-111.

Nelson, T.C. 1927. Report of the department of biology. In: Ann. Rep. Agric. Exp. Sta. New Brunswick New Jersey. 1926. pgs103-113.

Nelson, T.C. and E.B. Perkins. 1931. Annual report of the department of biology, July 1, 1929-June 30, 1930. N. J. Agrric. Exp. Stn. Bull. 522:3-47.

Newell, R.I.E. 1988. Ecological Changes in Chesapeake Bay: Are they the result of the American oyster, *Crassostrea virginica*?, p. 536-546. *In:* M.P. Lynch and E.C. Krome (eds), Understanding the estuary: Advances in Chesapeake Bay research. Chesapeake Research Consortium, Gloucester Point, Virginia.

North, E.W., Z. Schlag, R.R. Hood, M. Li, L. Zhong, T. Gross, and V.S. Kennedy. 2008. Vertical swimming behavior influences the dispersal of simulated oyster larvae in a coupled particle-tracking and hydrodynamic model of Chesapeake Bay. Mar. Ecol. Prog. Ser. 359:99-115.

Officer, C.B., R.B. Biggs, J.L. Taft, L.E. Cronin, M.A. Tyler, and W.R. Boynton. 1984. Chesapeake Bay anoxia: Origin, development, and significance. Science 223:22-27.

Pedersen T.M., J.L.S. Hansen, A.B. Josefson, B.W. Hansen. 2008. Mortality through ontogeny of soft-bottom marine invertebrates with planktonic larvae. J. Mar. Syst. 73:185-207.

Pierson, J.J., Frost, B.W., and A.W. Leising. 2007. The lost generation of *Calanus pacificus*: Is the diatom effect responsible? Limnol. Oceanogr. 52(5):2089-2098.

Pineda, J., J.A. Hare, S. Sponaugle. 2007. Larval dispersal and transport in the coastal ocean and consequences for population connectivity. Oceanogr. 20, 22–39.
Puckett, B.J., D.B. Eggleston, P.C. Kerr and R.A. Luettich Jr. 2014. Larval dispersal and population connectivity among a network of marine reserves. Fish. Ocenogr. 23(4):342-361.
Ricker, W.E. 1975. Computation and interpretation of biological statistics of fish populations. Fish. Res. Bd. Canada Bull. 191.
Rumrill, S.S. 1990. Natural mortality of marine invertebrate larvae. Ophelia 32:163-198.
Sanford, L.P., K.G. Sellner, and D.L. Breitburg. 1990. Covariability of dissolved oxygen with physical processes in the summertime Chesapeake Bay. J. of Mar. Res. 48:567-590.
Seliger, H.H. Boggs, J.A. Rivkin, R.B. Biggley, W.H. Aspden, K.R.H. 1982. The transport of oyster larvae in an estuary. Mar. Biol. 71:57-72.
Shanks, A.L. and L. Brink. 2005. Upwelling, downwelling, and cross-shelf transport of bivalve larvae: test of a hypothesis. Mar. Ecol. Prog. Ser. 302:1-12.
Steinberg, P.D., and V.S. Kennedy. 1979. Predation upon *Crassostrea virginica* (Gmelin) larvae by two invertebrate species common to Chesapeake Bay oyster bars. The Veliger 22(1):78-84.
Stevenson, C.H. 1894.The oyster industry in Maryland. U.S. Fish Commission Bulletin for 1892 12: 205-297.
Tapia F.J., J. Pineda. 2007. Stage-specific distribution of barnacle larvae in nearshore waters: potential for limited dispersal and high mortality rates. Mar. Ecol. Prog. Ser. 342:177-90.
Vaughn, D. and Allen, J.D. 2010. The peril of the plankton. Integr. Comp. Biol. 50(4):552-570.
Widdows, J., R.I.E. Newell and R. Mann. 1989. Effects of hypoxia and anoxia on survival, energy metabolism, and feeding of oyster larvae (*Crassostrea virginica*, Gmelin). Biol. Bull. 177:154-166.
Wilberg, M.J., M.E. Livings, J.S. Barkman, B.T. Morris, and J.M. Robinson. 2011. Overfishing, disease, habitat loss, and potential extirpation of the oysters in upper Chesapeake Bay. Mar. Ecol. Prog. Ser. 436:131-144.
Wood, L. and W.J. Hargis, Jr. 1971. *In:* D.J. Crisp (eds.). Transport of bivalve larvae in a tidal estuary. Fourth European marine biology symposium. Cambridge University Press, New York. pp. 29-44.

Chapter 5

Dame, R.F. 2012. Population processes, *In*: Ecology of marine bivalves an ecosystem approach P. Petrailia, and H. Linna (eds.), 2nd ed. CRC Press Taylor Frances Group. pp. 75-103.
Hare, M. P., S. R. Palumbi, and C. A. Butman. 2000. Single-step species identification of bivalve larvae using multiplex polymerase chain reaction. Mar. Biol. 137:953-961.

Henzler, C. M., E. A. Hoaglund, and S. D. Gaines. 2010. FISH-CS - a rapid method for counting and sorting species of marine zooplankton. Mar. Ecol. Prog. Ser. 410:1-11.

North, E.W., Z. Schlag, R.R. Hood, M. Li, L. Zhong, T. Gross, and V.S. Kennedy. 2008. Vertical swimming behavior influences the dispersal of simulated oyster larvae in a coupled particle-tracking and hydrodynamic model of Chesapeake Bay. Mar. Ecol. Prog. Ser. 359:99-115.

Liaw, A., and M. Wiener. 2002. Classification and regression by random forrest. R news. (2/3):18-22.

Lutz, R. J., and others. 1982. Preliminary observations on the usefulness of hinge structures for identification of bivalve larvae. J. Shell. Res. 2(1): 65-70.

Pineda, J., J.A. Hare, S. Sponaugle. 2007. Larval dispersal and transport in the coastal ocean and consequences for population connectivity. Oceanogr. 20, 22–39.

Sanchez, A., J. Quinteiro, M. Rey-Mendez, R.I. Perez-Martin, and C.G. Sotelo. 2014. Identificaiton and quanitificaiton of two species of oyster larvae using real-time PCR. Aquatic living resources. 27(3-4):135-145.

Wight, N. A., J. Suzuki, B. Vadopalas, and C.S. Friedman. 2009. Development and optimization of quantitative PCR assays to aid *Ostrea lurida* Carpenter 1984 restoration efforts. J. Shell. Res. 28(1): 33-41.